VOLUME AND PETROLOGIC CHARACTERISTICS OF THE KOLOA VOLCANICS, KAUAʻI, HAWAIʻI

A THESIS SUBMITTED TO THE GRADUATE DIVISION OF THE UNIVERSITY OF HAWAIʻI IN PARTIAL FULFILLMENT OF THE REQUIREMENTS FOR THE DEGREE OF

MASTER OF SCIENCE

IN

GEOLOGY AND GEOPHYSICS

April 2006

By

Christian Erick Gandy

Thesis Committee:

Michael O. Garcia, Chairperson
Chuck Blay
G. Jeffrey Taylor

We certify that we have read this thesis and that, in our opinion, it is satisfactory in scope and quality as a thesis for the degree of Master of Science in Geology and Geophysics.

THESIS COMMITTEE

_____

Chairperson

_____

_____

Acknowledgements

I would like to thank the U.S. Geological Survey Water Resources Division in Honolulu and geologist Scot Izuka for allowing us access to water well data and other information helpful to the project. Many thanks to Chuck Blay for providing housing during the field sessions and for his extensive geologic knowledge of the island of Kaua`i. Mahalo goes out to Bruce Robinson and Lissa Dunford of Gay & Robinson Sugar Co. for granting me access to their lands on Kaua`i. Also, I'd like to thank Jerry Taniguchi of Gay & Robinson for his expert knowledge of the geography of the island. Thank you to Mike Furakawa at Grove Farm Co. in Lihue for access to the Kilohana area. Chipper Wichman of National Tropical Botanical Garden in Lawai, the folks at A & B Property, and David Pirie at Halfway Bridge Quarry also deserve thanks for providing access to their lands. I would like to thank Christine Meyers, Jennifer Dermer, and Rebecca Carey for their valuable help in the field. Additional thanks go out to Steve Sahetepy-Engel for his understanding of GIS applications, as well as Mike Vollinger and Mike Rhodes at University of Massachusetts, Amherst, for XRF analyses. Thanks to Hiroki Sano and sharing unpublished data. This project was partially funded through a Harold T. Stearns Foundation grant from the Dept. of Geology and Geophysics at the Univ. of Hawai`i, overhead return funds to Dr. Michael Garcia, in addition to NSF grant EAR 05-10482. I would like to extend my deepest gratitude to my thesis committee, composed of Michael O. Garcia, Chuck Blay, and Jeff G. Taylor, for their patience and support throughout this study. Last but not least, I would like to thank the family and friends who have supported me in

so many ways: Christine Meyers, Rebecca Carey, Kevin Hannigan, Jim & Lois Gandy, and Marvin Gandy. This study is in memory of Thelma Gandy.

TABLE OF CONTENTS

Acknowledgements……iii

List of Tables……vii

List of Figures……viii

1.0 Abstract……1

2.0 Introduction……3

3.0 Geologic setting……7

4.0 Methods

4.1 Petrography and geochemistry……13

4.2 Volume calculations……15

5.0 Results

5.1 Petrography……20

5.2 Mineral chemistry……27

5.3 Whole rock chemistry……31

5.4 Volume……47

6.0 Discussion

6.1 Rock type temporal variations: Implications for melting history ..58

6.2 Duration of Koloa volcanism……61

6.3 Source models for rejuvenation volcanism……63

6.4 Mechanisms for the generation of rejuvenated magmas……65

6.5 Evaluation of mechanisms for rejuvenated volcanism ……68

6.6 Trends in duration and surface area of Hawaiian rejuvenated volcanism: Implications for future eruptions ……73

7.0 Conclusions……83

8.0 Future Work……85

Appendix

A. Petrographic summary of Koloa lavas……87

B. Well summary for wells located within the Koloa Volcanics……93

C. Normative analyses of representative Koloa lavas……100

References……103

LIST OF TABLES

Table **Page**

1. Modes for representative Koloa lavas based on 100 point counts/sample.....24

2. Composition of olivine cores and rims from the representative Koloa Volcanics, Kaua'i….29

3. XRF whole rock data for the Koloa Volcanics…….....41

4. XRF trace element data for the Koloa Volcanics……..44

.

5. Comparison of models for rejuvenation volcanism……..80

LIST OF FIGURES

Figure **Page**

1. Lithospheric melting by conductive heating (CH) and Secondary zone of mantle plume melting (SP)……6

2. A schematic cross-section of the flexure-induced decompressional melting model (FM)..6

3. Geologic map of Kaua`i with sample names and locations……12

4. Residual masses of Koloa lavas in Koai`e Canyon……19

5. Olivine mol % forsterite vs. whole rock Mg# for olivine phenocrysts from Koloa lavas…..28

6. Total alkali vs. silica (TAS) diagram for 60 Koloa Volcanics samples..…….....35

7. Normative nepheline vs. alkalinity index for 60 Koloa Volcanics samples……...36

8. P_2O_5 variation diagrams for SiO_2, MgO, TiO_2, CaO/Al_2O_3……..37

9. MgO variation diagrams for CaO/Al_2O_3 and modal olivine……37

10. CaO/Al_2O_3 vs. modal clinopyroxene……38

11. Incompatible element plots of Ce, Zr, and Sr vs. Nb, and La, Zr, Ba vs. Ce……...39

12. Modal abundances of olivine, plagioclase and clinopyroxene phenocrysts in Koloa lavas vs. Ni, Sr and Cr concentrations…….. 40

13. Distribution and thickness of Koloa Volcanics in Lihue Basin region…….....53

14. Distribution and thickness of Koloa Volcanics in Koloa region……..54

15. Distribution and thickness of Koloa Volcanics in Hanapepe region…….....55

16. Distribution and thickness of Koloa Volcanics in North Coast region……..56

17. Cross-sections of Kaua‘i showing Koloa Volcanics……..57

18. Surficial distribution of Koloa rock types……...75

19. Normative nepheline vs. age for 45 dated Koloa lavas..……76

20. Sr and Nd isotopes vs. rock type for Koloa lavas……...77

21. Age ranges for shield, postshield, and rejuvenated stages for the main Hawaiian Islands versus distance from Kīlauea Volcano……78

22. Total alkali vs. silica diagram (TAS) for Hawaiian postshield rocks and older Koloa rocks……..79

23. Histogram of Koloa lava ages……...81

24. Variations in rejuvenated volcanism along the Hawaiian chain

a. Duration of rejuvenated volcanism vs. distance from Kīlauea Volcano……..82

b. Surface area of rejuvenated lavas vs. distance from Kīlauea Volcano……..82

1.0 Abstract

The Koloa Volcanics on the island of Kauaʻi represent the most voluminous example of the rejuvenated-stage in Hawai`i. They provide an excellent opportunity to evaluate the cause of rejuvenated-stage eruptions through the study of their volume and petrologic characteristics. We have conducted an extensive field study of the Koloa Volcanics, collecting 164 samples and measuring sections from most regions of the island where Koloa rocks are exposed. New field and geochronological work on Koloa lavas show they range in age from 2.6 to 0.15 Ma. These weakly to strongly olivine-phyric lavas are picrobasalts, alkalic basalts, basanites, foidites, and melilite foidites. There is no temporal correlation in rock types (e.g., alkalic basalts and basanites were erupted during the entire duration of Koloa volcanism). Most olivine compositions are forsterite 83-86, which is too low to be in equilibrium with the whole rock compositions (Mg#), indicating that the rocks have variable amounts of olivine accumulation and/or resorption of ultramafic xenoliths. Olivine compositions indicate Koloa parental magmas had Mg#s of 62.5-67.5. Major-oxide and trace element variation diagrams show trends indicating low but variable degrees of partial melting from a somewhat heterogeneous source. Data from 41 measured sections, 80 water well logs, and previous geologic studies of Kauaʻi were synthesized using ARC/GIS to create four subsurface images of the Koloa Volcanics for volume calculations. A conservative estimate for the subaerial volume of Koloa Volcanics is ~58 km^3. This is the first quantitative volume estimate for Hawaiian rejuvenation volcanism. When

compared with new volume estimates for Kaua‘i (~57,000 km^3), the Koloa Volcanics represent ~0.1% of the total volume of the island, consistent with a previous guesstimate (<<1%).

Current models for rejuvenated stage volcanism provide predictable consequences for the volumes and duration of volcanism. The flexure-induced decompressional melting and convective mantle plume upwelling models predict a hiatus of 0.85-2 m.y. between shield and rejuvenated volcanism, and an eruptive duration for rejuvenation volcanism close to those observed for Kaua‘i (1.75-3 m.y. vs. 2.45 m.y.). Both of these models suggest a plume-derived source for rejuvenated lavas, consistent with recent seismic evidence for a thinned lithosphere and Nd, Sr, Pb, Lu, Hf, isotopic data that advocates a plume source. A third model, lithospheric melting by conductive heating, proposes a lithospheric source, a much larger volume of magma produced over a longer period than observed, and little or no volcanic hiatus. These predictions are inconsistent with new observations. The trends of eruptive duration and surface areas of rejuvenated lava flows on Hawaiian Islands south of Kaua`i are suggestive that the islands of Oahu, Molokai, and Maui may experience additional rejuvenated-stage eruptions.

2.0 Introduction

Many oceanic islands experience rejuvenation in eruptive activity after a main shield-building stage of volcanism (e.g., Hawaii, Canaries, Samoa, Marquesas). This second pulse of volcanism usually occurs after a ~1 m.y. hiatus (Gramlich et al., 1971; Schminke, 1973; Lamphere & Dalrymple, 1980; Natland, 1980; Woodhead, 1992). The Koloa Volcanics on the island of Kaua`i are the most voluminous example of rejuvenated-stage eruptions in Hawai`i (Macdonald et al., 1983). Studying the volume, age, and petrologic characteristics of these lavas provide an excellent opportunity to evaluate the cause(s) of rejuvenated-stage eruptions.

Three models are commonly cited as the cause of rejuvenated-stage volcanism: (1) Lithospheric melting by conductive heating (CH; Gurriet, 1987; Li et al., 2004; Fig. 1), (2) Secondary zone of mantle plume melting (SP; Ribe & Christensen, 1999; Fig. 1), and (3) Flexure-induced decompressional melting (FM; Jackson & Wright, 1970; Clague & Dalrymple, 1987; Bianco et al., 2005; Fig. 2). These models were designed to generate alkalic magmas and average magma flux rates that were thought to be appropriate. The flux rate is variable for the SP and FM models, which should result in temporal variations in lava composition. Each model predicts the duration of rejuvenated volcanism. When duration is combined with the magma flux rate, a volume for rejuvenated volcanism is produced. For example, the CH model suggests a long duration and high flux rate resulting in a large volume of lava. Conversely, the SP and FM models were designed to produce smaller volumes of rejuvenated lavas.

Another important characteristic of rejuvenation volcanism is the length of the hiatus from shield to rejuvenation eruptions. Modeling of the eruptive hiatus varies from little to no gap to 1 – 2 m.y. Hence, constraining these characteristics will help identify which, if any, of the current models explains the observed features of Hawaiian rejuvenated-stage volcanism.

The objective of this study of Kaua`i rejuvenated lavas was to test the proposed models for the causes for rejuvenated-stage lavas by collecting new petrologic and volume data and, via a companion study with Hiroki Sano of Kyoto University to obtain new K-Ar ages. New petrograhic analyses of 164 Koloa rocks show that they are alkali basalts, and foidites based on the classification scheme of Le Maitre (2002). A subset of 60 samples were classified using XRF analyses yielding picrobasalts, alkalic basalts, basanites, foidites, and melilite foidites (Le Bas, 1986). Contrary to previous suggestions (e.g., Reiners et al., 1999), there is no correlation of rock types with age (i.e., extent of partial melting). For example, alkalic basalts were erupted throughout the period of Koloa Volcanics (Clague & Dalrymple, 1988; Sano, 2006) and with basanites represent ~60% of surface rejuvenated lavas. Thus, there is no apparent systematic variation in the extent of partial melting, especially towards low degrees, during the ~2.5 m.y. of Koloa volcanism as previously suggested.

New whole-rock major and trace element analyses were made on the 60 freshest Koloa and late shield lavas collected during 49 days of field work. These data are consistent with previous petrographic observations reported for Koloa lavas (e.g., Macdonald et al., 1960; Feigenson, 1984; Clague & Dalrymple,

1988; Maaloe et al., 1992). Whole rock analyses show a positive correlation of TiO_2, Fe_2O_3, CaO/Al_2O_3, and to a lesser degree MgO with P_2O_5. SiO_2 has an inverse correlation with P_2O_5, which is thought to reflect varying degrees of partial melting (Maaloe et al., 1992). Ce, Zr, and Sr abundances are correlated with Nb, and La, Zr, and Ba abundances are correlated with Ce concentrations. Secondary alteration has led to the formation of clay, calcite, zeolite and iddingsite, which has modified the abundance of elements susceptible to low temperature modification (e.g., Ba, K, and Sr). However, the loss-on-ignition values for the fresher samples that were selected for chemical analyses are mostly low (<2 wt.%), especially compared to some previous studies (4-10 wt.%; Reiners and Nelson, 1998).

Here we present the first quantitative volume estimates for rejuvenated volcanism in Hawai`i. Using published and unpublished water well logs, field observations, and data from geologic maps, a conservative subaerial volume estimate of 58 km^3 (vesiculation corrected) was calculated for the Koloa Volcanics. Previous estimates include <1% of island volume (Clague and Dalrymple, 1987) to magma flux rates of 13 km^3/m.y. (Walker, 1990).

The predictions of the SP and FM models for the length of volcanic hiatus, duration, and source of volcanism agree with the observations of the Koloa Volcanics. Nonetheless, the melt volume flux predictions of the SP and FM models were less than (10-13 km^3/m.y. vs. 24 km^3/m.y.) the observed melt volume flux of Koloa lavas. However, at the time the SP and FM models were created, robust volume estimates of rejuvenated-stage volcanism did not exist.

Hence, the SP and FM models are the most probable scenarios for the generation of Hawaiian rejuvenated-stage volcanism.

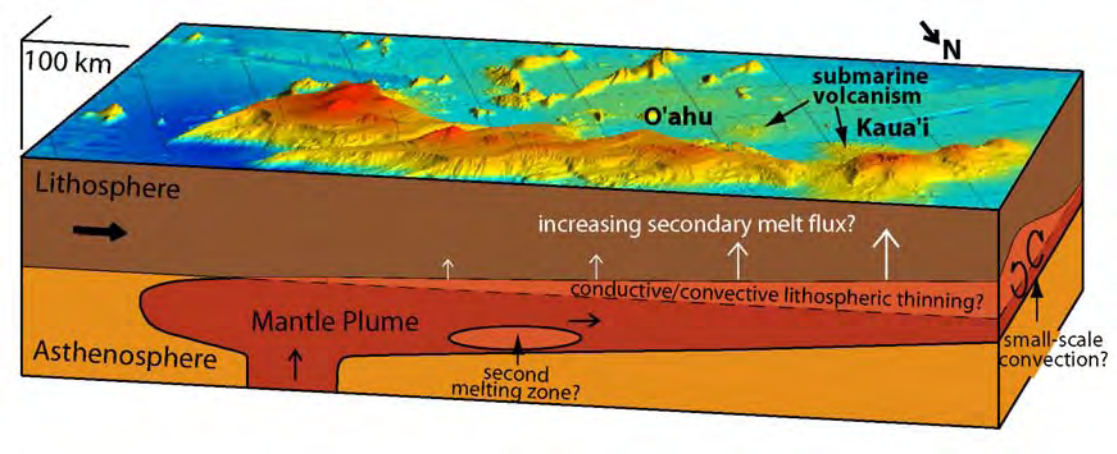

Figure 1. Block diagram illustrating the lithospheric melting by conductive heating (CH) and secondary zone of mantle plume melting (SP) models. The lithospheric thinning is in response to thermal and physical erosion. Physical erosion is thought to occur via roll-like instabilities creating convection within the upper mantle (Ribe, 2004; figure by B. Taylor, 2004, pers. comm.).

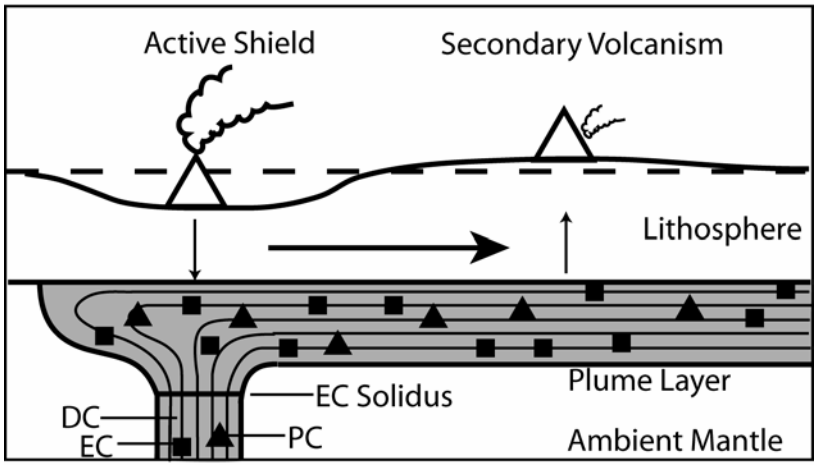

Figure 2. A schematic cross-section of the flexure-induced decompressional melting model (FM). Growth of the active shield pushes downward (downward pointing arrow) on the lithosphere beneath the shield and causes flexural uplift (upward pointing arrow) and secondary volcanism away from the shield. The curved line is an exaggerated example of how the lithosphere will flex compared to the unloaded lithosphere (dashed). The horizontal arrow shows the direction of plate motion which shears the buoyantly spreading plume layer beneath the lithosphere (Bianco et al., 2005).

3.0 Geology of Kaua`i

Kaua`i is located near the northwestern end of the Hawaiian Islands (Fig. 3), and is the second oldest of the eight principal islands (Macdonald et al., 1983). The island is commonly thought of as a single shield volcano (Macdonald et al., 1960; Macdonald et al., 1983), although geochemical and structural features prompted a suggestion that it consists of two shields (Holcomb et al., 1997). Kaua`i's subaerial shield and post-shield lavas are known as the Waimea Canyon basalts, which have been split into four members based on structural and stratigraphic relations (Macdonald et al.,1960). The oldest member is the Napali. However, the age relations of the other younger members (Haupu, Olokele, and Makaweli) are less certain and may overlap (Macdonald et al., 1960; Clague and Dalrymple, 1988).

Towards the end of the shield volcanism, a roughly 16 km diameter caldera collapsed and was subsequently filled with Olokele member lavas. This caldera may have formed at or near the same time as a smaller edifice, the Haupu member, formed on the southeastern flank of the island (Macdonald et al., 1960). Lava is thought to have breached the rim of the main caldera and flowed into a graben on the southwest of the island forming the Makaweli member. The Olokele and Makaweli lavas are capped locally by hawaiite or mugearite, indicating a change to post-shield volcanism near 4 Ma (Clague and Dalrymple, 1988).

After an eruptive hiatus, rejuvenation volcanism occurred on the eastern two thirds of the island forming the Koloa Volcanics (Hinds, 1930; Stearns, 1946;

Macdonald et al., 1960; Clague and Dalrymple, 1988). Koloa lavas erupted from roughly 40 vents aligned along possible rift zones trending north-south, and N60^{o}E (Macdonald et al., 1960; Palmiter, 1975). The presence of some vents has been inferred from the location of bosses of alkali gabbro, tuff, cinder, and spatter cones, and lava domes (Macdonald et al., 1960). These vents are widespread on Kaua`i, although most are located on the southern flank of the island (Fig. 3). The southern Koloa exposures are much fresher in appearance than those in the north (Macdonald et al., 1960). This may be a result of the trade winds distributing more rain on the northern part of the island (Hinds, 1930).

Koloa lavas partially filled many deeply dissected valleys and flooded the coastal plains of Kaua`i. The ancestral Hanapepe, Wailua, Waimea and Hanalei valleys contained hundreds of meters of Koloa lava flows and have since been eroded to a depth close to the original extent of erosion prior to Koloa volcanism (Macdonald et al., 1960). The deeply incised valleys of Hanapepe, Koula, Wailua, Waimea and Hanalei vary in length from ~6.5 to ~10.5 km (Fig. 3). The upper reaches of Hanalei Valley contain the thickest exposures of Koloa lavas, the thickest is in the east wall of the valley at ~650 m and exposures ≥300 m are prevalent (Macdonald et al., 1960).

The contact between the shield and post-shield lavas of the Waimea Canyon basalts, and the rejuvenated lavas of the Koloa Volcanics is marked by 10-30 m thick sequences of soil, sand, conglomerates and volcanic breccias (Macdonald et al., 1960; Reiners et al., 1999). Additionally, significant zones of

weathering and deposition have been identified within the Koloa lavas indicating considerable time gaps and episodic volcanism (Hinds, 1930; Reiners et al., 1999). At the base and interbedded within the Koloa lavas is the Palikea Breccia member (Macdonald et al., 1960; Reiners et al., 1999). The Palikea member is a mixture of debris from both the Waimea Canyon basalts and the Koloa Volcanics. The thickest exposure is at the type locality Palikea Ridge (~200 m), 5 km southeast of the island's summit, Mt. Kawakini (Reiners et al., 1999).

Subaerial shield volcanism has been dated by K-Ar methods at 5.1 – 4.3 Ma (McDougall, 1979). Olokele and Makaweli member lavas, which represent a transition from shield to the post-shield stage of volcanism, have reported K-Ar ages ranging from 4.16 – 3.91 Ma (McDougall, 1964; Clague and Dalrymple, 1988). Koloa lavas have been K-Ar dated at 0.52 to 3.65 Ma (Clague and Dalrymple, 1988), suggesting a brief period of quiescence between the shield and rejuvenated volcanism (<0.3 m.y.; Clague and Dalrymple, 1988). However, the majority (80%) of Koloa ages fall between 2.01 and 0.97 Ma, with only two ages older than 2.01 Ma (Clague and Dalrymple, 1988). The oldest dated sample (3.65 Ma) was collected in Waimea Canyon from a lava flow which caps an older breccia along the Kukui trail (D. Clague, 2005, pers. comm.). Other workers (Tagami et al., 2003; Sano, 2006) have suggested that the oldest dated Koloa sample is from the post-shield stage. This would increase the time gap between shield (or post-shield) and rejuvenation eruptions to ~1 m.y. Two new young ages (0.375 Ma, Ar-Ar date, Hearty et al., 2005; and 0.15 Ma, K-Ar date, Sano, 2006) have extended Koloa volcanism to relatively recently.

Previous Work on Koloa Volcanics

The earliest geologic inquiry of Kaua`i was by J.D. Dana (1849) during the 1840-1841 Wilkes Exploration Expedition. Dana observed the young looking cones in the Koloa area (south coast) on Kaua`i and those in southeast O`ahu, and theorized that they were a result of younger volcanism. Hitchcock (1909) also commented on the presence of "two classes of volcanic discharge" on Kaua`i. The first being the shield lavas, and the second in the Koloa area, described as an "inferior degree of activity". Powers (1915) was also aware of rejuvenated eruptive products and was first to identify their "rift" structures based on the location of cones. Hinds (1930) described what he called "parasitic", rejuvenated cones in the Koloa region and postulated that the cones were from a later stage of volcanism and that they had erupted at different times (not coeval). Stearns (1946) was first to present a reconnaissance geologic map of Kaua`i showing Koloa lavas. A detailed geologic map of Kaua`i showing the Koloa volcanics was published by Macdonald et al. (1960).

The first petrographic inspection of Koloa rocks was by Cross (1915) on four samples. More comprehensive petrographic studies of Koloa lavas were made by Macdonald et al. (1960) and later by Palmiter (1975).

The geochemistry of the Koloa Volcanics has been given in several studies. The earliest geochemical study was four samples evaluated by Cross (1915) by wet chemical analysis. Other studies reporting geochemical analyses were Macdonald et al. (1960) on 11 samples, Macdonald and Katsura (1964) on 15 samples, and Macdonald (1968) on 13 samples. Major oxide data was

reported on 29 samples (Palmiter, 1975) and major and trace element data on 3 Koloa lava flows by Kay and Gast (1973).

Feigenson (1984) provided Sr and Nd isotopic ratios for three Koloa lava flows in the first attempt to model its source. Maaloe (1992) and Reiners et al. (1998) provided major-oxide, trace element data, Nd and Sr isotopic data for Koloa lavas in a more recent effort to address the sources for rejuvenated-stage lavas on Kaua'i. Reiners et al. (1999) attempted to constrain the structural and petrologic evolution of the Lihue Basin by evaluating major and trace element, and Sr and Nd isotopic data for lavas in five Lihue basin drill holes. Os, Nd, and Sr isotopes were used in the latest attempt to model the source of Koloa eruptions (Lassiter et al., 2000).

Evernden et al. (1964) and McDougall (1964) were the first to provide radiometric ages for Koloa Volcanics. Clague and Dalrymple (1988) provided a more comprehensive set of K-Ar isotopic data in an attempt to constrain Koloa eruptive chronology and source.

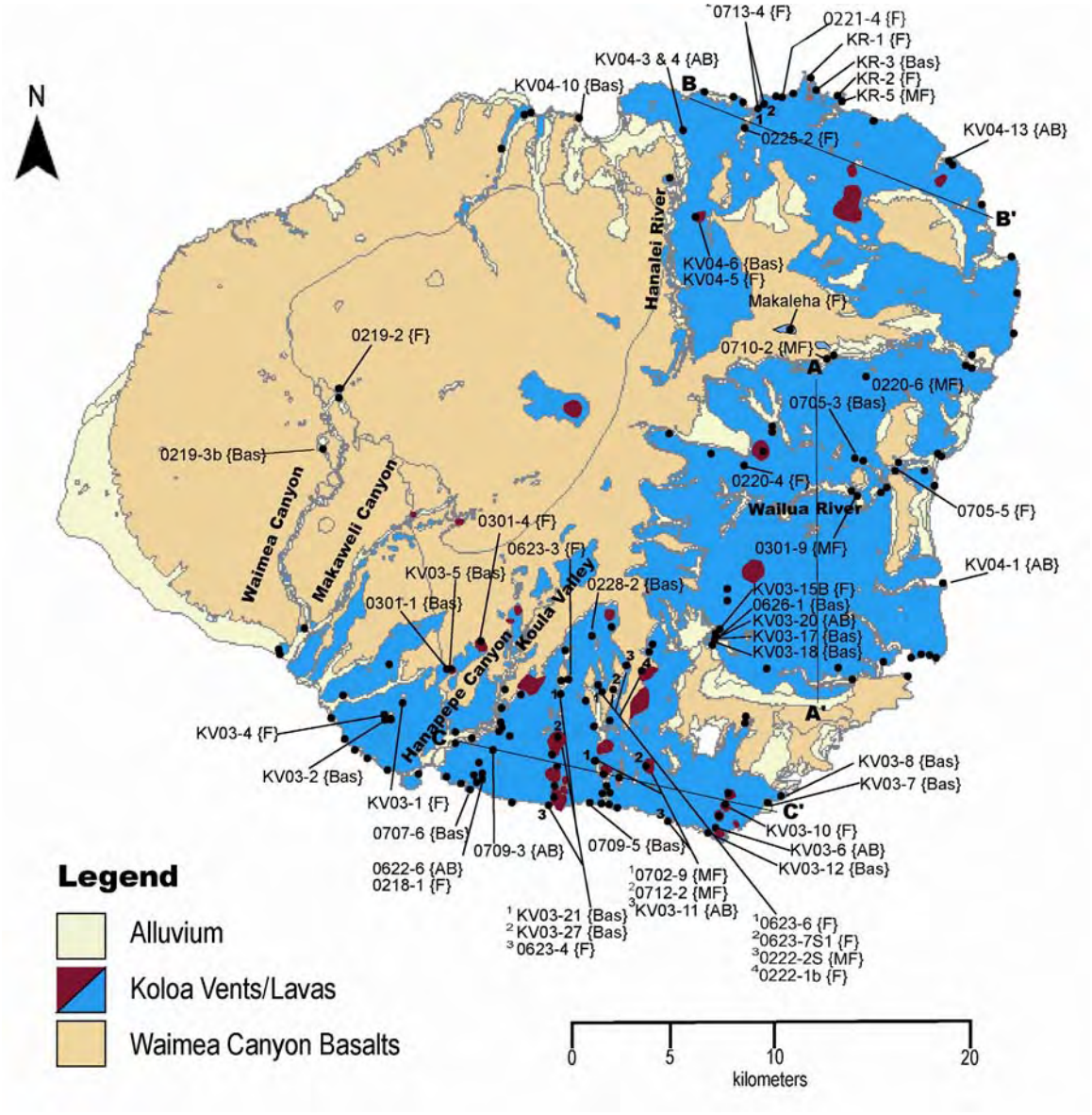

Figure 3. Geologic map of Kaua`i with sample names and locations. Data from Macdonald et al. (1960) and Sherrod et al. (2005).

4.0 Sampling and Analytical Methods

4.1 Petrography and Geochemistry

During seven weeks of field work between February, 2004 and February, 2005, 129 samples were collected from most parts of Kaua`i where Koloa lavas are exposed. Thirty-four additional Koloa samples were donated from other studies (M. Garcia, 2005, pers. comm.; KV03 and KV04 series) and one from the personal collection of Glen Bauer (Makaleha). Some Koloa exposures mapped by Macdonald et al. (1960) at the head of canyons, the summit region, or on private property were not sampled.

Koloa rocks share many physical properties such as mineralogy, color, crystallinity and texture. Therefore to discriminate rock types, thin section petrography was used to classify the 164 Koloa samples. The volcanic quartz-alkali feldspar-foid mineral classification method (QAPF; Le Maitre, 2002) was employed here. However, only two categories of the classification apply to Koloa rocks because they lack quartz and potassic feldspar (Cross, 1915; Macdonald et al., 1960; Palmiter, 1975; Maaloe et al., 1992; this study). These two categories are: basalts and foidites, based on the presence of foidic minerals such as nepheline and/or melilite (Appendix A).

Although considerable effort was made to collect the freshest possible samples at each outcrop, most samples were deemed too altered to be used for X-ray fluorescence (XRF) analyses. Sixty Koloa samples were chosen for modal and XRF analysis (Table 1; Fig. 3). These samples were unaltered or contained only minor amounts of iddingsite on olivine phenocrysts, and/or calcite, and

zeolites in vesicles. These 60 samples span the range of Koloa rock types, and were collected from the northern, eastern and southern regions of the island where Koloa rocks are common. Thus, the sample suite provides good spatial coverage. In addition, the ages of rocks chosen for XRF analyses span the duration (2.45 m.y.) of Koloa volcanism on Kaua`i (Clague & Dalrymple, 1988; Hearty et al., 2005; Sano, 2006). Modal analyses consisted of 100 point counts using an automated point counter. The error with these point counts is ±3 vol.% for values of 10% volume (Folk, 1974).

For XRF analysis, rocks were broken into small (1-8 mm) fragments with a WC-tipped rock press. Fragments with signs of alteration were removed before powdering the sample. Rock chips were cleaned in a beaker with ionized water and dried in an oven at 70° C for 24 hours to drive off excess water. Fragments were powdered in a tungsten carbide mill using a Rocklabs shatterbox for 1 – 3 minutes.

All XRF analyses were performed at the University of Massachusetts XRF laboratory where whole-rock major and selected trace element abundances (Nb, Zr, Y, Sr, Rb, Th, Pb, Ga, Zn, Ni, Cr, V, Ce, Ba, and La,) were measured. The major and trace element analytical procedures are discussed by Rhodes and Vollinger (2004). One sigma accuracy and precision estimates for the XRF data are ≤0.5% for majors and 0.5 – 2.0% for trace elements (Rhodes, 1996).

Loss-on-ignition (LOI) analysis represents a measurement of alteration from volatile loss. Five grams of a powdered sample were heated in a muffle

furnace at 1020°C for 10 minutes to limit the amount of ferrous iron formation (Rhodes and Vollinger, 2004). The weight loss is LOI.

Olivine compositions were measured at the University of Hawai`i using a five-spectrometer, Cameca SX-50 electron microprobe. Natural mineral standards (San Carlos olivine for Si and Mg; magnetite for Fe; augite for Ca; and NiO for Ni) were used for calibration, and a PAP-ZAF matrix correction was applied to all analyses. The beam conditions used for the analyses were a 15 kV accelerating voltage and a focused, 20 nA beam. Peak counting times for Si, Mg, Fe, Ca, and Ni were 40 seconds. Background counting times were half of peak counting times. Reported analyses are the average of three spot analyses for core and a single analysis for rims. Relative analytical error, based on counting statistics, is <1% for Si, Mg, and Fe; <5% for Ca and Ni.

4.2 Volume Calculations

Volume estimates for Koloa lavas were made using published (Reiners et al., 1999; Izuka, 2005) and unpublished well logs (USGS Honolulu office), measured sections, and topographic maps. Previous field observations (Stearns 1946; Macdonald et al., 1960) provide a minimum depth of Koloa Volcanics at coastal locations and remote areas such as the upper reaches of Olokele Canyon, Waimea Canyon, and Hanalei Valley. The volume of Koloa lava flows in Hanalei Valley, Makaweli Canyon, Olokele Canyon, Hanapepe Canyon, Lumahai Valley, Wainiha Valley and Waimea Canyon was inferred from isolated residual masses of Koloa lavas preserved on valley walls (Fig. 4). The

topographic relief of Koloa lavas is considered to be a minimum flow thickness within these valleys and canyons. In some cases residual masses of Koloa lavas are found on both sides of the canyon. This implies the width of the canyon/valley confining these previous Koloa lava flows may not have changed substantially since their eruption. The presence of these isolated masses at or near stream level led Macdonald et al. (1960) to conclude many of the larger canyons on Kaua`i have been eroded to approximately the same depth prior to being filled with Koloa lavas. Hence, we have calculated the volume of these canyon/valley confined flows from thickness of the residual masses (derived from field observations or topographic maps) and the width of the confining structure (canyon or valley). Volume calculations were aided by measuring 41 sections at coastal exposures, valley walls, roadcuts, and waterfalls that cut through Koloa rocks.

Water well log data for 386 wells drilled throughout Kaua`i was examined. Only 80 of the wells provided useful information for estimating Koloa thickness (Appendix B). Six of these wells in Lihue Basin were analyzed by Reiners et al. (1999). Two new wells in the Lihue Basin were drilled by the state of Hawai`i for ground water exploration and evaluated by the U.S. Geological Survey (S. Izuka, 2005, pers. comm.). Three wells near the southern coast of Kaua`i were analyzed by Macdonald et al. (1960). The other well log information was recorded by various drillers using different terminology, many lacking specific geologic terms. Because the quality of the well logs is variable, the following criteria were used to interpret Waimea Canyon shield basalts (WCB), from Koloa

lavas. Shield lavas (WCB) are considered to be more continuous and lack sedimentary horizons that are common in Koloa flows (S. Izuka, 2004, pers. comm.). Higher vesicularity and large (4 – 5 mm) olivine phenocrysts are common amongst shield-stage lavas (Macdonald et al., 1960). Koloa lavas commonly display thick sedimentary packages (up to 30 m thick) of weathered, clay-rich, sandy and/or coralline deposits. Although none of these criteria were found to be applicable to all well logs from the shield-stage or rejuvenated-stage, the majority (~90%) of well logs analyzed suggest these observations are valid for determining the depth of Koloa lavas within a well (Appendix B).

ArcMap (GIS) was used to synthesize the thickness data into a volume estimate for the Koloa Volcanics. Volume calculations were produced by combining the depth of Koloa lavas with a GIS-based geologic map of Hawai`i (Sherrod et al., 2005). The island of Kaua`i was divided into four regions for the purposes of volume calculations. A layer for each region shows the location and maximum depth of Koloa lavas in all wells. By projecting the contact between the Waimea Canyon basalts and the Koloa Volcanics from one well to another using water well data, field observations, and topographic maps, intervening depths are estimated. The actual (from the well log) and estimated depths of Koloa lavas in some locations were projected deeper where adjacent wells indicate greater depth. The Koloa Volcanics can then be evaluated using the “3D analyst” function, which converts the features to “triangulated irregular network”, or TIN. A TIN is defined as a representation of a surface derived from irregularly spaced sample points and features (ESRI, 2004). The TIN data set includes

topological relationships between points (X,Y,Z) and their proximal triangles. Data points are connected by edges to form a set of non-overlapping triangles that can be used to represent a surface (Enviromental Systems Research Institute, 2004). By creating a TIN of the well depths, a relief map for the Koloa contact depth was produced for each area. In order to calculate the volume of this map, the ArcMap surface analysis function was used. Volume estimates were derived by calculating below a plane of zero elevation. This procedure eliminates the need for considering the elevation of the well, which involves a more time consuming process of subtracting the elevation of the well from the depth of the Koloa lavas within the well at many locations. This method does not account for topography related to cones or vents which are mostly minor (total volume of all cones is ~0.1 km^3). The total volume calculation is a conservative estimate for the volume of Koloa Volcanics. The term “conservative” is used because our volume measurements are not a minimum. In areas where Koloa depth information is lacking, thicknesses of Koloa lavas have been projected according to nearby data. Therefore, we have attempted to interpret the depths using geologic principles, or extrapolate thicknesses which make sense geologically. As a result, volume projections (Figs. 13, 14, 15, & 16) are not bare minimums and do not represent the pre-rejuvenated surface of Kaua`i, but rather the depth of Koloa lavas at any point from zero elevation. The volume calculations have ~±10% error associated with well log interpretation, and potentially up to ±20% error for extrapolating Koloa thickness to areas lacking information. The combined error for our volume calculations is ±30%.

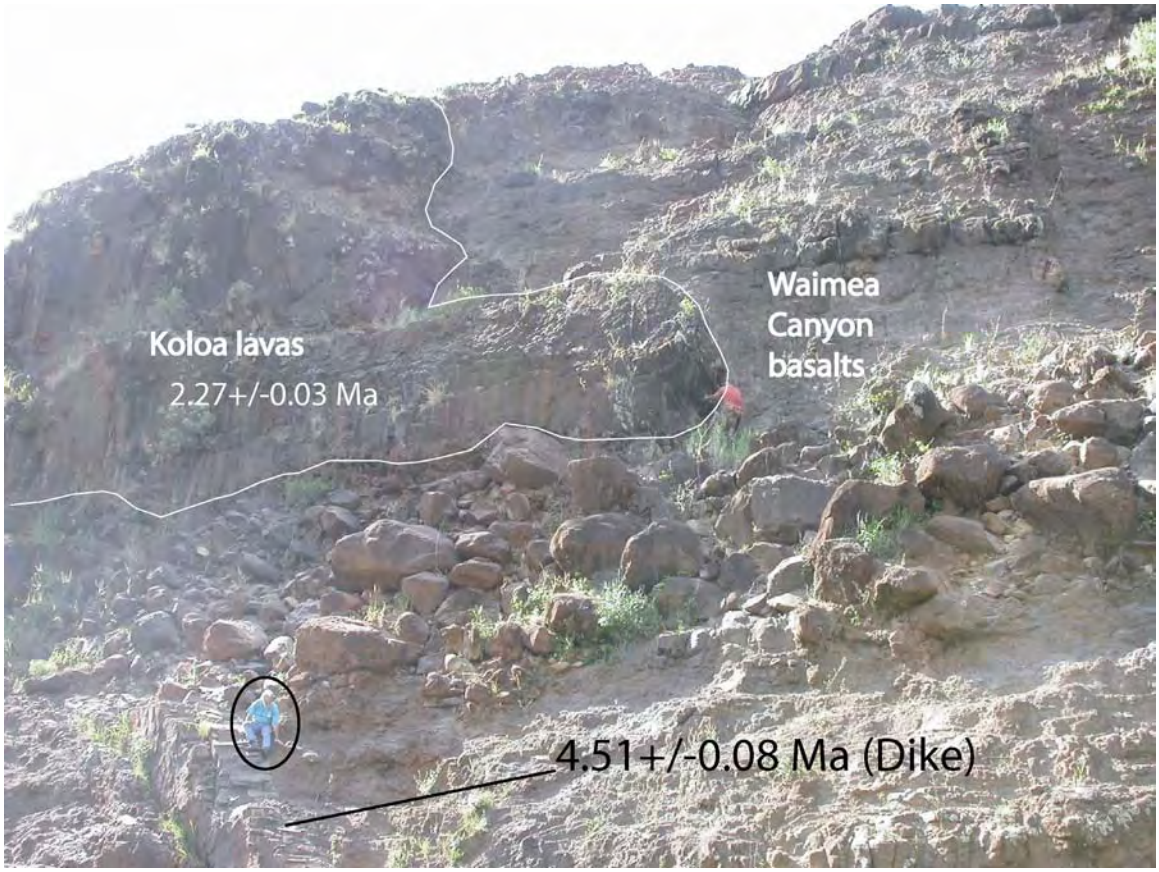

Figure 4. Residual mass of Koloa lavas in Koai`e Canyon. Notice Koloa lavas adhering to Waimea Canyon basalts on the western wall of Koai`e Valley, near Waimea Canyon. Notice person for scale (age data from Sano, 2006).

5.0 Results

5.1 Petrography

Textures

Rocks of the Koloa Volcanics are fine-grained with variable amounts of olivine (Appendix A), as noted in previous studies (Cross, 1915; Macdonald et al., 1960; Palmiter, 1975; Maaloe, 1992). The most common groundmass textures in these rocks are hyaloophitic and hypocrystalline. A smaller number of samples with plagioclase exhibit intersertal (<5%) or sub-ophitic (7%) textures. The majority of Koloa samples have ≤6% vesicles, although rare samples contain up to 50% vesicles. Where vesicles are present, secondary mineralization (calcite and/or zeolites, clay) is common.

The groundmass of Koloa lavas consists of variable amounts of glass, clinopyroxene, olivine, plagioclase, nepheline, opaques and phlogopite. Koloa lavas can be divided into two categories on the basis of the presence of plagioclase or nepheline in the groundmass (Le Maitre et al., 2002). These minerals do not occur together in any of the lavas collected. Rocks with plagioclase are classified here as alkalic basalts; those containing nepheline and/or melilite are foidites (Table 1).

Dunite, wehrlitic or lherzolitic xenoliths were found in ~5% of Koloa rocks. Dunites are the more common (Macdonald et al., 1960; Appendix A), and are generally more angular than lherzolitic and wehrlitic xenoliths. All xenoliths display an intergranular texture. Where xenolithic orthopyroxene is in contact with the silica-undersaturated host lava, granoblastic rims (1 -2 mm wide) of

augite are present. Lherzolitic xenoliths occur mostly in foidic rocks as noted in a previous study (White, 1966; Appendix A).

Koloa lavas may contain phenocrysts of olivine and clinopyroxene (augite or titanaugite), and microphenocrysts of olivine, clinopyroxene, plagioclase or melilite, and accessory minerals (chromite, magnetite, and/or ilmenite). Nepheline, apatite and biotite occur mainly in the groundmass. The two prevailing crystallization sequences for these minerals are: (1) spinel $\rightarrow$ olivine $\rightarrow$ clinopyroxene/plagioclase $\rightarrow$ nepheline/magnetite/ilmenite $\rightarrow$ phlogopite; and (2) spinel $\rightarrow$ olivine $\rightarrow$ melilite/clinopyroxene $\rightarrow$ nepheline/magnetite/ilmenite $\rightarrow$ phlogopite.

Minerals

Olivine is the most common mineral in Koloa lavas (Table 1), as noted in previous studies (Cross, 1915; Macdonald, et al., 1960; Palmiter, 1975; Maaloe, 1992). It occurs as phenocrysts (>0.5 mm), microphenocrysts (0.1-0.5 mm) and in the matrix. Many olivines are euhedral, although some crystals show disequilibrium features such as partial resorption and embayment, resulting in subhedral and anhedral shapes. Deformed olivine phenocrysts contain kinks and are present in <5% of Koloa rocks. The alteration of olivine to iddingsite is widespread in Koloa Volcanics, as noted by Maaloe (1992). Where present, iddingsite varies from thin rims (0.01-0.1 mm) to replacing entire phenocrysts (Appendix A).

The pyroxene in Koloa rocks is augite, although the varietal form titanaugite is also present (mostly as microphenocrysts). Only 16% of the 164 samples examined were found to have clinopyroxene phenocrysts, although most contain microphenocrystic or groundmass clinopyroxene (Appendix A). Clinopyroxene phenocrysts range from subhedral to euhedral and are ≤3 mm in diameter. Zoning in clinopyroxene phenocrysts and microphenocrysts is ubiquitous and commonly concentric. Some titanaugite crystals have hourglass twinning. Groundmass clinopyroxene is commonly prismatic and elongate (aspect ratios of 2 to 3).

Phenocrysts of plagioclase are rare in Koloa rocks. Only three samples contain plagioclase phenocrysts. However, microphenocrystic and groundmass plagioclase occur in many more samples (55% of 164 samples; almost all alkalic basalts contain plagioclase mph; Table 1). Most plagioclase is < 0.1 mm. Previous studies (Macdonald et al., 1960; Palmiter, 1975) suggest there is 10-25% plagioclase in the mode (phenocryst or microphenocryst were unspecified) of some Koloa lavas, which is consistent with observations from this study (Table 1). Plagioclase microphenocrysts and phenocrysts are euhedral. Plagioclase composition ranges from anorthite (An) 45 (andesine) to An 52 (sodic labradorite), based on the Michel-Levy method (Nesse, 1991). These values are slightly more sodic than previous petrographic observations of Koloa rocks (An 50 to An 75; Palmiter, 1975).

The foidic minerals in Koloa rocks are nepheline and melilite. They are present in 40% of the samples (Appendix A). Nepheline was found in 40% of the

rocks examined and commonly occurs interstitially as anhedral masses. It was only identified as microphenocrysts or phenocrysts in five samples (Appendix A). Melilite was observed in 10 samples (6%); seven of these samples also contain nepheline (Appendix A). Previous studies suggest melilite occurs in 20% of the rocks that contain nepheline, which is twice that found in this study (10%) (Macdonald et al., 1960). Although Macdonald et al. (1960) considered peg structure (a sign of alteration) to be rare in Koloa melilite foidites, it was found to be common in the new samples. Other criteria to identify melilite were first-order gray to yellow birefringence, parallel extinction and lack of twinning. It occurs as subhedral to euhedral crystals.

Other minerals in rocks of the Koloa Volcanics include euhedral to subhedral magnetite and chromite. Palmiter (1975) observed that these opaques occur in greater abundance in nepheline-bearing rocks than plagioclase-bearing rocks. However, no correlation was found in the new samples (Appendix A). Chromite occurs as inclusions in olivine and in the groundmass. An elongate, opaque mineral (ilmenite?) was observed in 8% of the samples. Apatite, which forms acicular inclusions in plagioclase, nepheline and phlogopite, and in the matrix was observed in 2% of samples. Phlogopite was found in ~2% of the samples.

Table 1. Modes for Koloa lavas with XRF analyses, based on 100 point counts/sample.

	Olivine		Clinopyroxene		Melilite		Neph		Plag		Magt	Phlog		Rock type	
Sample	Ph	Mph	Ph	Mph	Ph	Mph	Ph	Mph	Ph	Mph	Mph		Matrix	Modal	TAS
KV03-19	6	3	-	-	-	-	-	-	-	-	-	-	91	Basalt	PB
0622-6	3	4	9	7	-	-	-	-	-	17	-	-	60	Basalt	AB
0709-3	6	5	*	6	-	-	-	-	-	5	1	-	77	Basalt	AB
KV03-6	3	1	-	8	-	-	-	-	-	*	-	-	88	Basalt	AB
KV03-20	1	15	-	8	-	-	-	-	-	1	-	-	75	Basalt	AB
KV03-11	3	3	-	3	-	-	-	-	-	2	-	-	89	Basalt	AB
KV04-1	10	13	-	5	-	-	-	-	1	13	-	-	58	Basalt	AB
KV04-3	8	13	-	2	-	-	-	-	-	-	3	-	74	Basalt	AB
KV04-13	*	10	-	-	-	-	-	2	-	-	-	-	88	Basalt	AB
0219-3b	8	9	-	-	-	-	-	-	-	*	3	-	80	Basalt	Bas
0220-3	-	-	-	-	-	-	-	-	-	-	-	2	98	Basalt	Bas
0228-2	-	4	-	-	-	-	-	-	-	4	-	-	92	Basalt	Bas
0301-1	7	7	-	-	-	-	-	-	-	*	1	-	85	Basalt	Bas
0626-1	2	12	-	2	-	-	-	-	-	1	2	-	81	Basalt	Bas
0705-3	3	7	-	-	-	-	-	-	-	*	-	-	90	Basalt	Bas
0707-6	1	16	-	3	-	-	-	-	-	14	4	-	62	Basalt	Bas
0709-5	6	8	-	13	-	-	-	-	-	*	-	-	73	Basalt	Bas
KV03-2	6	2	-	11	-	-	-	-	-	*	1	-	80	Basalt	Bas
KV03-5	8	1	1	*	-	-	-	-	-	4	2	-	83	Basalt	Bas
KV03-7	-	9	-	-	-	-	-	-	-	1	1	-	89	Basalt	Bas
KV03-8	-	9	-	4	-	-	-	-	4	8	1	-	74	Basalt	Bas
KV03-12	1	4	1	5	-	-	-	-	-	*	1	-	88	Basalt	Bas
KV03-17	1	6	-	3	-	-	-	-	-	*	-	-	90	Basalt	Bas
KV03-18	7	16	-	-	-	-	-	-	-	*	-	-	77	Basalt	Bas
KV03-21	5	5	-	10	-	-	-	-	-	1	-	-	79	Basalt	Bas
KV03-27	-	9	-	*	-	-	-	-	-	*	-	-	91	Basalt	Bas
KV04-4	2	18	-	-	-	-	-	-	-	11	3	-	66	Basalt	Bas
KV04-6	7	11	-	-	-	-	-	-	-	*	-	-	82	Basalt	Bas
KV04-10	10	11	-	9	-	-	-	-	-	6	6	-	58	Basalt	Bas

Table 1. cont.

KR-3	-	1	-	-	-	-	-	-	-	-	-	-	99	Basalt	Bas
0218-1	5	2		2	-	-	-	*	-	-	-	-	91	Foidite	F
0219-2	9	9	-	*	-	-	-	-	-	-	-	-	82	Foidite	F
0220-4	7	7	-	*	-	-	-	*	-	-	-	-	86	Foidite	F
0221-4	14	8	-	*	-	-	-	*	-	-	-	-	78	Foidite	F
0222-1b	2	13	1	1	-	-	-	*	-	-	4	-	79	Foidite	F
0225-2	1	13	-	-	-	-	-	*	-	-	-	-	86	Foidite	F
0301-4	2	9	-	-	-	-	-	*	-	-	-	-	89	Foidite	F
0623-3	2	14	-	-	-	-	-	*	-	-	-	-	84	Foidite	F
0623-4	5	9	1	2	-	-	-	2	-	-	1	-	80	Foidite	F
0623-6	2	3	-	-	-	-	-	*	-	-	3	*	92	Foidite	F
0623-7S1	7	8	-	-	-	-	-	*	-	-	2	*	83	Foidite	F
0705-5	3	6	-	-	-	-	-	*	-	-	-	-	91	Foidite	F
0713-4	2	17	-	1	-	-	-	*	-	-	2	-	78	Foidite	F
KV03-1	6	3	-	3	-	-	1	3	-	-	-	-	82	Foidite	F
KV03-4	10	2	-	-	-	-	-	2	-	-	1	-	85	Foidite	F
KV03-10	-	8	-	-	-	-	*	3	-	-	-	-	89	Foidite	F
KV03-15B	6	11	-	-	-	-	-	*	-	-	-	-	83	Foidite	F
KV04-5	2	12	-	-	-	-	-	2	-	-	-	-	84	Foidite	F
KV04-8	2	10	-	3	-	-	-	*	-	-	-	-	85	Foidite	F
KV04-9	1	6	-	3	-	-	-	*	-	-	-	-	90	Foidite	F
KR-1	2	8	-	-	-	-	-	1	-	-	-	-	89	Foidite	F
KR-2	4	9	-	-	-	-	-	-	-	-	-	-	87	Foidite	F
Makaleha	2	5	-	-	-	-	-	-	-	-	-	-	93	Foidite	F
0220-6	3	12	-	-	-	*	-	-	-	-	-	*	85	Foidite	MF
0222-2s	6	9	-	-	-	*	-	3	-	-	4	-	78	Foidite	MF
0301-9	3	13	-	-	-	*	-	-	-	-	-	-	84	Foidite	MF
0702-9	14	6	-	1	-	5	-	*	-	-	2	-	73	Foidite	MF
0710-2	1	3	-	-	-	*	-	*	-	-	2	-	94	Foidite	MF
0712-2	8	6	2	23	1	12	-	5	-	-	5	-	38	Foidite	MF
KR-5	4	8	-	-	-	5	-	6	-	-	-	-	77	Foidite	MF

Table 1. cont.

PB - picro-basalt, AB - alkalic basalt, Bas - basanite, F - foidite, MF - melilite foidite, phlog - phologopite, magt - magnetite, neph - nepheline, plag - plagioclase, mel - melilite
Total alakali vs. silica (TAS) classification from Le Bas et al. (1986)
Modal classification from Quartz-Alkali-Plagioclase-Foidite diagram, Le Maitre et al. (2002)

5.2 Mineral Chemistry

New analyses of olivine phenocrysts and microphenocrysts (5 to 10 phenocrysts per sample) in nine Koloa lavas range in forsterite (Fo) composition from $Fo_{73.7}$ to $Fo_{86.5}$. However, most phenocrysts cores are Fo_{83} to Fo_{86} (Table 2), which is slightly lower than previously reported for Koloa lavas (Fo_{85} to $Fo_{88;}$ Maaloe et al., 1992). Most olivine are normally zoned or unzoned. Reverse zoning was observed on seven of the 55 crystals in four of the nine analyzed samples (only four grains shown in Table 3). The maximum extent of reverse zoning from core to rim is $Fo_{73.7}$ to $Fo_{83.3}$, although more typically the average range is smaller ($Fo_{80.5}$ to $Fo_{82.5}$). Reversely zoning was more common in the slightly lower forsterite crystals ($Fo_{80.5}$ to $Fo_{84.5}$). There does not appear to be a correlation between rock type, Fo%, or zonation of olivine phenocrysts (Table 2).

The Fo content of the olivine may vary considerably within individual rocks when compared to whole rock Mg #, which is defined as $100[Mg/(Mg+Fe^{2+}]$, assuming a Fe^{2+}/Fe^{3+} ratio of 0.85 (Fig. 5). Most phenocrysts plot in a tight cluster, however samples KV03-5, KV03-10, and KV03-18 have significant variation. This may be a result of magma mixing as evidenced by the reverse zoning of these samples. Some olivine in rocks with Mg #'s between 62.5 and 67.5 are in equilibrium with their Fo composition. Lavas with higher Mg #'s typically plot below the equilibrium field. These rocks have higher olivine abundances or are related to flows with peridotite xenoliths (Fig. 5; Appendix 1). Therefore, these higher Mg# rocks may have accumulated olivine. Thus, the compositions of olivines in Figure 5 (Fo_{84} to $Fo_{86.5}$) suggest that parental magmas

for these lavas had a Mg # between 62.5 and 67.5 (Fig. 5). Previous studies showed olivines in equilibrium with Mg #'s between 66.5 and 69 (Maaloe et al., 1992).

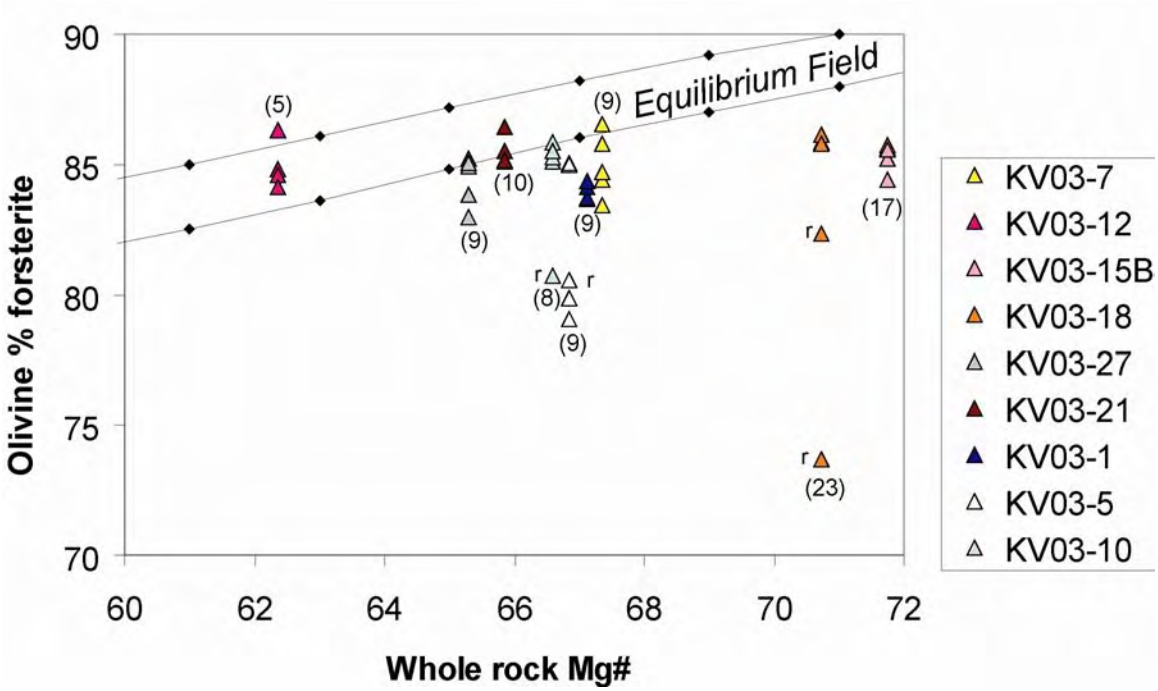

Figure 5. Olivine % forsterite vs. whole rock Mg# for olivine phenocrysts from Koloa lavas. Most olivine are normally zoned or unzoned, those with reverse zoning are indicated by (r). Some rocks phenocryst with Mg#'s between 62 and 67.5 have equilibrium olivine. Phenocrysts below the equilibrium field may have accumulated olivine (numbers in parenthesis indicate number of olivine phenocrysts in 100 point count per sample). There is no apparent correlation between % olivine in rock and location of olivine relative to equilibrium field.

Table 2. Representative olivine cores and rims from the Koloa Volcanics, Kaua`i.

Sample	Si	Fe	Ni	Mg	Ca	Total	Fo (%)	Fo avg.	Zoning	Rock Type
KV03-1.1c	39.32	15.25	0.31	44.23	0.17	99.28	83.62	83.3	**N**	F
KV03-1.1r	40.31	14.82	0.19	43.83	0.58	99.73	82.16			
KV03-1.6c	39.48	15.42	0.26	44.10	0.22	99.47	83.22	83.5	**R**	F
KV03-1.6r	39.28	15.03	0.21	44.43	0.36	99.30	83.92			
KV03-5.4c	38.88	18.59	0.24	41.60	0.21	99.53	79.68	79.0	**N**	Bas
KV03-5.4r	38.24	21.10	0.12	39.35	0.51	99.33	76.51			
KV03-5.9c	40.02	12.42	0.47	46.58	0.27	99.75	86.52	86.5	**N**	Bas
KV03-5.9r	40.13	13.32	0.32	46.01	0.35	100.14	85.43			
KV03-5.10c	38.50	19.27	0.18	41.25	0.23	99.42	79.40	79.8	**R**	Bas
KV03-5.10r	39.12	16.86	0.24	42.82	0.36	99.40	81.48			
KV03-7.1c	39.51	12.90	0.42	46.25	0.27	99.36	86.53	86.4	**N**	Bas
KV03-7.1r	39.62	13.36	0.21	45.78	0.34	99.31	85.76			
KV03-7.5c	39.60	14.15	0.30	45.20	0.39	99.63	84.75	83.0	**N**	Bas
KV03-7.5r	38.21	19.79	0.29	40.11	0.53	98.93	77.92			
KV03-10.1c	39.00	18.15	0.32	42.33	0.04	99.84	80.64	81.7	**R**	F
KV03-10.1r	39.94	14.16	0.35	45.36	0.28	100.09	84.59			
KV03-10.5c	39.99	13.52	0.36	45.87	0.23	99.97	85.39	85.2	**N**	F
KV03-10.5r	39.93	14.25	0.28	45.05	0.37	99.89	84.21			
KV03-12.5c	39.24	17.88	0.21	42.06	0.58	99.98	79.91	80.4	**R**	Bas
KV03-12.5r	39.55	17.17	0.27	42.94	0.50	100.43	80.90			
KV03-15B.1c	40.06	13.75	0.27	45.95	0.39	100.41	85.22	83.7	**N**	F

Table 2 (cont.)

KV03-15B.1r	39.03	19.06	0.15	41.54	0.53	100.30	79.07			
KV03-15B.2c	39.78	13.41	0.36	45.91	0.38	99.84	85.62	83.7	**N**	F
KV03-15B.2r	38.56	20.02	0.24	40.65	0.51	99.96	78.14			
KV03-18.1c	40.42	12.93	0.31	46.17	0.53	100.37	86.25	85.6	**N**	F
KV03-18.1r	40.37	13.40	0.37	45.82	0.30	100.25	84.92			
KV03-18.5c	37.77	23.65	0.21	37.89	0.14	99.65	74.33	78.8	**R**	F
KV03-18.5r	39.58	15.11	0.26	44.23	0.33	99.51	83.34			
KV03-21.8c	39.80	13.02	0.40	46.59	0.29	100.10	86.44	86.4	**N**	Bas
KV03-21.8r	38.12	20.94	0.17	39.78	0.62	99.63	77.20			
KV03-27.4c	39.92	14.00	0.38	45.59	0.27	100.15	84.93	84.4	**N**	Bas
KV03-27.4r	39.63	15.31	0.27	43.96	0.43	99.61	82.84			
KV03-27.5c	40.06	13.78	0.40	45.72	0.25	100.20	84.98	83.2	**N**	Bas
KV03-27.5r	38.92	19.77	0.14	40.46	0.54	99.82	77.63			

Zoning: N **-** normal zoning, R **-** reverse zoning, c - core, r - rim
Fo avg. = represents an average of four points within a single grain

5.3 Whole Rock Chemistry

Major Elements

The total alkali vs. silica (TAS) diagram (Fig. 6) was used for classification of Koloa rocks. Rocks were divided into four groups using this diagram: (1) Picrobasalts (PB), (2) Alkalic basalts (AB), (3) Basanites (Bas), and (4) Foidites (F). A fifth group was defined by the presence of melilite in the foidic rocks; melilite foidites (MF; Table 1). These groupings are comparable to other measures for evaluating alkalinity, normative nepheline vs. alkalinity index (Fig. 7). Rocks with an alkalinity index >0 are considered alkaline, rocks <0 are deemed tholeiitic (Rhodes & Vollinger, 2004). The greater the alkalinity index, the greater the deviation from the Macdonald-Katsura line, which is commonly used to indicate whether a rock is alkalic or tholeiitic (Macdonald & Katsura, 1964). An increase in alkalinity and normative nepheline (e.g., alkalic basalts to melilite foidites) is thought to be representative of rocks produced by lower degrees of melting (Clague & Frey, 1982). For example, rocks produced from higher degrees of melting (alkalic basalts) have lower normative nepheline and alkalinity index, whereas those produced from lower degrees of melting (foidites, melilite foidites) have higher normative nepheline and alkalinity index. There is some overlap of basanites and foidites (Fig. 7). However, these rocks still fall within the general trend of increasing alkalinity with increasing normative nepheline (Fig. 7). The foidites and melilite foidites display a tangential trend to the alkalic basalts and basanites. This may result from the nepheline normative axis only considering one component of alkalinity and not leucite and larnite.

Unlike previous classification schemes for Hawaiian rejuvenated lavas (e.g., Clague & Frey, 1982), the term nephelinite is not used.

Many of the new Koloa Volcanics samples are not fully crystallized (as evidenced by the differences in modal and normative mineralogy; Fig. 7). Therefore, deriving rock names on the basis of modal analysis may be ineffective for all Koloa rocks. CIPW norms (Appendix C) were calculated using an Excel spreadsheet created by Kurt Hollocher of Union College (http://www.union.edu/PUBLIC/GEODEPT/hollocher/kth/). A ratio of 0.15 for Fe_2O_3/total iron was chosen for normative calculations, which is considered probable for Hawaiian rejuvenated-stage rocks (Le Bas, 1989). Normative analyses shed light on complications that may arise when trying to classify rocks on the basis of modal appearance or absence of a mineral. Samples with modal nepheline all contain normative nepheline, although many nepheline normative Koloa rocks do not have nepheline in the mode. The absence of nepheline may be related to the the poorly crystallized nature and its late appearance in Koloa lavas. Holocrystalline samples are expected to more closely mimic the normative mineral phases (Appendix C). Koloa rocks with melilite in the mode generally yield higher abundances of normative nepheline and leucite, but none exceed 20% normative nepheline, the amount required for classification as a nephelinite (Le Maitre et al., 2002).

The 60 new Koloa samples (Table 3) show major-element trends (Fig. 8) comparable to those previously reported for Koloa Volcanics (Macdonald et al., 1960; Macdonald, 1968; Palmiter, 1975; Feigenson, 1984; Clague and

Dalrymple, 1988; Maaloe et al., 1992; Reiners et al., 1998. However, the new Koloa samples extend to slightly lower SiO_2, and higher CaO/Al_2O_3 than the 72 previous Koloa samples (Fig. 8). P_2O_5 is used here for displaying compositional variations because it is incompatible in Hawaiian rejuvenated lavas and is relatively unsusceptible to alteration (e.g., Clague and Frey, 1982).

The major element compositional variation for the new data is similar to previous data (e.g., SiO_2 vs. P_2O_5 show almost perfect overlap; Fig. 8). TiO_2 and CaO/Al_2O_3 are positively correlated with P_2O_5, and to a much less degree with MgO (Fig. 8). Conversely, SiO_2 is negatively correlated with P_2O_5 (Fig. 8).

The range of P_2O_5 (0.3 – 1.5 wt%) in the Honolulu Volcanics is larger than observed in the new Koloa samples (0.3 – 1.1 wt%; Clague & Frey, 1982). Thus, the Koloa lavas may reflect a somewhat smaller range in extent of partial melting or a distinct source. P_2O_5 has also been used to infer the relative extent of partial melting in Hawaiian rejuvenated lavas (Clague & Frey, 1982).

A poor correlation exists between modal olivine and MgO with large ranges in model olivine at a given MgO content (e.g., 4 -23 vol% olivine at 14 wt% MgO; Fig. 9). Thus, the high MgO of Koloa rocks is not necessarily related to olivine accumulation. Foidic rocks (F, MF) generally have higher CaO/Al_2O_3. A plot of CaO/Al_2O_3 vs. modal clinopyroxene does not show a correlation indicating that the higher abundances of CaO in foidic rocks are not related to the presence of clinproxene phenocrysts (Fig. 10). Instead, the high CaO/Al_2O_3 in foidic rocks is probably related to the incompatible behavior of CaO at low degrees of melting, as noted for the Honolulu Volcanics (Clague & Frey, 1982).

Trace Elements

The new XRF data display positive, well-defined linear trends for all but a few samples on most incompatible element plots (Fig. 11). These trends are similar to previous data. However, the new Koloa data extend to higher Nb than previous studies. Likewise, the new Koloa data have higher Ce than previous studies when plotted against La, Zr, and Ba (Fig. 11). Foidic rocks (F, MF) have the greatest abundance of incompatible elements. This observation is consistent with their derivation from low degrees of partial melting as shown the Honolulu Volcanics (Clague and Frey, 1982). Although plots of Ce, Zr, and Sr vs. Nb, and Ba, Zr, and La vs. Ce show a general correlation of elements (Fig. 11), plots of Sr vs. Nb and Ba vs. Ce show more variability (Fig. 11). This variability is probably attributable to an increase in Sr and Ba from secondary mineralization (calcite and zeolites, which contain high Sr and Ba).

Some Koloa lavas have olivine (>20 vol%), clinopyroxene (>15 vol%), and plagioclase (>17 vol%) phenocrysts in high abundance. However, there is no correlation of the abundance of these minerals in Koloa rocks with trace elements that are compatible in the minerals (Fig. 12). Basanites are scattered for the entire range of Ni, Sr, and Cr. Additionally, foidites have widely varied modal abundance of clinopyroxene with no apparent relation to the abundance of Cr. Thus, the Koloa rock compositions have not been strongly affected by the accumulation of these minerals.

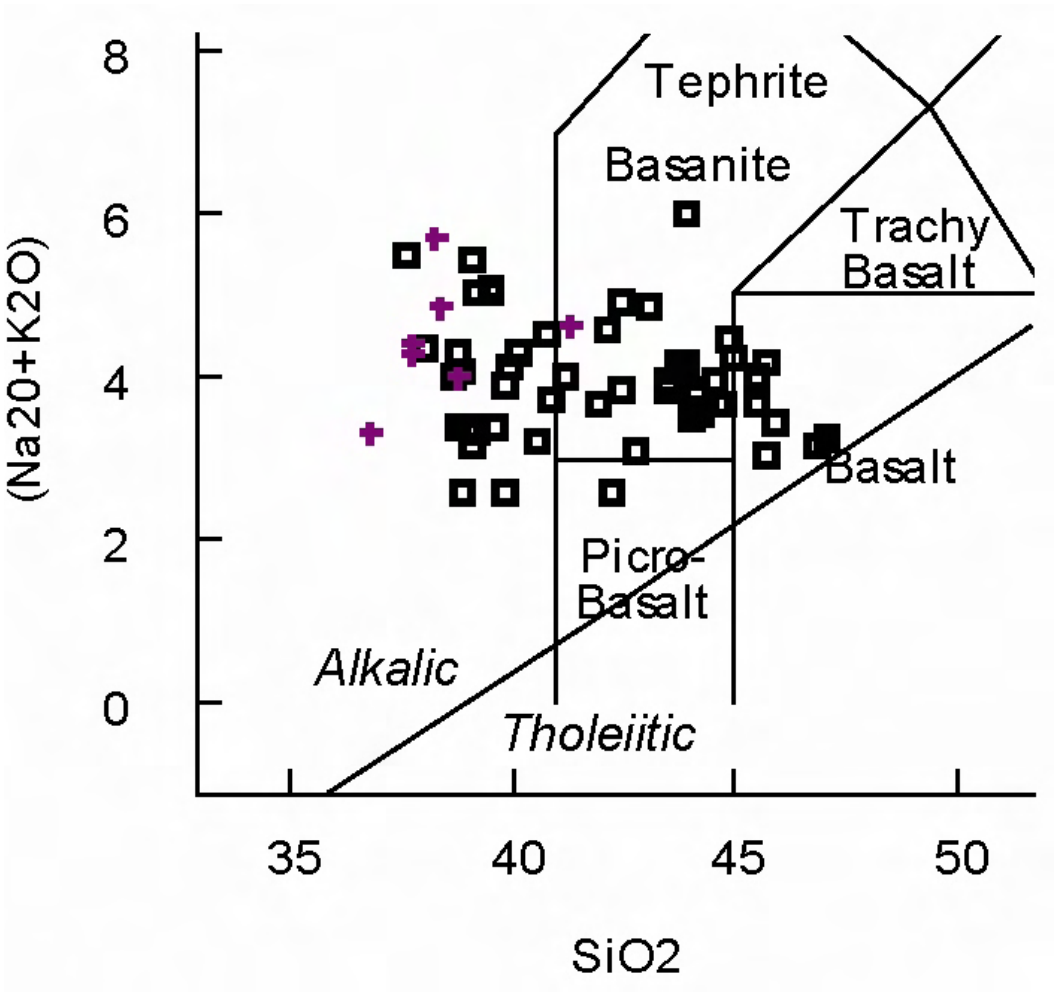

Figure 6. Total alkali versus silica (TAS) diagram for 60 Koloa Volcanics samples. All values are in weight %. Koloa lavas are classified as picrobasalts, alkalic basalts, basanites, foidites, melilite foidites. Gray crosses are melilite foidites. Notice one sample has modal melilite and plots as a basanite. In this instance the modal appearance of melilite supercedes TAS classification.

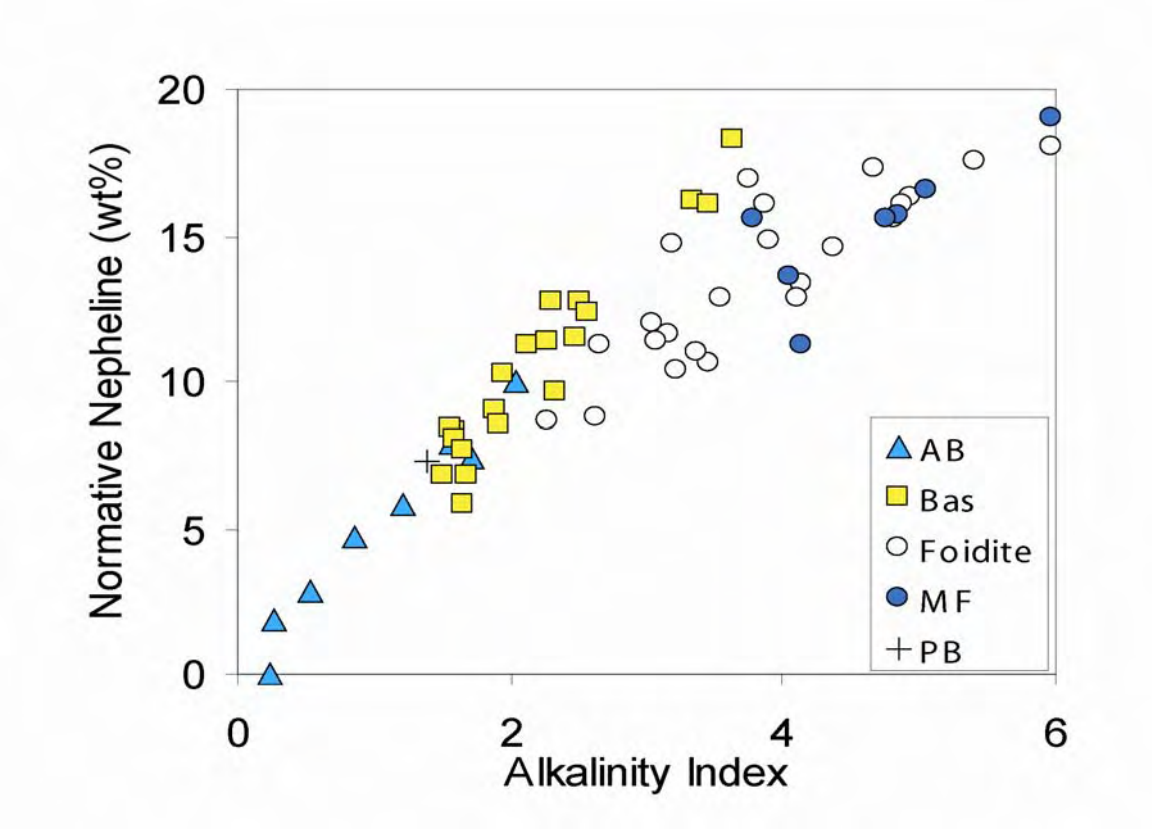

Figure 7. Normative nepheline vs. akalinity index for 60 Koloa samples. This plot shows the similarity and differences with the three classification schemes: TAS, normative nepheline, and alkalinity index. Rock names are based on TAS method. The classification schemes are thought to correlate rock type with the degree of melting (Clague & Frey, 1982; Rhodes & Vollinger, 2004). Alkalic basalts generally show low alkalinity and low normative nepheline (higher degrees of melting), and melilite foidites are the most alkalic rocks, consistent with high normative nepheline (low degrees of melting). Basanites and foidites overlap. Notice that foidites and melilite foidites define a different trend than alkalic basalts and basanites. This may be a result of the normative nepheline axis only considering one component of alkalinity and not leucite and larnite. Data is from Table 3 and Appendix B.. AB – alkalic basalts, Bas – basanite, F – foidites, MF – melilite foidites.

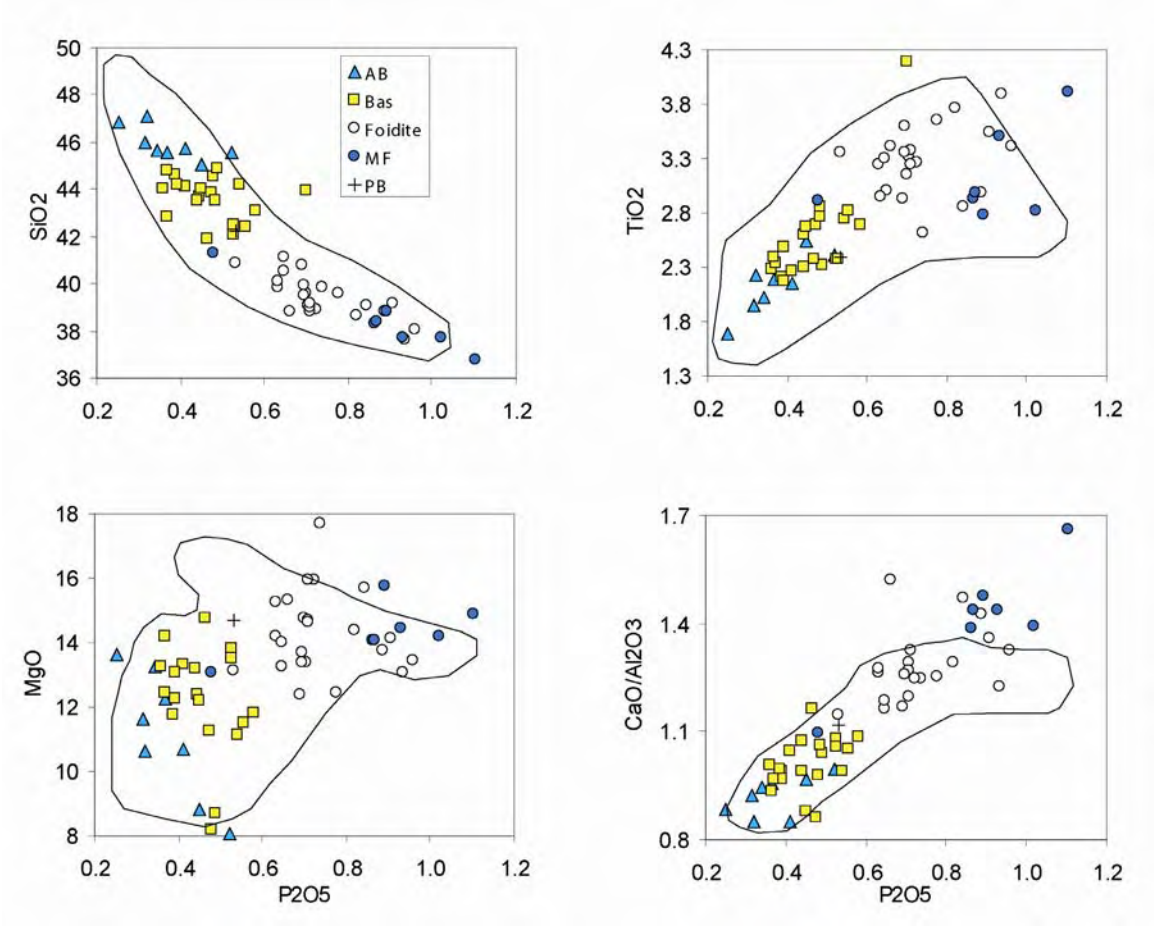

Figure 8. P_2O_5 variation diagrams for SiO_2, MgO, TiO_2, CaO/Al_2O_3. Field shows data from previous studies of Koloa lavas (60 samples; Feigenson, 1984; Clague and Dalrymple, 1988; Maaloe et al., 1992). There is a general correlation of rock type with P_2O_5 abundance. Foidic rocks containing nepheline and melilite contain higher P_2O_5 contents (data from Table 3).

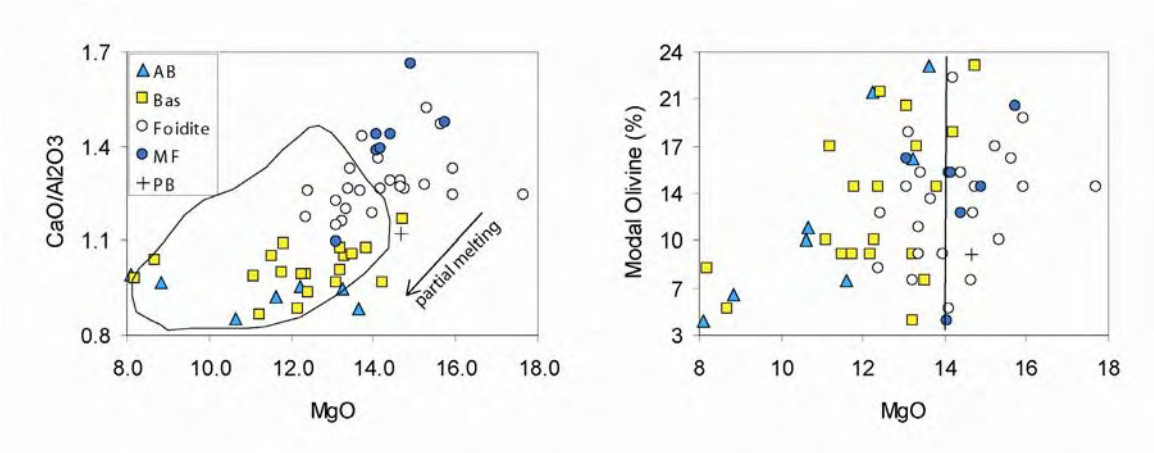

Figure 9. MgO variation diagrams for CaO/Al_2O_3 and modal olivine. CaO/Al_2O_3, rock type and modal olivine are variable at a given MgO. At ~14% MgO all rock types are represented. Field data from Feigenson (1984), Clague and Dalrymple (1988), Maaloe et al. (1992). New data from Tables 1 and 3).

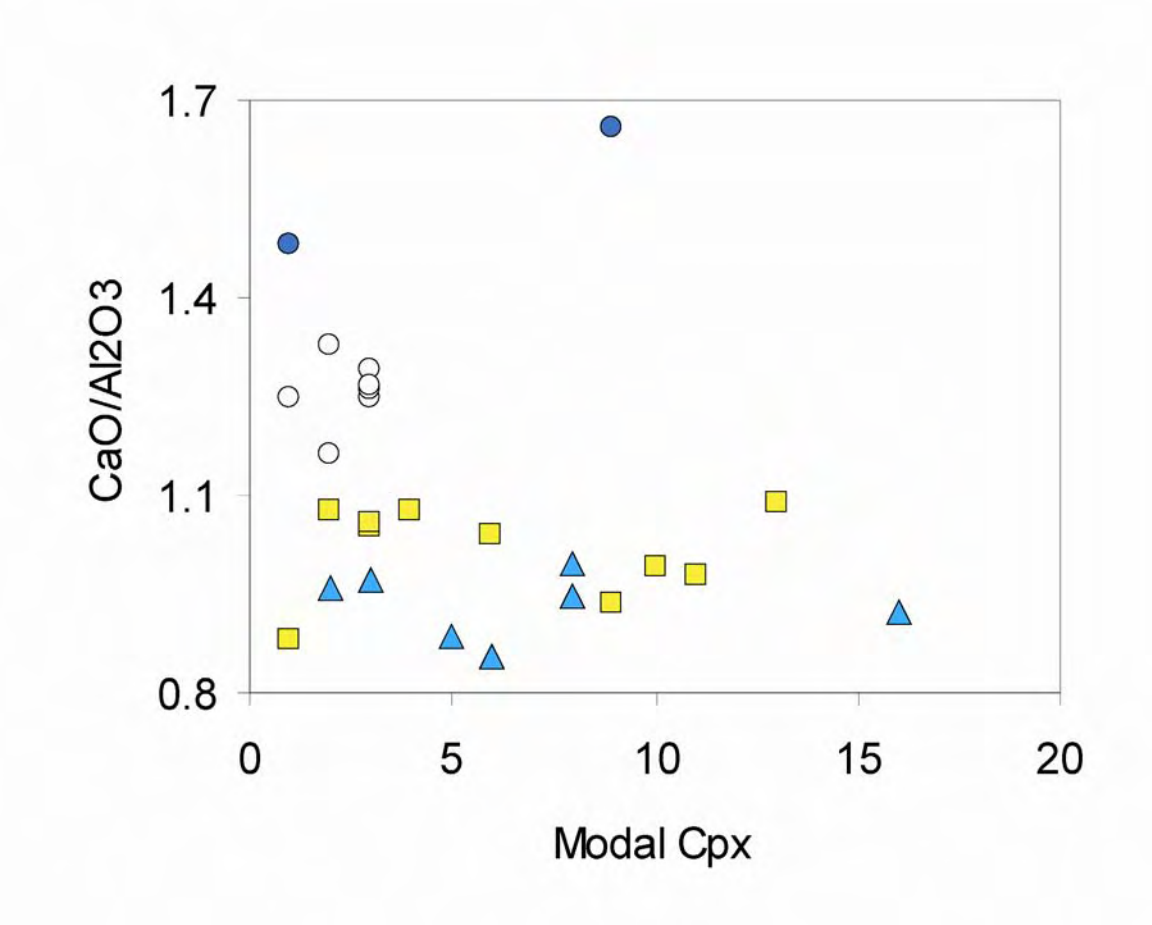

Figure 10. CaO/Al_2O_3 vs. modal clinopyroxene. There is not a correlation between CaO/Al_2O_3 and modal CPX. Hence, the high CaO/Al_2O_3 in foidic rocks is not related to the presence of cpx and is more likely related to partial melting, as noted by Clague & Frey (1982) for Honolulu Volcanics).

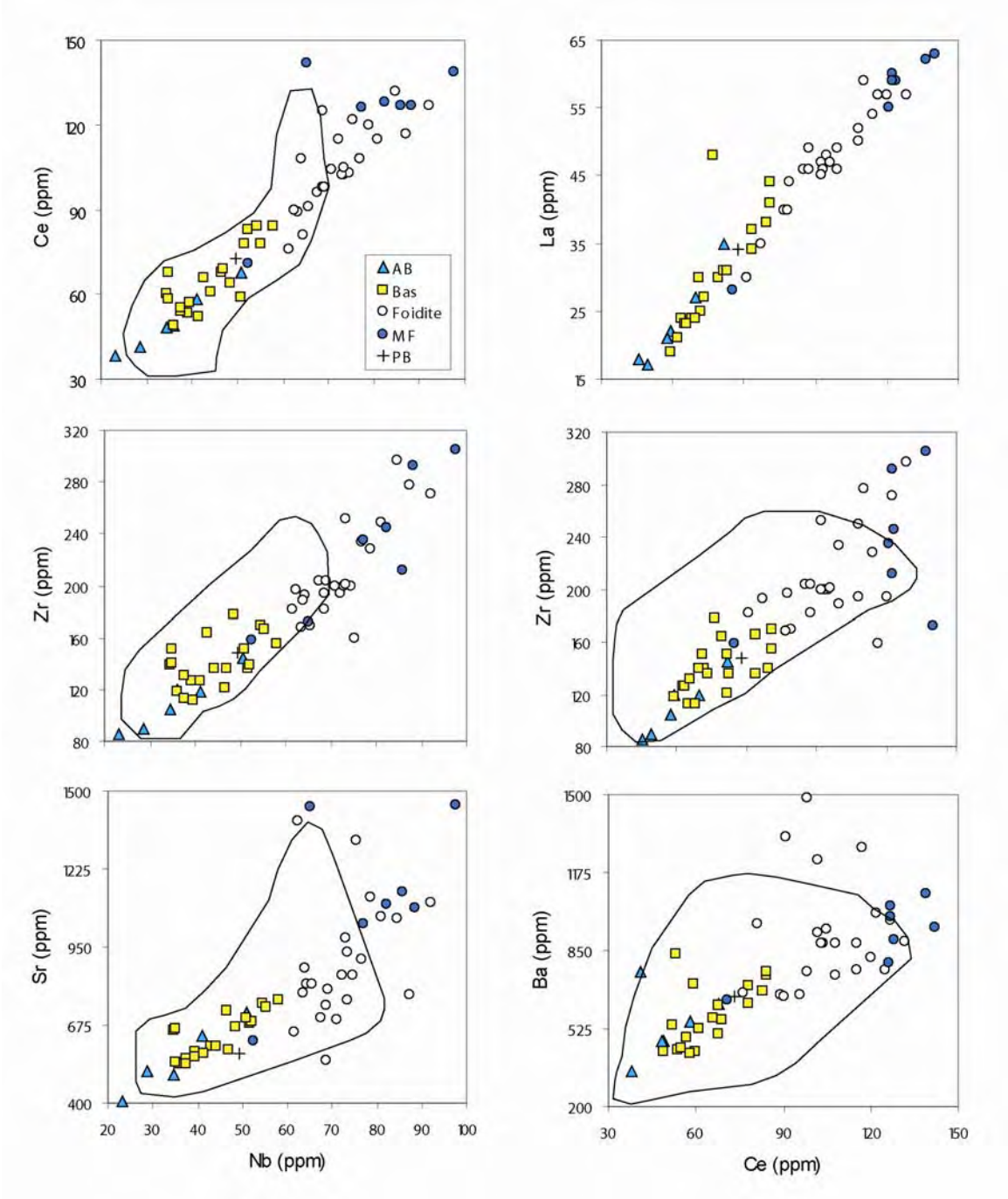

Figure 11. Incompatible element plots of Ce, Zr, and Sr vs. Nb, and La, Zr, and Nb vs. Ce. Elements are generally correlated with the exception of Sr vs. Nb and Ba vs. Ce. The scatter on the Sr vs. Nb and Ba vs. Ce plots are thought to result from of secondary mineralization. Field from Clague and Dalrymple (1988), Maaloe et al. (1992). Data from Table 4.

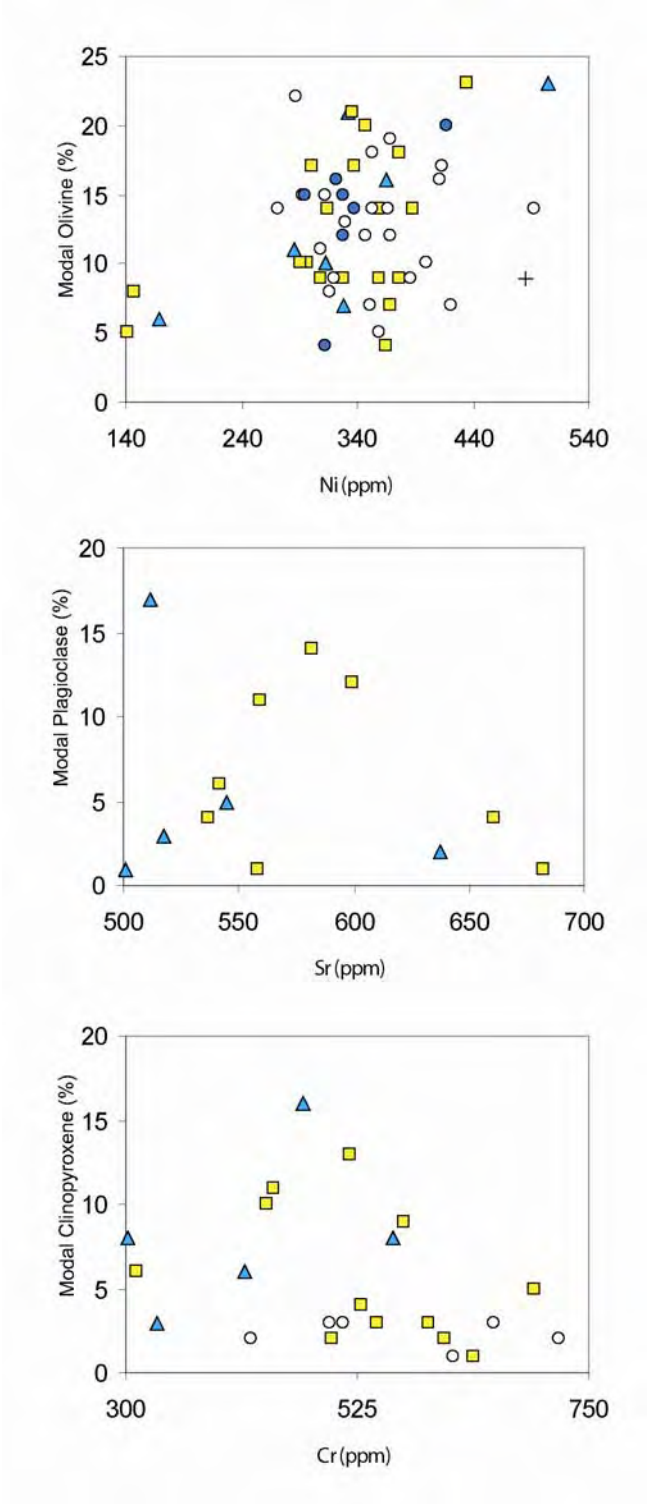

Figure 12. Modal abundances of olivine, plagioclase and clinopyroxene phenocrysts in Koloa lavas vs. Ni, Sr and Cr concentrations. Overall, phenocryst abundances are not related to rock type or an element (Ni, Sr, Cr) compatible in either olivine, plagioclase, or clinopyroxene. Kd's for minerals are as follows: Ni in olivine (12.2), Sr in plagioclase (2.94), Cr in clinopyroxene (5.3; Kd's from Faure, 1986; data from Tables 1 and 4).

Table 3. XRF whole rock major element (wt%) data for selected Koloa Volcanics.

Sample	SiO_2	TiO_2	Al_2O_3	$Fe_2O_3^T$	MnO	MgO	CaO	Na_2O	K_2O	P_2O_5	Total	LOI	CaO/Al2O3
Picrobasalt													
KV03-19	42.22	2.350	10.69	14.38	0.19	14.66	12.01	1.98	0.598	0.534	99.61	2.27	1.12
Alkalic Basalt													
0622-6	45.97	1.91	12.35	12.66	0.18	11.61	11.38	2.68	0.75	0.32	99.80	0.41	0.92
0709-3	45.72	2.10	12.71	12.97	0.19	10.66	10.83	3.26	0.94	0.41	99.79	-0.37	0.85
KV03-6	45.55	2.36	13.38	12.55	0.18	8.09	13.30	2.84	1.136	0.52	99.91	0.71	0.99
KV03-11	45.01	2.48	12.97	13.07	0.19	8.82	12.56	3.23	1.02	0.45	99.80	0.04	0.97
KV03-20	45.68	1.97	11.70	12.60	0.19	13.24	11.07	2.23	0.78	0.34	99.81	0.35	0.95
KV04-1	46.82	1.63	11.45	12.79	0.18	13.64	10.15	2.58	0.58	0.25	100.07	0.41	0.89
KV04-3	45.55	2.14	11.48	13.41	0.19	12.22	10.99	2.77	0.87	0.37	99.98	-0.17	0.96
KV04-13	47.08	2.17	12.41	13.33	0.18	10.63	10.53	2.51	0.72	0.32	99.89	0.85	0.85
Basanite													
0219-3b	43.89	2.64	12.52	13.77	0.19	11.22	10.79	3.24	0.91	0.48	99.64	-0.34	0.86
0220-3	43.91	4.138	15.98	13.78	0.21	5.59	9.04	4.57	1.448	0.701	99.37	0.08	0.57
0228-2	44.04	2.23	11.28	13.68	0.21	13.22	11.37	2.66	0.81	0.36	99.86	0.34	1.01
0301-1	43.67	2.55	11.42	13.68	0.19	12.38	11.32	3.08	1.12	0.44	99.85	0.09	0.99
0626-1	42.49	2.33	10.88	13.98	0.20	13.83	11.72	2.81	1.01	0.53	99.77	0.54	1.08
0705-3	44.16	2.43	11.66	13.55	0.19	12.27	11.55	2.70	1.09	0.39	99.99	0.26	0.99
0707-6	44.09	2.22	10.99	13.38	0.19	13.30	11.52	2.89	0.93	0.41	99.92	-0.20	1.05
0709-5	43.09	2.64	11.17	13.21	0.19	11.81	12.15	3.49	1.35	0.58	99.68	0.63	1.09
KV03-2	44.57	2.72	13.20	13.08	0.19	8.19	12.94	2.82	1.15	0.48	99.34	1.13	0.98
KV03-5	44.06	2.62	11.93	14.09	0.19	12.18	10.51	2.65	0.89	0.45	99.57	0.03	0.88
KV03-7	44.65	2.16	11.94	13.30	0.19	11.76	11.91	2.82	0.83	0.39	99.95	0.46	1.00
KV03-8	43.53	2.25	11.00	13.44	0.19	13.20	11.83	2.85	0.96	0.44	99.69	0.49	1.08
KV03-12	44.92	2.27	12.95	12.22	0.19	8.68	13.45	3.39	1.09	0.49	99.65	0.18	1.04
KV03-17	42.10	2.32	10.89	13.98	0.20	13.51	11.54	3.46	1.13	0.53	99.66	-0.55	1.06
KV03-18	41.90	2.33	10.13	14.21	0.21	14.73	11.79	2.64	1.01	0.47	99.41	0.32	1.16

Table 3. cont.

KV03-21	44.17	2.70	12.04	13.44	0.19	11.11	11.91	2.41	1.20	0.54	99.71	1.70	0.99
KV03-27	42.41	2.76	11.16	14.27	0.20	11.51	11.71	4.22	0.68	0.56	99.48	0.05	1.05
KV04-4	44.22	2.11	11.66	13.55	0.20	13.08	11.26	2.65	0.89	0.39	100.01	0.19	0.97
KV04-6	42.82	2.29	11.40	14.45	0.20	14.21	11.02	2.25	0.83	0.37	99.84	0.90	0.97
KV04-10	44.81	2.34	11.61	13.60	0.19	12.41	10.86	2.78	0.89	0.37	99.86	0.02	0.94
KR-3	43.53	2.81	13.55	13.40	0.19	6.88	14.39	2.67	1.30	0.49	99.20	1.96	1.06
Foidite													
0218-1	41.16	2.95	10.75	14.02	0.20	13.24	12.50	3.14	0.85	0.65	99.46	2.15	1.16
0219-2	40.84	3.31	10.83	14.24	0.20	13.11	12.41	2.55	1.19	0.53	99.20	1.03	1.15
0220-4	37.66	3.85	10.36	15.51	0.23	13.08	12.67	3.87	1.62	0.94	99.78	-2.21	1.22
0221-4	39.85	3.19	10.48	15.32	0.22	14.19	13.22	1.86	0.72	0.63	99.68	3.46	1.26
0222-1b	38.04	3.37	10.56	14.73	0.23	13.43	14.02	3.70	0.62	0.96	99.66	2.83	1.33
0225-2	39.57	3.11	10.16	14.74	0.23	14.77	12.80	2.49	0.89	0.70	99.45	2.32	1.26
0301-4	39.09	3.26	10.72	14.28	0.21	13.36	12.84	3.78	1.67	0.71	99.92	0.27	1.20
0623-3	39.11	2.80	9.27	15.15	0.22	15.66	13.63	2.44	0.68	0.84	99.81	2.59	1.47
0623-4	39.87	2.56	9.08	14.45	0.24	17.68	11.30	2.77	1.10	0.74	99.79	2.15	1.24
0623-6	39.18	3.50	9.22	14.86	0.21	14.13	12.55	3.49	1.51	0.91	99.56	0.67	1.36
0623-7S	38.63	3.72	9.89	14.99	0.20	14.40	12.75	2.85	1.14	0.82	99.39	2.28	1.29
0705-5	40.52	3.25	10.62	14.39	0.20	13.97	12.59	2.40	0.82	0.65	99.40	2.56	1.19
0713-4	38.92	3.21	9.93	14.30	0.25	15.95	12.36	2.76	1.31	0.73	99.72	1.49	1.24
KV03-1	39.48	3.54	9.54	15.28	0.20	13.38	12.02	3.33	1.67	0.70	99.14	0.59	1.26
KV03-4	39.55	3.60	9.89	15.45	0.23	12.42	12.41	3.43	1.65	0.78	99.41	1.35	1.25
KV03-10	40.75	2.88	10.84	14.49	0.21	12.38	12.68	3.45	1.07	0.69	99.43	1.38	1.17
KV03-15B	40.14	2.89	9.76	14.01	0.22	15.25	12.47	3.18	1.13	0.63	99.69	0.74	1.28
KV04-5	38.81	3.20	9.77	14.27	0.20	15.95	12.94	2.26	1.12	0.71	99.23	2.30	1.32
KV04-8	38.95	3.32	9.88	15.52	0.22	14.68	12.75	2.35	1.00	0.71	99.38	2.32	1.29
KV04-9	39.19	3.32	9.88	15.62	0.22	14.65	12.53	2.22	1.07	0.71	99.41	1.38	1.27
KR-1	38.85	3.35	9.31	14.57	0.21	15.32	14.15	1.88	0.70	0.66	99.00	1.87	1.52
KR-2	39.90	3.31	10.14	14.44	0.21	13.67	12.75	3.61	0.49	0.70	99.21	1.36	1.26
Makaleha	38.79	2.94	9.72	15.18	0.21	13.74	13.88	3.13	1.18	0.89	99.66	1.76	1.43

Table 3. cont.

Melilite Foidite													
0220-6	38.29	2.88	9.40	15.05	0.21	14.09	13.04	4.07	1.63	0.87	99.52	-0.41	1.39
0222-2s	37.71	2.76	10.18	14.79	0.24	14.18	14.18	3.35	1.03	1.02	99.44	1.57	1.39

Table 3. cont.

0301-9	41.31	2.85	10.79	14.15	0.20	13.08	11.84	3.33	1.31	0.48	99.34	-0.11	1.10
0702-9	38.83	2.73	9.12	14.67	0.22	15.75	13.47	2.92	1.06	0.89	99.67	1.70	1.48
0710-2	38.40	2.93	9.61	15.22	0.22	14.07	13.81	3.55	1.29	0.87	99.96	0.73	1.44
0712-2	36.81	3.85	8.87	15.92	0.22	14.90	14.71	2.42	0.92	1.10	99.73	2.89	1.66
KR-5	37.75	3.46	9.25	15.39	0.23	14.42	13.29	3.32	0.98	0.93	99.01	1.29	1.44

* = phenocrysts + microphenocrysts
T = total iron

Table 4. XRF trace element analyses (ppm) for selected Koloa Volcanics.

Sample	Nb	Zr	Y	Sr	Rb	Ba	La	Ce	Th	Pb	Ga	Zn	Ni	Cr	V
Picrobasalt															
KV03-19	49.5	148	20.9	573	15.7	656	34	73	5	2	18	123	485	694	287
Alkalic Basalt															
0622-6	28.6	90	19.5	512	17.8	764	17	41	2	1	19	105	328	473	233
0709-3	36.1	120	21.4	545	23.4	476	22	49	3	2	20	117	285	415	240
KV03-6	50.7	145	24.3	716	26.4	632	35	68	4	2	20	112	134	302	272
KV03-11	41.1	119	23.0	638	26.1	552	27	58	3	3	20	113	169	330	283
KV03-20	34.5	105	18.2	501	19.7	473	21	48	3	1	18	110	366	560	231
KV04-1	23.2	85	25.0	404	13.4	345	18	38	2	1	17	107	505	698	207
KV04-3	36.2	137	91	519	21	445	46	53	4	2	18	122	334	501	252
KV04-13	28.5	116	73	470	15	393	57	139	2	2	19	119	315	494	256
Basanite															
0219-3b	34.5	139	33.6	657	22.5	426	25	60	3	1	19	109	301	582	284
0220-3	58.0	200	31.0	1203	30.8	686	37	92	4	2	21	123	12	-	233
0228-2	35.9	118	19.8	537	19.4	426	19	49	3	1	18	114	365	571	268
0301-1	42.8	164	22.5	601	24.4	566	30	66	3	2	19	112	314	526	286
0626-1	51.8	136	20.2	682	25.3	701	37	78	5	3	18	123	388	611	284
0705-3	41.3	126	18.9	578	27.6	541	21	52	3	2	19	112	298	529	273
0707-6	39.3	126	18.9	582	22.2	836	24	53	3	2	18	110	338	544	254
0709-5	57.9	155	30.3	760	33.6	750	44	84	5	2	19	117	360	518	241
KV03-2	48.5	178	43	670	26	3079	48	64	3	0	19	116	148	437	299
KV03-5	35.0	151	27.1	661	20.4	503	31	68	3	2	19	119	359	638	290
KV03-07	37.5	113	19.4	559	19.6	434	23	54	3	2	19	116	328	482	255
KV03-8	44.3	136	20.0	600	23.3	528	27	61	3	2	19	118	377	529	253
KV03-12	46.6	121	22.6	724	26.6	618	31	68	4	2	20	103	142	311	261
KV03-17	52.2	139	20.4	686	28.5	678	38	83	5	3	18	120	370	594	281
KV03-18	47.1	136	19.4	588	25.6	565	31	69	4	2	18	123	435	672	295

Table 4. cont.

KV03-21	54.5	169	31.0	751	28.8	762	41	84	4	2	20	125	291	437	261
KV03-27	55.2	166	21.4	739	7.5	626	34	78	4	2	21	126	309	469	293
KV04-4	39.5	112	19.9	560	22.5	487	24	57	3	2	19	115	348	575	262
KV04-6	37.5	131	18.8	535	18.0	441	23	55	2	2	18	108	376	629	286
KV04-10	35.0	140	19.8	542	18.9	423	24	58	2	2	20	108	337	570	250
KR-3	50.8	151	21	699	30.4	708	30	59	-	-	-	111	336	310	59
Foidite															
0218-1	67.5	203	23.2	702	25.0	667	46	96	5	2	18	108	422	722	267
0219-2	61.5	182	19.9	653	38.8	675	30	76	4	1	19	113	354	664	336
0220-4	72.1	194	25.6	848	41.6	768	50	115	6	2	21	139	272	383	345
0221-4	64.3	192	20.1	817	34.5	961	35	81	5	2	20	123	288	422	334
0222-1b	75.4	159	25.5	1323	16.0	1004	57	122	7	0	19	135	294	425	322
0225-2	68.8	182	21.3	742	24.8	1482	49	98	6	2	18	123	367	674	312
0301-4	76.8	233	25.0	907	35.7	876	46	108	6	2	18	116	308	542	318
0623-3	78.8	228	22.9	1128	16.5	817	54	120	7	2	18	142	412	700	277
0623-4	68.7	194	30.0	551	24.1	768	57	125	6	1	16	123	494	659	266
0623-6	84.7	297	26.5	1050	30.2	885	57	132	7	4	20	142	360	542	295
0623-7S	81.0	249	23.2	1057	33.3	880	52	115	6	3	20	130	312	404	310
0705-5	65.5	169	20.7	816	24.8	1321	44	91	5	2	20	128	321	415	319
0713-4	70.9	200	22.0	693	32.0	876	48	104	5	3	18	113	370	618	316
KV03-1	73.5	252	23.6	761	39.2	924	47	102	6	2	21	144	387	539	315
KV03-4	87.3	277	34.5	784	39.3	1280	59	117	7	2	22	160	369	494	325
KV03-10	64.1	189	24.5	873	20.2	744	49	108	6	3	20	135	317	520	290
KV03-15B	63.4	168	20.6	790	32.8	669	40	89	5	2	18	122	413	648	303
KV04-5	74.5	200	21.4	853	35.9	881	46	103	6	2	18	112	353	618	317
KV04-8	72.9	200	21.1	980	25.6	1230	45	102	6	2	20	130	348	512	324
KV04-9	73.3	201	21.0	932	29.5	941	47	105	6	2	20	132	351	498	326
KR-1	62.4	196	20.3	1395	17.8	658	40	90	-	-	-	108	400	612	335
KR-2	69.1	203	22.0	802	10.4	763	46	98	-	-	-	111	331	528	270
Makaleha	92.2	271	26.0	1108	24.7	976	60	127	7	3	20	149	315	488	274

Table 4. cont.

Melilite Foidite

0220-6	77.2	235	23.7	1034	33.0	801	55	126	6	2	19	148	329	493	278
0222-2s	65.1	172	27.8	1441	30.7	944	63	142	8	2	17	143	295	559	313

Table 4. cont.

0301-9	52.5	158	19.1	619	37.6	646	28	71	4	2	19	117	323	494	300
0702-9	85.9	212	22.9	1146	26.1	1032	60	127	7	2	17	135	417	645	283
0710-2	82.3	245	24.3	1100	27.1	893	59	128	7	3	19	144	313	511	285
0712-2	97.7	305	25.4	1452	33.9	1088	62	139	8	3	18	154	339	385	300
KR-5	88.4	292	25.4	1085	27.1	991	59	127	-	-	-	135	329	493	323

5.4 Volume Results

Thickness information from 80 wells and tunnels on Kaua`i have been synthesized with field observations and data from topographic maps using ARC/GIS to produce a conservative volume estimate for the Koloa Volcanics (see Methods section for procedures). The island has been divided into four sections for volume calculations to minimize errors in extrapolating thicknesses between distant areas of the island. The areas are: Lihue Basin, Koloa, Hanapepe, and North Coast.

Lihue Basin region

Koloa lava outcrops within the Lihue basin are limited. Kilohana cone, a prominent feature on the surface of the Lihue Basin, yielded only a single outcrop, a ~12 m waterfall at the southwestern margin of the cone. Koloa lavas exposed in the walls of Wailua River canyon are at least 60 m thick, the maximum exposed thickness of Koloa lavas in Lihue Basin. The conservative volume estimate for Koloa lavas in the Lihue Basin is derived mostly from six deep wells (Reiners et al., 1999). Analyses of chips from drill cores yield a depth of 250 – 300 m for Koloa lavas in the central and southeastern Lihue Basin (Reiners et al., 1999). Logs for wells 0121-01, 0123-01, 0124-01, 0023-01 and 5923-08 within 3.5 km south of the Wailua River also suggest Koloa lavas are much deeper (~150 m) than the exposed sections (Fig. 13; Appendix B). Hence, we have extrapolated the depth of Koloa lavas to 150 m in the area of the Wailua River (Fig. 13). The depth of Koloa lavas in the northern end of the basin is extrapolated from wells 0620-01 and 0523-02 (Fig. 13). Data in the western end

of the basin is sparse, although wells 0327-01 (70 m depth) and 0126-01 (135 m depth) provide a basis for extrapolation to the western boundary of the Lihue Basin (Fig. 13). Koloa lavas are found to be 280 m thick in well 5824-01 in southern Lihue Basin, the greatest subsurface depth of Koloa known on the island (Fig. 13). Other wells in the southern Lihue Basin (5821-01, 5721-01 and 5821-02) have Koloa lavas exposed to the depth of the well (Appendix B). Areas near these wells which do not have well data have been projected to a comparable depth.

The Palikea breccia member is interbedded with Koloa lavas in the Lihue basin (Reiners et al., 1999). Therefore, in order to provide a minimum volume estimate, the thicknesses of the Palikea member breccia in Koloa have been subtracted from the maximum depth of Koloa lavas. The average depth of the Palikea member breccia in Lihue basin is 50 m, determined from 6 wells (Reiners et al., 1999). This value has been extended through the entire basin and depth values for Koloa lavas in the Lihue Basin have been modified accordingly (Fig. 13). The resultant conservative volume for Koloa lavas in the Lihue Basin is estimated to 30 km^3.

Koloa region

Southern Kaua`i has been divided into two regions separated by the Hanapepe River; Koloa and Hanapepe (Figs. 14 & 15). The Koloa region extends from Carter Point, at the southern tip of Nawiliwili Harbor, west to Hanapepe River (Fig. 14). The conservative volume estimate for Koloa lavas in the Koloa region is based on field observations and data from 16 water wells

(Fig. 14). Because rock exposures and well data are limited in the area southwest of Kilohana Cone near Papuaa Reservoir and further west near Kanaele Swamp, estimates are biased by wells to the south (Fig. 14). For instance, well 5631-01 has Koloa lavas to a minimum depth of 54 m and is located on the seaward side of a peak of shield lavas (Fig. 14). Koloa lavas north of this well may thicken towards the source (Macdonald et al., 1960). In support of this assumption are cones mapped by Macdonald et al. (1960) in the areas north of the well. Hence, the Koloa thicknesses in areas north of well 5631-01 in the Koloa region are assumed to be at least 50 m.

Koloa lavas are 213 m deep in the Eleele Tank Well, the deepest well in this region (Izuka, 2005). This thickness has been extended eastward across the flow field to well 5531-01, where Koloa lavas are found at a depth of 207 m. Koloa lavas are 200 m deep in well 5530-02 (Macdonald et al., 1960) to the northeast. Eastward of this well, the Koloa lavas thin to the coast in wells 5529-02 (162 m), 5428-01 (133 m) and 5426-01 (100 m; Fig. 14). Koloa lava thicknesses along the south coast are based on field exposures, which provide only a minimum thickness (10-30 m). Koloa lavas in the northern Koloa region are poorly constrained because of a lack of thickness information. In this case a value of 20 m was used. This assumption is based on two observations: an average single-flow thickness for Koloa lavas of ~5 m and no Koloa lavas were observed as singular flows. The resultant conservative volume for the Koloa Volcanics in the Koloa region is 10 km^3.

Hanapepe region

The volume for the Hanapepe region is largely defined by field observations and topographic maps because only three wells provide data (Fig. 15). Two of the wells are shallow (5635-01; 21 m and 5537-01; 45 m), and they terminated in Koloa rocks, so they provide only minimum thicknesses. However, well 5634-01 yielded Koloa lavas to a depth of at least 132 m. Residual masses of Koloa lavas were mapped above the confluence of Waimea Canyon and Koaie Stream (Stearns, 1946; Macdonald et al., 1960). Koloa lavas in the western wall of Koaie Stream are located at elevations of 430 to 310 m and are gently sloping downstream. Thus, the minimum Koloa thickness is 120 m. This thickness was been projected down-canyon ~10 km to where other residual masses of Koloa lavas gave a thickness of ~75 m (Fig. 15). Similarly, Olokele Canyon and Kahana Valley, which flow into Makaweli Canyon, contain residual masses of Koloa lavas (Fig. 15). The depths estimates east of Makaweli Canyon (40 m), which form Nonopahu Ridge, represent the relief of Koloa lavas in the eastern wall of Makaweli Canyon (Fig. 15). Flow thicknesses of Koloa lavas on Aaka Ridge and Waikai Valley to the east are projected to a minimum depth of 40 m, in accordance with the thickness observations in the eastern wall of the adjacent Makaweli Canyon (40 m; Fig. 15). Koloa lavas in well 5635-01 are a minimum of 21 m. However, areas nearby have been projected to 40 m because the contact between Koloa lavas and the underlying shield lavas was not found. Therfore, we suggest a projection of Koloa lavas to a depth of 40 m near well 5635-01 is reasonable.

Estimates for depths of lava flows in Hanapepe and Koula valleys are derived from mapped residual masses in the canyon walls (Fig. 15). Depths of Koloa lavas in coastal areas have been estimated from outcrops along the shoreline. They range between 10-15 m but have been projected deeper in accordance with well 5537-01, which has lavas to a depth of 45 m. In areas where no field observations or well data are available, and where topographic maps provide no relief for mapped Koloa lavas, a minimum thickness of 20 m has been ascribed based on the assumptions given above. The resultant conservative volume for the Koloa lavas in the Hanapepe region is 3.3 km^3.

North Coast region

The volume estimate for the North Coast is largely based on field observations and topographic maps because most of the 29 water wells in the region are shallow (<50 m) and located near the coast (Figs. 16 & 17). Residual masses of Koloa lavas were mapped in Wainiha, Lumahai and Hanalei Valleys by Stearns (1946) and Macdonald et al. (1960). The thickness of Koloa lavas was estimated from the exposures along the valley walls. Lava flows were only projected up these valleys (towards the summit) to cover known outcrops of Koloa lavas. The Koloa lavas bounded by Hanalei and Kalihiwai Valleys are estimated from the steep cliffs of Koloa lavas found in the eastern wall of Hanalei Valley and the western wall of Kalihiwai Valley mapped by Macdonald et al. (1960; Fig. 16). These exposures of Koloa range in thickness from 20 – 240 m.

Surface depths for Koloa lavas in the north are from wells 1020-03 (168 m), 1225-02 (100 m) and 1327-02 (110 m), which penetrated the contact

between the older shield lavas and the overlying Koloa lavas (Figs. 16 & 17). From these data, depths in between the wells were estimated (Fig. 16). Where Koloa lavas extend to the base of the well, the depth is noted in parentheses (Figs. 13-16). Koloa lavas were projected deeper in these areas if data from nearby wells suggest Koloa lavas are deeper (e.g., well 1120-03 has Koloa lavas to ~30 m, although well 1020-03, ~1.5 km to the southwest, has Koloa lavas logged by the late geologist D.C. Cox to a thickness of 168 m, corrected for 68 m of Palikea member). Some sea cliffs along the northern coast of the island expose Koloa lavas at least 60 m thick. These thicknesses are extrapolated inland if well data were not available. Combining these data yields a conservative volume of Koloa lavas from the North Coast, from Kapaa Stream to Wainiha Valley, of 18.2 km^3.

Total Volume for Koloa Volcanics

Combining the volumes of Koloa lavas for the four regions of the islands yields a total volume of 61.5 km^3. This estimate does not include the roughly 40 cones of the Koloa Volcanics because their volume contribution is minimal (~0.1 km^3). However, a potentially important correction for this estimate is to remove vesicles to get a dense rock equivalent value of magma volume. Modal analyses of 25 thin sections spanning the range of rock types, yielded an average vesicularity of ~6 vol.%. Adjusting the volume estimate for 6 vol.% vesicularity, a dense rock conservative volume estimate for the Koloa Volcanics is ~58 km^3.

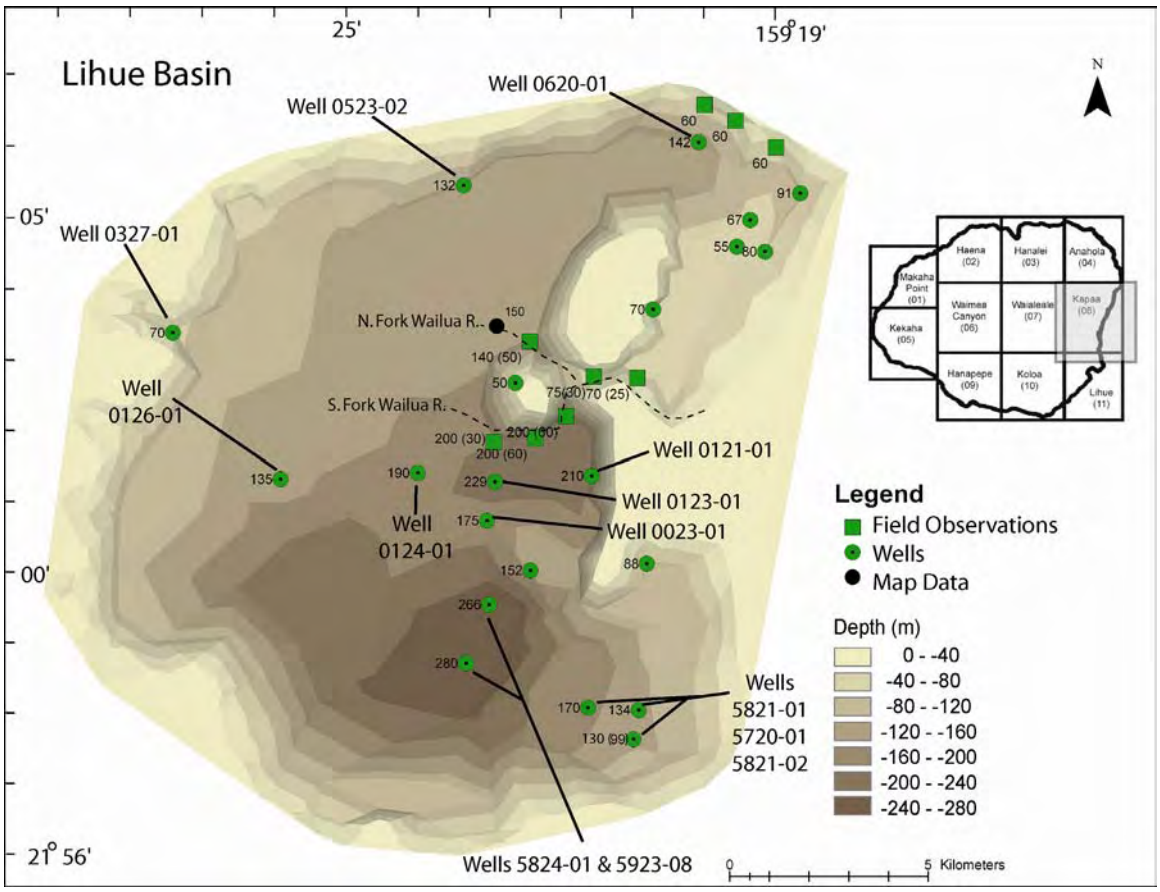

Figure 13. Distribution and thickness of Koloa lavas in the Lihue Basin. Numbers in parenthesis show the actual thickness/depth of Koloa lavas obtained from water well logs or field observations. The number not in parenthesis is the projected depth, derived from nearby data (Reiners et al., 1999; Izuka, 2005; unpublished water well logs). Map data represents volumes estimated from field observations that were not observed in this study (Stearns, 1946; Macdonald et al., 1960). Total conservative estimate for the volume of Koloa lavas in the Lihue Basin region is 30 km^3.

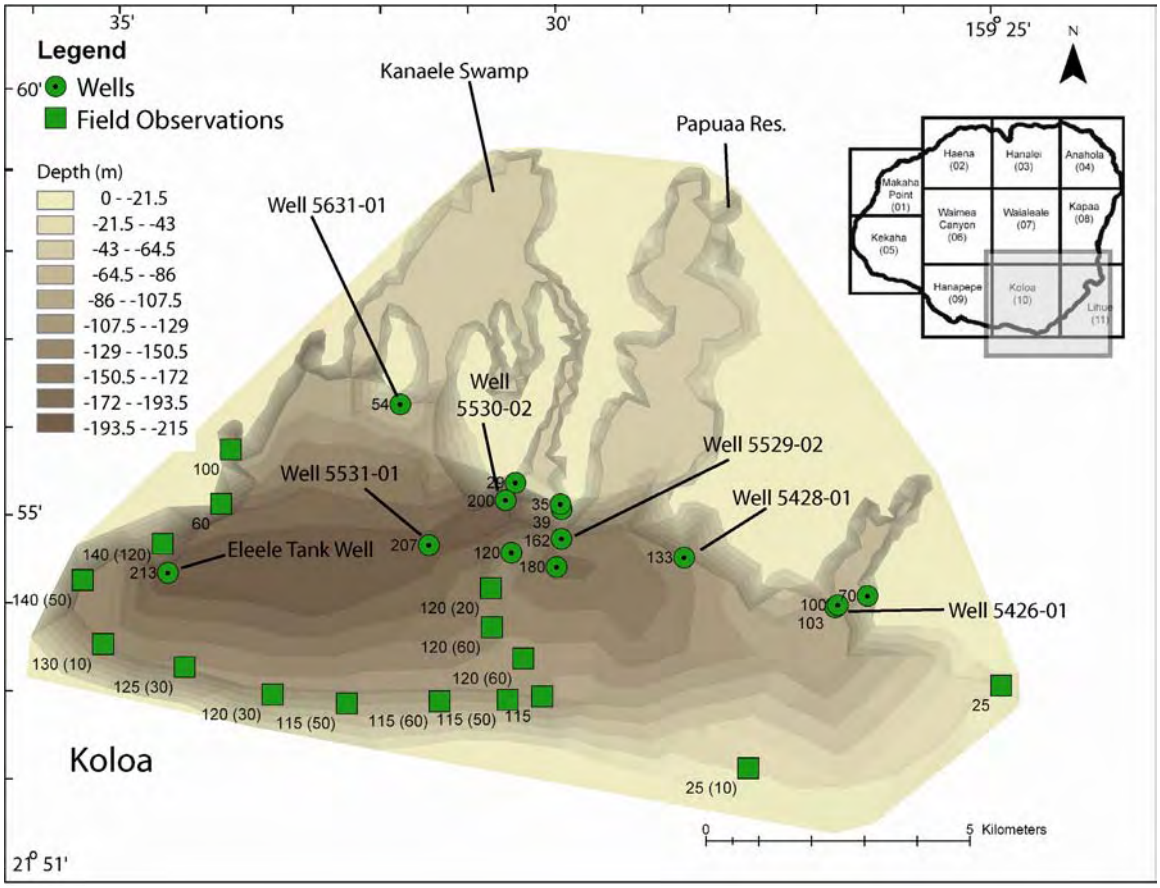

Figure 14. Distribution and thickness of Koloa lavas in the Koloa region. Symbols and definitions are the same as Figure 13. Data from Macdonald, et al. (1960), Izuka (2005), and unpublished water well logs. Total conservative estimate for the volume of Koloa lavas in the Koloa region is 10 km^3.

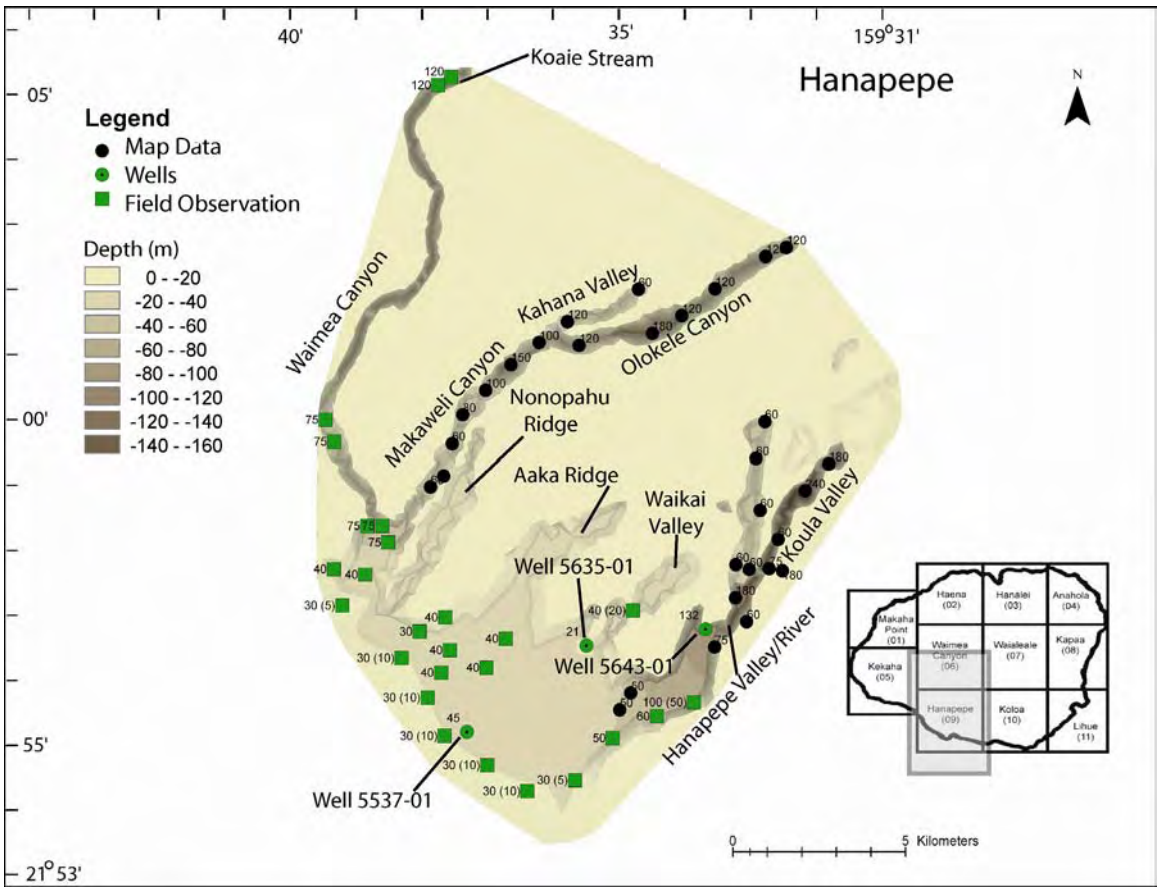

Figure 15. Distribution and thickness of Koloa lavas in the Hanapepe region. Symbols and definitions are the same as in Figure 13. Data from Stearns (1946), Macdonald et al. (1960), and unpublished water well logs (USGS Honolulu Office). See text for more explanation of how thicknesses were determined. Total conservative estimate for volume of Koloa lavas in the Hanapepe region is 3.3 km^3.

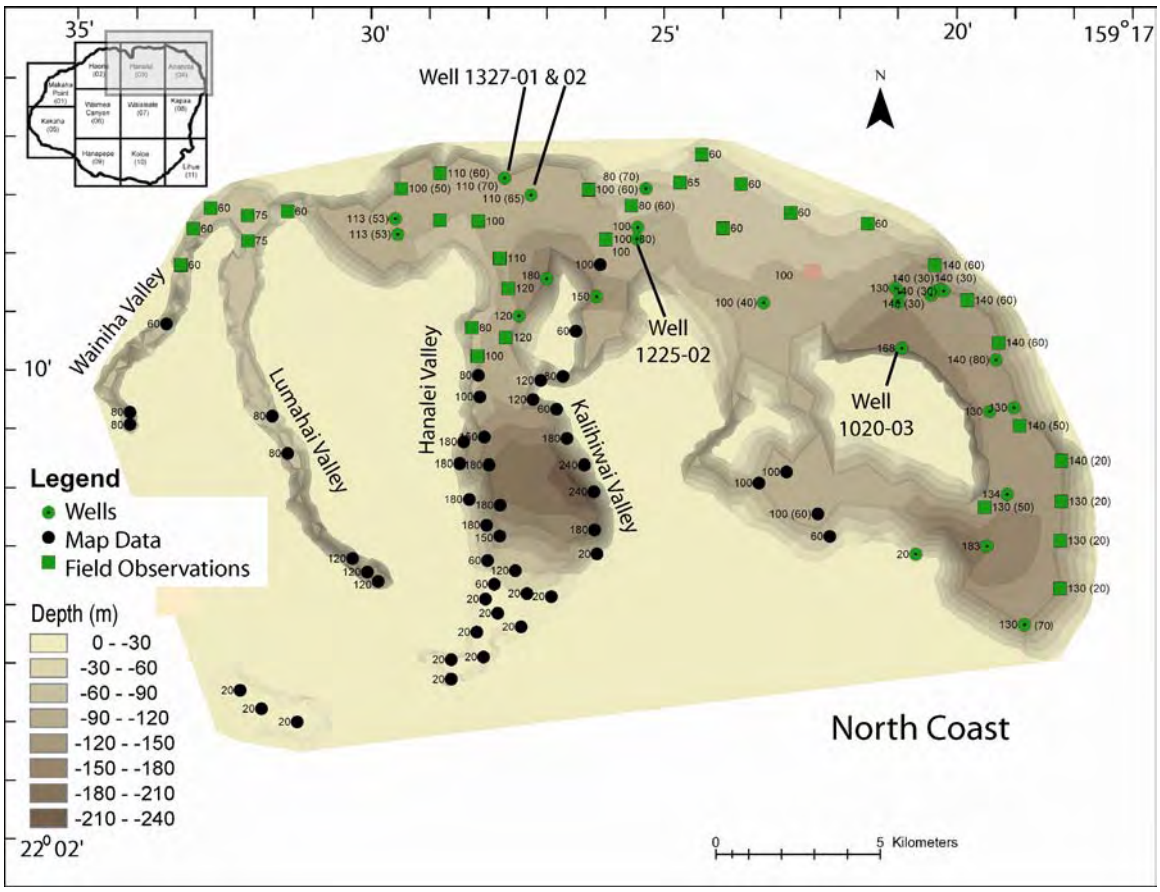

Figure 16. Distribution and thickness of Koloa lavas in the North Coast region. Symbols and definitions are the same Figures 13. Data from Stearns (1946), Macdonald et al. (1960), and unpublished water well logs. Total conservative estimate for volume of Koloa lavas in the North Coast region is 18.2 km^3.

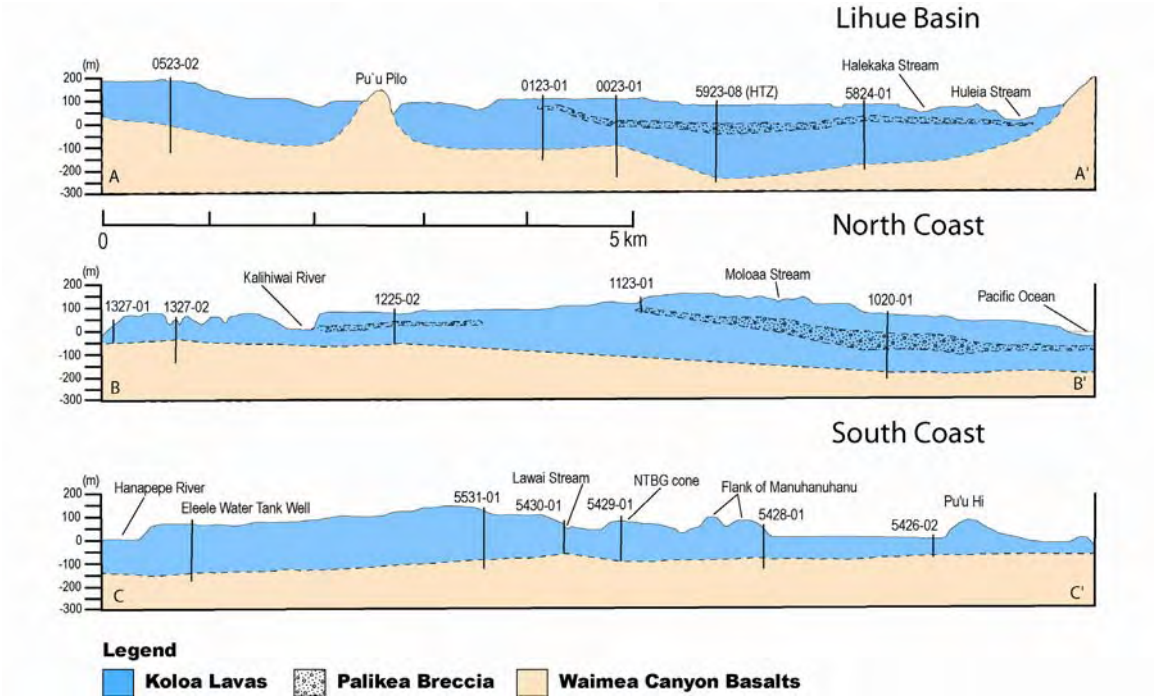

Figure 17. Cross-sections of Kaua`i showing Koloa Volcanics. Dashed lines represent the base of Koloa lavas. Vertical lines show well locations used in the cross-sections. Numbers listed next of well indicate well number. "NTBG" is abbreviated from National Tropical Botanical Garden. See Figure 1 for location of sections. Data from Macdonald et al. (1960), Reiners et al. (1999), Izuka (2005), and unpublished well data.

6.0 Discussion

6.1 Rock type temporal variations: Implications for melting history

The Koloa Volcanics include a wide range of alkalic compositions (picrobasalt to foidite; Figs. 3 & 18). These compositions are thought to reflect varying degrees of partial melting of a common source (Clague & Dalrymple, 1988; Maaloe et al., 1992). Some previous studies (Reiners & Nelson, 1998; Reiners et al., 1999; Clague et al., 2006) suggested that the Koloa Volcanics show a temporal decrease in extent of melting (from older alkalic basalt and basanite, to younger foidite and melilite foidite). This interpretation is supported by cuttings from 300-350 m deep water wells in the Lihue basin (Reiners & Nelson, 1998; Reiners et al., 1999). If this trend is valid for all Koloa lavas, it has important implications for the process(es) creating rejuvenation volcanism. However, Maaloe et al. (1992) found the opposite trend in a 17 flow sequence along the south coast of Kaua`i. We have used our data (164 petrographic analyses and 60 geochemical analyses) to assess whether there is a temporal variation in composition among Koloa rocks, and to gain insight into the process(es) creating rejuvenation volcanism.

Our investigation of the Lihue basin included visiting several active rock quarries where the youngest lavas are alkalic basalts. These flows and other surface flows in the basin originated from Kilohana or Hanahanapuni cones. Other young alkalic basalt lavas from unknown vents were sampled along the N. fork of Wailua River in the eastern part of Lihue basin. The presence of these young alkalic basalts is contrary to the results from the drill holes (Reiners et al.,

1999). Perhaps the youngest flows from the Kilohana and Hanahanapuni cones did not reach the drill sites or were eroded. Another problem with the drill core study was the extensive alteration of the chips, which reduced the alkalic contents in these rocks (Reiners and Nelson, 1998). Reiners and Nelson (1998) also observed opposite trends (towards less alkalic compositions up section) within shorter intervals of the drill core. They concluded these opposite trends were related to monogenetic mantle melting processes. Another study also found a trend towards less alkalic basalts for the south coast of Kaua`i (Maaloe et al., 1992). Thus, there appears to be a temporal trend towards younger alkalic basalts in both the Lihue Basin and the south coast of Kaua`i.

An alternative approach to evaluating the temporal chemical evolution hypothesis is to examine the surface distribution of Koloa rock types (Fig. 18). The combination of our new results with previous sampling by Macdonald et al. (1960), Palmiter (1975), Clague and Dalrymple (1988), Maaloe et al. (1992) and Reiners et al. (1999) shows that ~60% of the surficial rejuvenated lavas are alkalic basalts and basanites, whereas only ~36% are foidites or melilite foidites and 4% are unknown (no rock samples; Fig. 18). We recognize that foidites and melilite foidites present lower degrees of partial melting (Clague and Frey, 1982), so they may have been produced in smaller volumes and therefore may not completely cover older alkalic basalts and basanites. To evaluate this issue, we utilized previous and new K-Ar ages of Koloa lavas (Clague and Dalrymple, 1988; Sano, 2006) and compared them to rock types using % normative nepheline, which is thought to correlate inversely with the degree of partial

melting (e.g., Clague & Dalrymple, 1982). The normative nepheline content of Koloa lavas range widely (<1% to 18%) with no temporal variation (Fig. 19). For example, at ~1 Ma all rock types were erupted. Furthermore, basanites were erupted throughout the period of Koloa volcanism and alkalic basalts are some of the youngest rather than oldest lavas, which is contrary to the hypothesis of Reiners et al. (1999) that suggest alkalic basalts should be the oldest. The oldest dated Koloa lava is a foidite, although none of the youngest lavas (<0.9 Ma) are foidites (Fig. 19). Therefore, our new results based on ages for 45 samples indicate there was no temporal evolution in rock type or extent of melting during Koloa volcanism. Thus, the extent of melting did not vary systematically as would be predicted by some melting models (e.g., Ribe & Christiensen, 1999)

Koloa lavas might be expected to show a temporal variation in source of composition that may be indicative of the mechanism responsible for rejuvenated volcanism. Rejuvenated lavas are characterized by relatively low $^{86}Sr/^{87}Sr$, and high $^{143}Nd/^{144}Nd$, and limited isotopic variation (Feigenson, 1984; Maaloe et al., 1992; Reiners & Nelson, 1998; Reiners et al., 1999; Lassiter et al., 2000; Yang et al., 2003). Koloa lavas show a relatively large range in Sr and Nd isotopes (Fig. 20) compared to Honolulu rejuvenated lavas (Reiners & Nelson, 1998). Few Koloa lavas that have been dated have been analyzed for Sr, Nd or Pb isotopes. However, chips from a drill core, which provide a stratigraphic order, were analyzed for Sr and Nd isotopes. These chips show significant variation (e.g.,

$^{87}Sr/^{86}Sr$ ratios of 0.703066 to 0.703365) but no systematic variation with depth (Reiners and Nelson, 1998).

Reiners and Nelson (1998) also noted a correlation of Sr and Nd isotope data with rock type for Koloa Volcanics. Such a correlation is important in understanding the causes of rock type variation. For example, if each rock type has a distinct source control and there is no temporal variation in rock type, then the source must be heterogeneous on a small scale. Our compilation of Sr and Nd isotope data show basanites and foidites/melilite foidites span nearly the entire isotopic range for Koloa lavas (Fig. 20). Thus, it would appear that there is no correlation of rock type with Sr and Nd isotopes and that all rock types were produced from a somewhat heterogeneous source. The same interpretation was reported for the wide range of rock types at Loihi volcano (basanitic to tholeiitic; Garcia et al., 1995), where it was related to a progressive change in partial melting. This explanation does not appear valid for Koloa volcanism.

6.2 Duration of Koloa Volcanism

Shield volcanism on Kaua`i has been dated at 5.1 to 4.1 Ma (McDougall, 1979; Sano, 2006). Post-shield lavas are rare on Kaua`i; the few dated lavas range from 3.5 to 4.1 Ma (McDougall, 1964; Clague and Dalrymple, 1988; Sano, 2006). Rejuvenated volcanism on Kaua`i is reported to extend from 3.65 to 0.375 Ma (Clague & Dalrymple, 1988; Hearty et al., 2005), the longest duration in the Hawaiian Islands. However, there is a ~1 m.y. age gap between the two oldest Koloa ages (3.65 and 2.6 Ma; Clague and Dalrymple, 1988; Fig. 22). This

gap led Tagami et al. (2003) to question whether the older age represents Koloa volcanism. The locality in Waimea Canyon that yielded the old age was visited and sampled. The new age for this sample is comparable to the previous age (3.86 ±0.06 vs. 3.65 ±0.03 Ma; Clagaue & Dalrymplme, 1988; Sano, 2006). Thus, the old age is considered valid. Unfortunately, this flow caps a hill and a thick breccia, so its stratigraphic relationship to younger rocks is unknown.

Another old age was obtained from a large (~3 m across) boulder on the southern bank of the N. fork Wailua River (3.58±0.05; Sano, 2006). New chemical analyses of these "old" samples show they are both basanites similar to some Koloa lavas (Fig. 22). The older lava has a relatively low $^{87}Sr/^{86}Sr$ ratio (0.70324), typical of Koloa rocks (Clague and Dalrymple, 1988). However, such geochemical features are also found among Hawaiian post-shield lavas, including on Kaua`i, Haleakalā, Kaho`olawe and Wai`anae volcanoes (Reiners et al., 1999; Sherrod et al., 2003; Sano, 2006; I. Van der Zander, 2005, pers. comm.). Therefore, the division of the post-shield and rejuvenation stages of Hawaiian volcanoes cannot be made based solely on geochemistry. This notion is supported by a recent study (Sinton, 2005) which suggests that the divisions of the volcanic stages of a Hawaiian volcano are field based, not geochemical. Thus, our assessment of the length of the volcanic hiatus between post-shield and rejuvenated lavas is 1 m.y. for Kaua`i (Fig. 21). This is comparable to the gap for Molokai (~1 m.y.; Clague et al., 1983), somewhat longer than for West Maui (0.6 m.y.; Tagami et al., 2003) but shorter than observed for Ko`olau volcano (1.3 m.y.; Ozawa et al., 2005). Despite an extensive effort during this

and previous geochronological studies (total of 55 dated samples; McDougall, 1964; Clague & Dalrymple, 1988; Hearty et al., 2005; Sano, 2006), no lavas with ages between 2.6 – 3.6 Ma have been found. The apparent gap in volcanism and the geochemical similarity of the 3.58-3.86 Ma lavas to post-shield basanites on other Hawaiian volcanoes, leads us to conclude that these older lavas are not part of Koloa volcanism. Instead, they are probably post-shield stage lavas, which would extend the range from 3.95 to 3.58 Ma.

New ages for southern Kaua`i extend the younger age extent for Koloa volcanism to as recently as 0.15 Ma (Tagami et al., 2005; Sano, 2006). These ages date lavas that were considered by Macdonald et al. (1960) and Palmiter (1975) as the youngest Koloa lavas. Given these younger ages, it is possible that Koloa volcanism may not be extinct (see section 6.6).

6.3 Source models for rejuvenation volcanism

Before evaluating the implications of our new Koloa data on origin of rejuvenated volcanism, key observations and models for their source are summarized below. Rejuvenated-stage lavas are moderately to strongly alkalic and are somewhat isotopically variable, which led to the suggestion that they formed by low degrees of partial melting of a heterogeneous source (Winchell, 1947; Macdonald et al., 1960; Macdonald, 1968; Jackson & Wright, 1970; Clague & Frey, 1982; Clague, 1987; Clague & Dalrymple, 1988; Maaloe et al., 1992). Rejuvenated lavas are isotopically distinct from shield lavas, although both types of lavas may share one or more common components (Bianco et al., 2005; Frey

et al., 2005). Processes such as high-pressure fractional crystallization and crustal contamination of shield magmas are inadequate as potential explanations for the isotopic and geochemical characteristics of rejuvenated lavas (Clague & Frey, 1982; Clague & Dalrymple, 1988; Maaloe et al., 1992; Reiners & Nelson, 1998; Lassiter et al., 2000; Yang et al., 2003). Instead, various source mixing scenarios have been invoked to describe the distinctive characteristics of these lavas. Brief summaries of recent scenarios are given below starting with a lithospheric source followed by a plume source.

A lithospheric source for rejuvenated lavas was suggested by Lassiter et al. (2000) based on the similarity of Os isotopes in some rejuvenated Koloa and Honolulu lavas, and in pyroxenite xenoliths found at Salt Lake Crater on O`ahu. Mineralogical analyses suggest these pyroxenite-bearing xenoliths formed at depths of ~60-90 km, which was assumed to be in the lithosphere (Lassiter et al., 2000: Bizimis et al., 2005). However, recent seismic studies (Li et al., 2004; Kind et al., 2005) suggest the lithosphere has thinned to ~60 km thick below Kaua`i which implies that the pyroxenite xenoliths may have come from a depleted component within the plume. The Salt Lake Crater pyroxenite xenoliths have Lu/Hf isotope systematics which lie on a 1 Ga isochron (Bizimis et al, 2005). Thus, the Salt Lake Crater pyroxenites may not have been derived from the ~90 m.y. Pacific lithosphere. Furthermore, another recent study employed Sr, Nd, Hf, and Pb isotopes to contend that there is a depleted component common to the Detroit Seamount and Hawaiian rejuvenated lavas that are plume-borne (Frey et al., 2005).

A plume-derived, three component mixture of pyroxenite, enriched peridotite, and depleted peridotite has been advocated (Bianco et al., 2005). This scenario is supported by Sr, Nd, Pb, and Hf isotope systematics, which supports a depleted plume component for Hawaiian shield and rejuvenated stage lavas (Frey et al., 2005). The enriched and pyroxenite components begin melting deeper than the depleted component because of their lower solidi (Bianco et al., 2005). The three-component mixture yields greater flexibility for modeling the compositional and isotopic ranges of Hawaiian shield and rejuvenated lavas. Unlike other geochemical models for the origin of rejuvenated lavas, Bianco et al. (2005) provided a mechanism (discussed below) for eruption of rejuvenated lavas.

6.4 Mechanisms for the generation of rejuvenated magmas

There are three main physical models for rejuvenated volcanism: (1) Lithospheric melting by conductive heating, (2) second zone of mantle plume melting, and (3) flexure-induced decompressional melting. Each model generates low degrees of partial melting and alkalic magma, which is characteristic of rejuvenated volcanism. These models make predictions about the possible gap between shield and rejuvenated volcanism, the duration of rejuvenated volcanism, and the source components for the rejuvenated lavas.

The lithospheric melting by conductive heating (CH) model generates magma as a mantle plume heats the base of the overriding lithosphere to asthenospheric temperatures (Gurriet, 1987). Plume-derived heat diffuses into

the lithosphere generating ~1-5% melt from a thermal anomaly 10-40 km wide with a melt thickness of 25-150 m at the base of the lithosphere (Gurriet, 1987). Recent seismic studies indicate that the lithosphere has thinned from 100 km under the island of Hawai`i to 60 km under Kaua`i (Li et al., 2004; Kind et al., 2005). This thinning may be in response to both thermal and physical erosion of the base of this lithosphere by the plume as it moves laterally away from the island of Hawai`i (Li et al., 2004; Ribe, 2004). Roll-like instabilities of plume-derived material at the base of the lithosphere may facilitate this extensive erosion, which could not achieved in a few million years by conductive heating alone (Ribe, 2004). The CH model predicts little or no gap between postshield and rejuvenated volcanism and a prolonged period of rejuvenated volcanism (up to 5 m.y.; Gurriet, 1987).

A second zone of plume melting (SP) was found in a numerical model simulating 3-D convection of a Newtonian viscosity mantle plume beneath an overriding lithosphere (Ribe & Christensen, 1999). The modeling predicts a small zone of melting 320 to 520 kilometers downstream from the primary melting zone. Melting occurs as the buoyant plume spreads laterally and thins under the lithosphere causing it to rise again (Ribe & Christensen, 1999). Melt is derived primarily from the base of the plume, with little or no contribution from the lithosphere except by assimilation as the magma ascends (Ribe & Christensen, 1999). This model predicts a 1 - 2 m.y. hiatus in volcanism and a 2 - 3 m.y. duration for rejuvenated volcanism.

Flexure-induced decompressional melting (FM) is predicted from the rapid growth of Hawaiian shield volcanoes. These giant volcanoes depress the underlying lithosphere constructing a donut-shaped "flexural arch" at a radius that reflects the elastic thickness of the plate (Jackson & Wright, 1970; Clague & Dalrymple, 1987; Bianco et al., 2005). The plume beneath the flexural arch decompresses as it is flexes upward (Jackson & Wright, 1970; Clague & Dalrymple, 1987; Bianco et al., 2005). The plume material is presumed to be near its solidus, producing a moderate volume (up to 20 km^3/m.y. of alkalic melt within the flexural arch) by drawing magma from the decompressing mantle below an area of ~4760 km^2 (equal to a circular area of radius 39 km), although it does not assume a melt focusing mechanism (Bianco et al., 2005). This is comparable to the volume produced by the secondary zone melting model. This model predicts that rejuvenation volcanism takes place when the island rides over the flexural arch. Based on the ~10 cm/year rate of plate motion (e.g., Garcia et al., 1987), volcanism should occur ~2 m.y. after the volcano drifts downstream from the plume stem. The duration of volcanism should be ~1.75 – 2.25 m.y. Pooled, plume-derived melt at the base of the lithosphere escapes to the surface through stress fractures created in the lithosphere as a result of passage over the flexural arch (Bianco et al., 2005). This model has the added benefit of predicting volcanism on the flexural arch away from the Hawaiian chain, which is observed north of Oahu and south of the island of Hawaii (Lipman et al., 1989; Clague et al., 1990).

6.5 Evaluation of mechanisms for rejuvenated volcanism

One of the objectives of this study was to evaluate current models for rejuvenated volcanism using our new petrologic and volume data combined with new (Tagami et al., 2005; Hearty et al., 2005; Sano, 2006) and existing (McDougall, 1964; Clague & Dalrymple, 1988) age data. Based on these results, we have examined four key features of these models to evaluate: (1) length of volcanic hiatus between post-shield and rejuvenated stage of volcanism (m.y.), (2) duration of rejuvenated volcanism (m.y.), (3) melt volume flux (km^3/m.y.), and (4) source for rejuvenated lavas (section 6.3).

Volcanic hiatus length

The flexure-induced decompressional melting model (FM) predicts rejuvenated volcanism could start no sooner than when the volcano is 175 – 225 km from the active shields, depending on the load (e.g., Bianco et al., 2005). This prediction is based on calculations which consider an effective elastic thickness of the lithosphere of 25 – 35 km. At the current velocity of the Pacific plate (~10 cm/yr northwest; Clague & Dalrymple, 1987; Garcia et al., 1987), this model predicts a hiatus between post-shield and rejuvenated lavas on the order of 0.85 – 1.45 m.y. This assumes post-shield volcanism continues for ~80-90 km downstream from the area of loading (e.g., Kohala volcano is ~95 km from Kīlauea volcano and ended its postshield stage at ~60 ka; Spengler and Garcia, 1988). This value is within the range for the observed hiatus on Kaua`i and

other examples of Hawaiian rejuvenation except West Maui which has a volcanic hiatus of 0.6 m.y. and cannot be explained by any of the proposed models.

The SP model proposes a volcanic hiatus of 1 – 2 m.y. (Ribe & Christensen, 1999; Table 5). This range is also consistent with the gaps in volcanism observed on all of the Hawaiian examples of rejuvenated volcanism, except West Maui. It should be noted that there are exceptions to the normal Hawaiian volcanism model (Walker, 1990). For example, post-shield volcanism on Hāleakala volcano has continued well beyond the normal period (~1 m.y.; Sherrod et al., 2003), which may lead to a narrow age gap between post-shield and rejuvenated volcanism. However, there is no evidence for prolonged post-shield volcanism on West Maui (Tagami et al., 2003). The CH model predicts little or no volcanic hiatus from the shield to rejuvenated-stage of volcanism (Gurriet, 1987), which is inconsistent with the observed 0.6 - 1.3 m.y. gaps for rejuvenated volcanism (Fig. 21). Gurriet (1987) recognized this problem and suggested the magmas were stored prior to eruption. There is no petrologic or seismic evidence in support of this storage argument. The high MgO content of most rejuvenated magmas has been used to suggest they are relatively primitive magmas that were not stored or fractionated prior to eruption (e.g., Maaloe et al., 1992).

Duration of volcanism

The FM model predicts a volcanic duration between 1.75 – 2.25 m.y. (Table 5), depending on the elastic plate thickness and amount of loading

(Bianco et al., 2005). The maximum duration (2.25 m.y.) is comparable to the observed duration of the Koloa Volcanics (~2.45 m.y). The SP model suggests the duration of rejuvenation volcanism is 2- 3 m.y. (Ribe & Christensen, 1999). This range is consistent with the duration of rejuvenated volcanism on Koloa and Ni`ihau (Table 5), but considerably longer than observed on islands south of Kaua`i (all less than 1 m.y.). The CH model predicts a longer duration of rejuvenated volcanism (up to 5 m.y.; Gurriet, 1987) than observed on Kaua`i (2.45 m.y.). However, Koloa volcanism may not have ended. The most recent eruption is 0.15 Ma (Sano, 2006). Nonetheless, Koloa volcanism appears to be wanning.

Melt Volume Flux

The average flux rate for Koloa rejuvenated volcanism is ~24 km^3/m.y. based on our new lava volume estimate of ~58 km^3 (Table 5) and the new 2.45 m.y. estimate for the duration of volcanism (Clague & Dalrymple, 1988; Sano, 2006). This is the first quantitative estimate of the melt flux for Hawaiian rejuvenated volcanism. It is more than twice the guesstimate of Walker (1990), which was used for SP and FM modeling. Other estimates include <1% of the shield volume and <<1% (Clague and Dalrymple, 1987; 1988). Given a new volume estimate of 57,600 km^3 for the Kauian shield volcano (Robinson & Eakins, 2006), our new volume estimate indicates that Koloa volcanics represent ~0.1% of the total shield volume.

This new melt flux rate estimate is a minimum, since some fraction of the melt was not erupted due to storage in the crust and mantle (e.g., Francis et al., 1993), or it remained in the source because of incomplete extraction (e.g., Gurriet, 1987). Furthermore, it is unlikely that the flux of Koloa volcanism was constant. A histogram of ages suggests that eruptive frequency may have reached a maximum from 1.26 to 1.75 Ma and was lower before and after this peak (Fig. 23). Thus, any scenario for rejuvenated volcanism must be able to duplicate this roughly Gaussian pattern of volcanism and produce relatively high melt flux rates (>24 km^3/m.y.). However, the age pattern for Koloa volcanism contrasts with the two pulses of Honolulu volcanism (Ozawa et al., 2005) because no second major pulse of Koloa volcanism seems to have occurred.

Each of the physical models for rejuvenated volcanism attempted to generate the known magma flux rate at the time it was developed. The CH model was designed to produce 100 km^3 of magma per m.y. or ~1% of the total volume of the shield (Clague & Dalrymple, 1987; Gurriet, 1987), which is a relatively high flux rate. The CH model was initially derived from the lithospheric thinning and reheating concept proposed by Crough (1978). Gurriet (1987) modified this approach by considering the effect of using different bulk compositions and their related solidus temperatures. These compositions influence the thickness of the molten layer and the extent of melting (Gurriet, 1987).

The FM and SP models were designed to generate maximum magma flux rates of ~13 km^3/m.y. (Ribe & Christensen, 1999; Bianco et al., 2005), which is only ~55% of the average rate for Koloa volcanism and probably much less than

the peak rate. Furthermore, unpublished bathmetric data suggests the volume of submarine Koloa lavas may be at least equal to the subaerial volume (B. Taylor, 2005, pers. comm.). If true, the average melt volume flux for the Koloa Volcanics would be ~48 km^3/m.y. A value considerably larger than that suggested by the FM and SP models, although less than originally proposed by the CH model (<100 km^3/m.y.; Gurriet, 1987).

Model for Koloa Volcanism

None of the existing models for the generation of rejuvenated lavas accounts for all the observations of Hawaiian rejuvenated volcanism (Table 5). The SP model suggests an eruptive hiatus (1 – 2 m.y.) which closely matches that observed on Kaua`i (1 m.y.), O`ahu (1.3 m.y.), and Molokai (0.8 m.y.). Furthermore, the SP model does well predicting the 2.45 m.y. eruptive duration of the Koloa Volcanics (2 – 3 m.y.). The melt volume flux for the SP model is less than observed (Table 5). However, at the time the SP model was derived, there were no quantitative volume measurements for rejuvenated volcanism available, and the estimate was based on the best available estimate. The FM model successfully predicts the hiatus (0.8 – 1.45 m.y.) but suggests a volcanic duration, which at its maximum of 2.25 m.y. (Bianco et al., 2005), is somewhat less than the observed duration (2.45 m.y.). As with the SP model, the melt volume flux estimate for the FM model is the less than observed on Kaua`i. We attribute this discrepancy to the volume estimates available at the time of modeling and are not necessarily a fatal flaw of either the SP or FM models. The

CH model does not successfully predict the volcanic hiatus and duration. Furthermore, the CH model proposes a lithospheric source, which recent isotopic and seismic evidence does not support (Bizimis et al., 2005; Frey et al., 2005). The SP model does best at explaining the new Koloa age and volume data, and the plume source for rejuvenation lavas. However, the FM model does predict the observed volcanic hiatus and suggests a duration comparable to that observed for rejuvenated lavas. Refinement of the SP and FM models with our new volume estimate may delineate which of the two models best explain the causes of rejuvenated volcanism.

6.6 Trends in duration and surface area of Hawaiian rejuvenated volcanism: Implications for future eruptions

The duration of rejuvenated volcanism along the Hawaiian chain increases away from the active shield volcanoes on the Island of Hawai`i towards Kaua`i and Ni`ihau (Fig. 24a). Kaua`i has the longest duration (~2.45 m.y.; Sano, 2006; Clague & Dalrymple, 1988) of rejuvenated volcanism in the Hawaiian Islands, although Ni'ihau's record may be of similar duration (Fig. 24a). Islands southeast of Kaua`i have much shorter durations of rejuvenated volcanism. For example, the Honolulu Volcanics on O`ahu have an eruptive duration of ~0.75 m.y. (Gramlich et al., 1971; Lamphere & Dalrymple, 1980; Ozawa et al., 2005), whereas the four vents of the Lahaina Volcanics on W. Maui (McDougall, 1964; Naughton et al., 1980; Tagami et al., 2003) and the Kalaupapa Basalts from Molokai (Clague et al., 1983) are even shorter (~0.2 m.y.).

The surface area of rejuvenated lavas (Sherrod et al., 2005) also increases away from the active shield volcanoes, with the exception of Ni`ihau (Fig. 24b), which has undergone extensive erosion and subsidence (Clague et al., 2000). The rejuvenated lavas on Ni`ihau (Kiekie Volcanics) are abundant, with single cone volume estimates of ~7 km^3 (D. Clague, 2006, pers. comm.). Much of Ni`ihau's rejuvenation lavas are now submarine and were not considered in surface area estimates (Fig. 24b). If Ni`ihau is not included in the comparison of distance vs. surface area of rejuvenated lavas, the correlation coefficient improves from 0.31 to 0.87 (Fig. 24b). There is a significant difference in the surface area of the Koloa Volcanics when compared to rejuvenation lavas south of Kaua`i (Fig. 24b). Although the suface area vs. distance trend is mostly defined by the Kaua'i data point, the trend is suggestive that the islands of Oahu, Molokai, and Maui may experience future rejuvenated stage eruptions. However, it is important to note that not all Hawaiian shield volcanoes host rejuvenation-stage volcanism (e.g., Wai'anae). The lack of rejuvenation lavas on all Hawaiian volcanoes complicates predictions concerning their life stages. Nonetheless, our Koloa volume data, and comparisons of eruptive duration and surface area of Hawaiian rejuvenation lavas offers an indication that additional eruptions on the islands with rejuvenated lavas are possible.

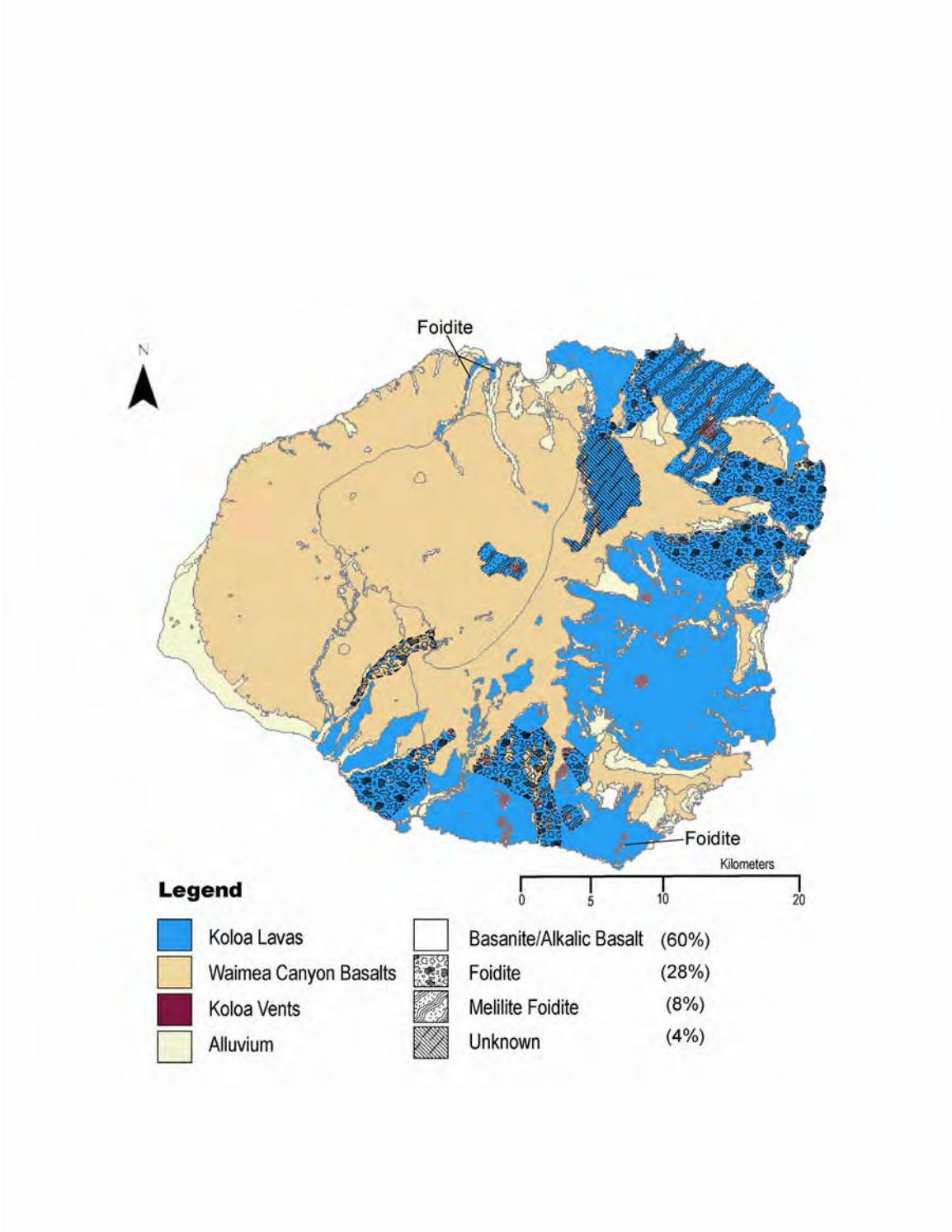

Figure 18. Surficial distribution of Koloa rock types. Alkalic basalts and basanites comprise 60% of the rejuvenated surface of Kaua`i, while foidites and melilite foidites cover 36% of the rejuvenated surface. Data from Macdonald et al.(1960), Palmiter (1975), Clague & Dalrymple (1988), Maaloe et al. (1992), Sherrod et al. (2006).

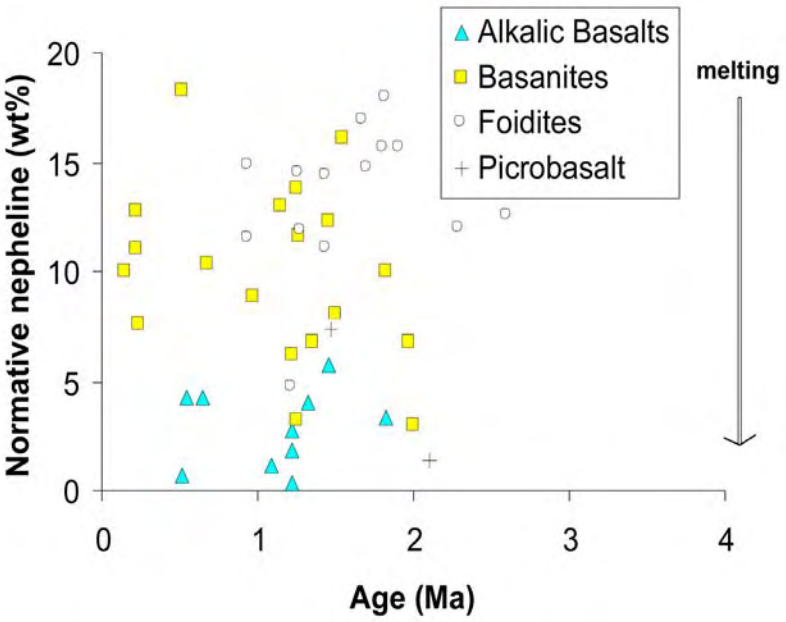

Figure 19. Normative nepheline vs. age for 45 dated Koloa samples. Normative nepheline is thought to reflect the degree of partial melting (e.g., Clague and Frey, 1982). There is no correlation between these two variables. All rock types were erupted ~1 m.y., indicating that the percent of partial melting is not related to age. Age data from Clague & Dalrymple (1988) and Sano (2006); normative nepheline values based on whole-rock data from Clague & Dalrymple (1988) and Appendix C.

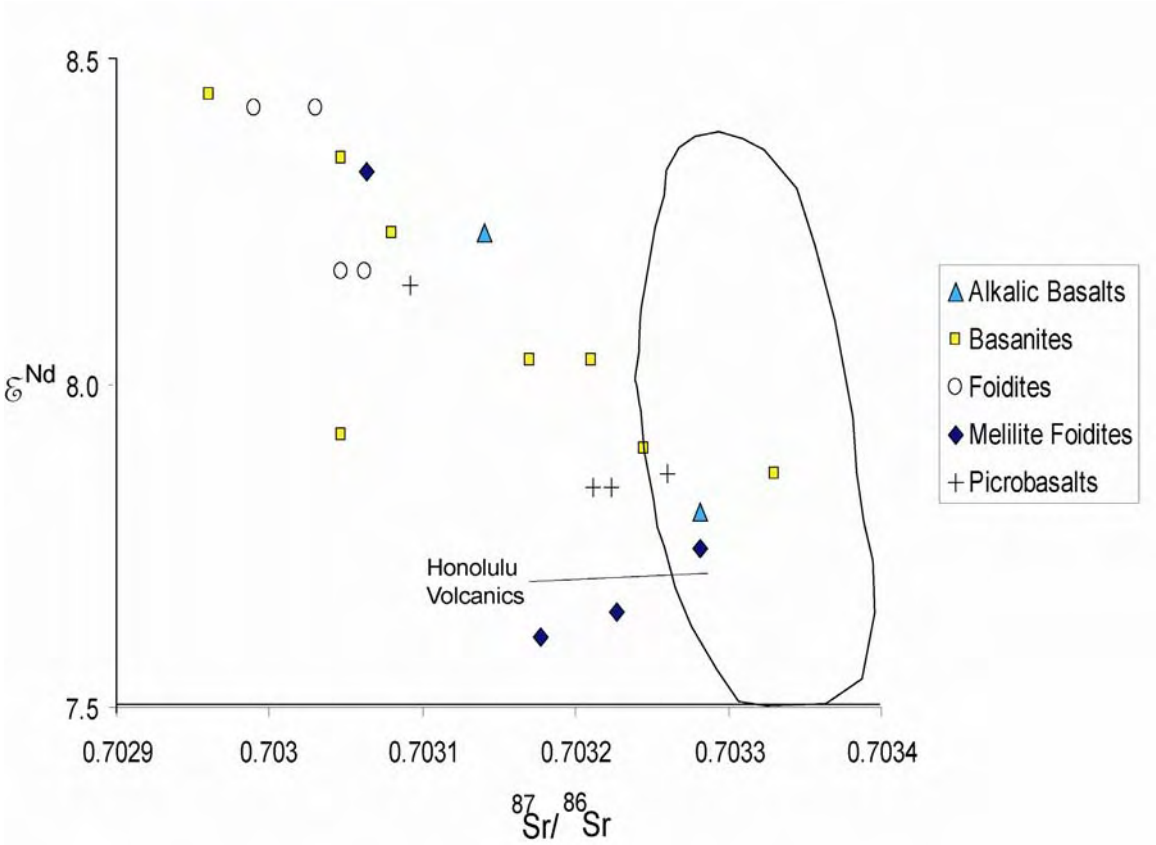

Figure 20. Sr and Nd isotopes vs. rock type for Koloa lavas. There is no relationship between rock type and Nd or Sr isotopic values (e.g., basanites are distributed throughout the plot). Thus, the source does not apparently play a role in controlling rock types. The variation in Sr and Nd isotopes suggest the source for rejuvenated lavas is heterogeneous with at least three components to explain the scatter, assuming sample leaching was sufficient to remove alteration effects. Data from Feigenson (1984), Maaloe et al. (1992), and Reiners & Nelson (1998). Field data from Xu et al. (2005).

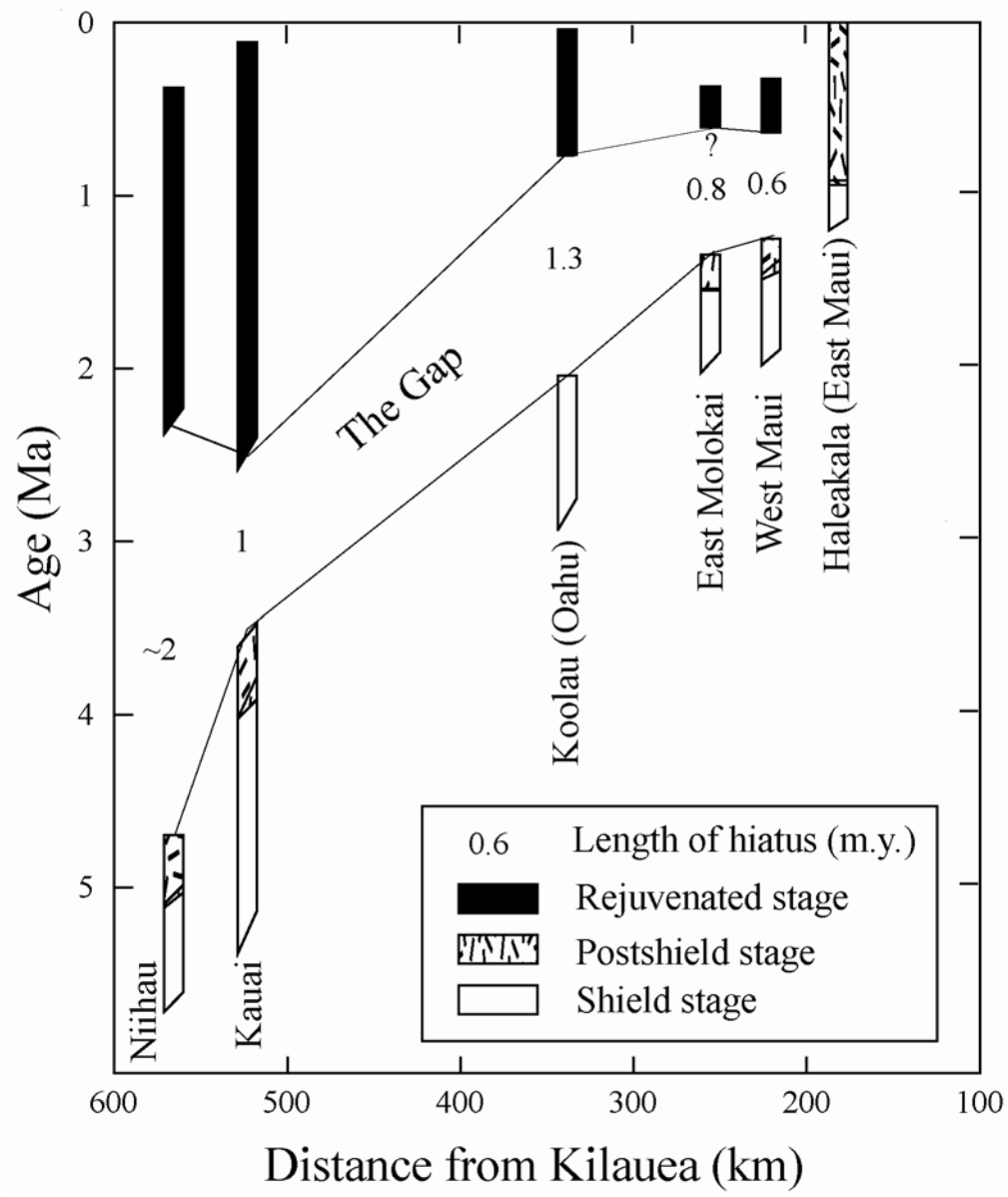

Figure 21. Age ranges for shield, postshield, and rejuvenated stages for the main Hawaiian Islands versus distance from Kīlauea Volcano. A recent study of Haleakalā shows no gap in volcanism and is thought to have a prolonged post-shield stage (Sherrod et al., 2003). Note that this figure presents a shorter period for the duration of Kaua`i rejuvenated volcanism then indicated by Clague & Dalrymple (1988; see discussion). The size of the gap is critical to modeling the origin of rejuvenated volcanism. Figure modified after Tagami et al. (2003) and includes new Koloa ages from Hearty et al. (2005) and Sano (2006).

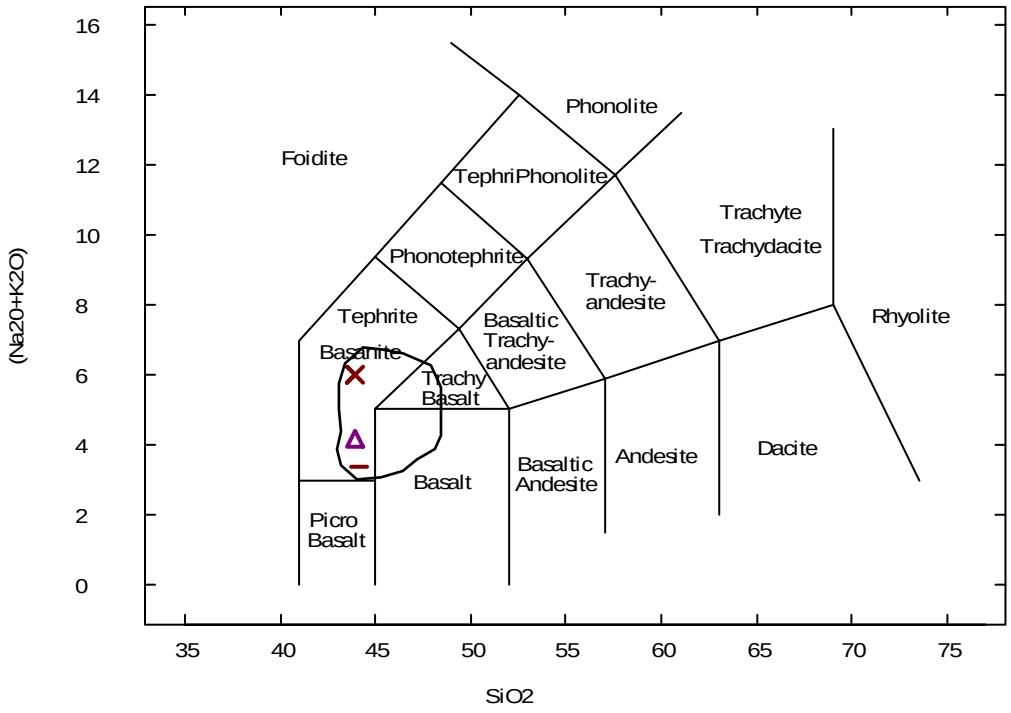

Figure 22. Total alkali vs. silica diagram (TAS) diagram for Hawaiian postshield basalts and older basanite samples from Kaua`i. Sample 86KA12 collected by Clague & Dalrymple (minus sign; 1988) plots closely with older basanites from this study (X = 3.58 Ma, triangle = 3.86 Ma; Sano, 2006). Notice the similarity of these rocks (Clague & Dalrymples 86KA12 and samples from this study) to post-shield rocks from other Hawaiian Islands (e.g. Waianae and Haleakala; data for field from Presley et al., 1997 and Sherrod et al., 2003).

Table 5. Comparison of rejuvenation volcanism models and data from Koloa Volcanics (Jackson & Wright, 1970; Feigenson, 1984; Gurriet, 1987; Clague & Dalrymple, 1987; Clague & Dalrymple, 1988; Maaloe et al., 1992; Ribe and Christensen, 1999; Lassiter et al., 2000; Li et al., 2004; Bianco et al., 2005; this study).

Mechanism	Average Melt Volume Flux (km^3/m.y.)	Length of Volcanic Hiatus	Duration of Rejuvenated Volcanism
Lithospheric Melting by Conductive Heating **(CH)**	<100	small (<0.25 m.y.) or no gap	long (~5 m.y.)
Secondary Zone of Mantle Plume Melting **(SP)**	10	1 - 2 m.y.	2 - 3 m.y.
Flexure-induced Decompressional Melting **(FM)**	13	0.85 - 1.45 m.y.	1.75 - 2.25 m.y.
Koloa Volcanics subaerial (observed)	24	1 m.y.	2.45 m.y.

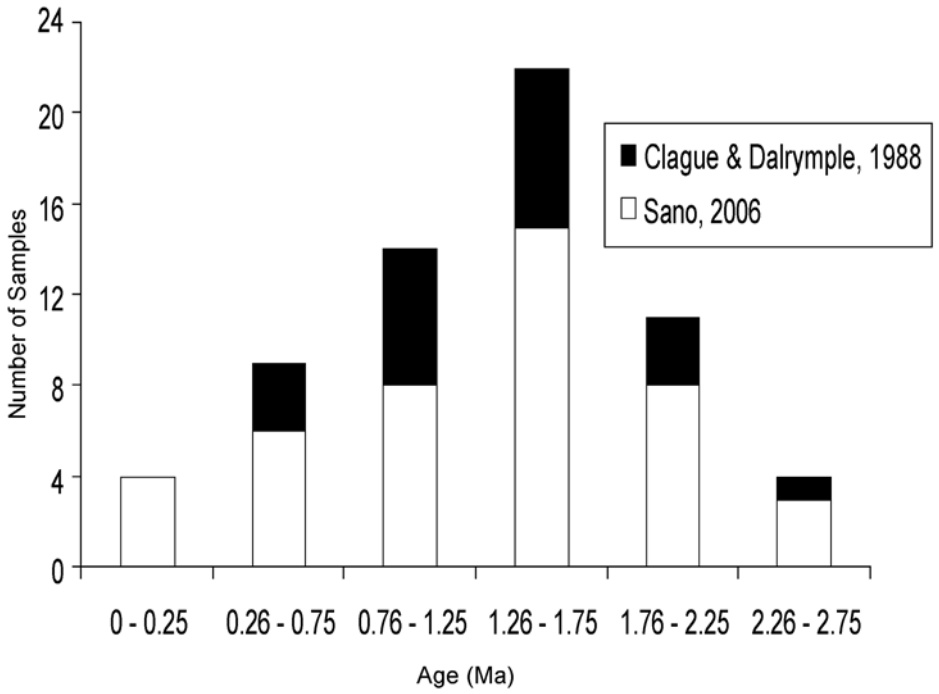

Figure 23. Histogram of Koloa lava ages. This plot shows a peak in volcanism between 1.26 – 1.75 Ma and that the pattern for melt volume flux for Koloa volcanism was apparently Gaussian. Hearty et al. (2005) Ar-Ar age of 0.375 Ma is included with Sano (2006). Data from Clague and Dalrymple (1988), Sano (2006).

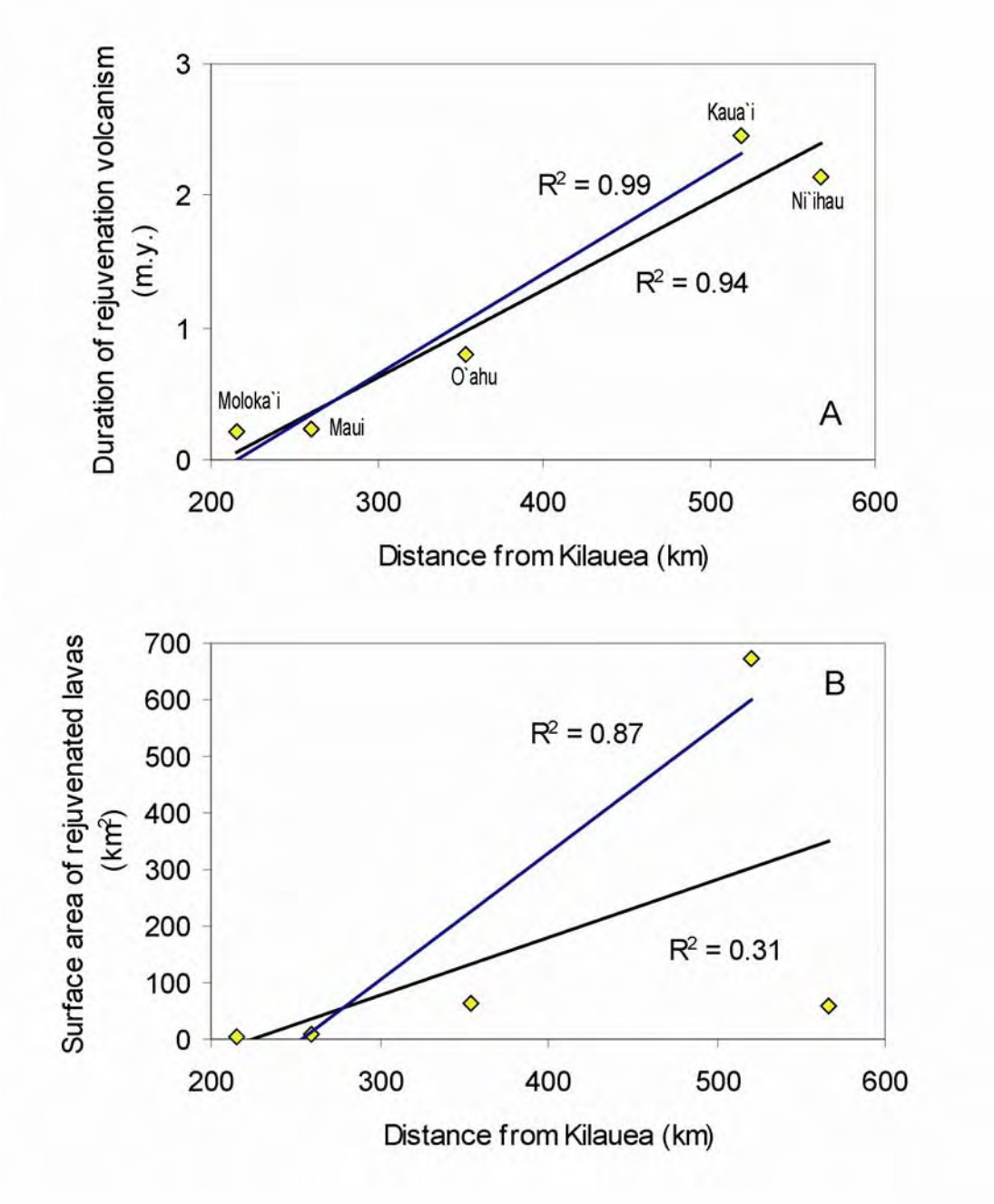

Figure 24. Variations in rejuvenated volcanism along the Hawaiian chain. a. Duration of rejuvenated volcanism vs. distance from Kīlauea Volcano. b. Surface area of rejuvenated lavas vs. distance from Kīlauea Volcano. Areas of volcanism (diamonds) from left to right are W. Maui, Moloka`i, O`ahu, Kaua`i, and Ni`ihau. The duration of rejuvenation volcanism increases from W. Maui to Ni`ihau. Plotting a second trend line without Ni`ihau, which has undergone extensive erosion and subsidence, yields a higher correlation coefficient (0.99). The surface area plot shows a similar trend. However, Ni`ihau has extensive areas of submarine rejuvenated volcanism (Clague et al., 2000). A trend line without Ni`ihau improves the correlation coefficient to 0.87. These plots are suggestive that the islands south of Kaua`i (O`ahu, Moloka`i, and Maui) may experience renewed rejuvenation volcanism. Data from McDougall (1964), Gramlich et al. (1971), Lamphere & Dalrymple (1980), Naughton et al. (1980), Clague et al. (1983), Tagami et al. (2003), Sherrod et al. (2004), and Ozawa et al. (2005).

7.0 Conclusions

New field and petrologic work on the Koloa Volcanics are combined with a tandem geochronological study by colleagues at Kyoto University to assess models for rejuvenated volcanism. The key variables that were determined were: Length of the gap between shield and rejuvenated volcanism, in addition to duration and volume of rejuvenated volcanism. Other variables that were examined include: Temporal variation in rock types, surface distribution of rock types, and the possibility of future rejuvenation-stage eruptions on the Hawaiian Islands.

The new results show Koloa lavas were erupted from 2.6 – 0.15 Ma with the majority of eruptions occurring between 1.26 – 1.75 Ma. A previous study proposed the oldest Koloa lavas were 3.65 Ma. However, two samples (3.58 and 3.86 Ma) dated by our colleagues in Kyoto are geochemically similar to Hawaiian post-shield basalts on Haleakala and Wai`anae volcanoes. Furthermore, despite a total of 45 K-Ar ages a gap in volcanism between 3.6-2.6 Ma remains. Thus, the volcanic hiatus between the shield stage and the rejuvenated stage of volcanism on Kaua`i is 1 m.y., not <0.25 m.y. as previously suggested.

Contrary to a previous suggestion, there is no temporal correlation, or a decrease in the extent of partial melting during Koloa volcanism. The youngest rocks are not strongly alkalic. Instead, weakly alkalic basalts were erupted throughout the duration of volcanism, and alkalic basalts and basanites cover ~60% of the rejuvenated surface of Kaua`i.

Water well and field relationships were used to make a conservative estimate for the volume of rejuvenated volcanism on Kaua`i, the first quantitative estimate for a Hawaiian volcano. This vesicle corrected estimate is ~58 km^3, which is a conservative estimate for subaerial Koloa Volcanics. Given the 2.45 m.y. eruptive duration of Koloa lavas, this produces an average melt volume flux of ~24 km^3/m.y. for the Koloa Volcanics. Yet the Koloa lavas are thought to be pervasive on the submarine flanks of the island with a volume equal to that of the subaerial lavas on Kaua`i. If this is true, the melt volume flux for the Koloa Volcanics would be at least ~48 km^3/m.y. This value is much larger than predicted by the SP and FM models. However, this may not be a fatal flaw of either model given that their predictions were based on the volume estimates available at the time. Although the CH model does well predicting a large (>100 km^3/m.y.) melt volume flux, this model does not account for the observed hiatus and predicts a longer duration. It also ultilizes a lithospheric source, in contrast to new evidence for a plume-derived source.

Hawaiian rejuvenated volcanism sequences show a range of volcanic hiatuses from 0.6 to 1.3 m.y., a duration up to 2.45 m.y. on Kaua`i, and evidence for a plume source for rejuvenated volcanism. These observations are generally consistent with the predictions of the SP and FM models. However, the FM model predicts a maximum duration (2.25 m.y.), which is less than observed on Kaua`i (2.45 m.y.), where volcanism may not have ended. Therefore, among current models for rejuvenated volcanism, the SP model does the best job in predicting the observed features.

8.0 Future Work

The scope of this study provided opportunities to investigate a vast portion of the Koloa Volcanics. However, there are still areas that have not been explored, and lavas that have not been sampled. In addition to field observations, there are major questions that remain unanswered concerning the evolution of the island, and the timing of certain events (i.e., Haupu member). The following questions are given with the hope that future studies may address these issues.

1. *Origin of Lihue Basin? A*re the Koloa rocks at the bottom of the cores examined by Reiners & Nelson (1998) and Reiners et al. (1999) similar to other 'older' rocks on the island in the upper reaches of the canyons and valleys, or the summit lavas? Specifically, are the foidic rocks at the summit region similar to the foidic rocks found in the cores of the basin by Reiners & Nelson (1998)? Are the lavas in the Lihue Basin a result of the two cones presently residing on its surface (Kilohana and Hanahanapuni)? If not, where did these other lavas originate?

2. *Extent of Postshield?* Are the Haupu member and the Olokele member related? These post-shield lavas may impact the volcanic hiatus since the lavas underlying the Haupu member are 4.1 Ma.

3. *Start of Koloa Volcansim?* How do the summit lavas compare to the lavas in the upper reaches of Wainiha, Lumahai, Hanalei, Koula, and Kahana valleys; Olokele and Waimea Canyons? Are these lavas possibly the oldest from Koloa?

4. *Volume?* What is the total (subaerial and submarine) of Koloa lavas? More Koloa lavas exist in the submarine depths offshore Kaua`i (Clague et al., 2006). Continued mapping and sampling of these lavas will certainly increase the volume estimate. B. Taylor (2005, pers. comm.) has suggested that the volume of submarine Koloa lavas may be equal to or greater than the subaerial portion. A cruise to survey and sample these submarine lavas is planned for 2007. Additional drilling on the island within the Koloa Volcanics may provide volume data in areas this study was unable to determine, and was forced to extrapolate from nearby well or field data.

5. *Rift Zones?* Are the rift zones defined by Macdonald et al. (1960) related by age or rock type?

Appendix A. Petrographic summary of new Koloa lavas

Primary minerals (size of largest grain)						**Secondary alteration**			**Classification**	**Rock Type**	**Xeno**
Slide	olivine	cpx	neph	mel	plag	iddingsite	calcite	zeolites			
0218-2	sub	mx	-	-	mx	major	-	-	Basalt	-	-
0218-3	an/sub	mx	-	-	mx	minor	-	-	Basalt	-	-
0219-3b	eu	mx	-	-	mx	minor	-	-	Basalt	Bas	-
0220-1	sub/eu	mx	-	-	mx	major	-	-	Basalt	-	-
0220-2	an	mx	-	-	mx	major	-	-	Basalt	-	-
0220-3	sub	mx	-	-	mx	minor	-	-	Basalt	Bas	-
0220-5	sun	mx	-	-	mx	minor	-	-	Basalt	-	-
0221-1	sub/eu	mx	-	-	mx	major	-	-	Basalt	-	-
0221-2	eu	mx	-	-	mx	major	-	-	Basalt	-	-
0221-3	sub	mx	-	-	mx	major	-	-	Basalt	-	-
0223-1	sub	mx	-	-	mx	major	-	-	Basalt	-	-
0223-2	sub	mx	-	-	mx	major	-	-	Basalt	-	-
0223-5	sub	mx	-	-	mx	major	-	-	Basalt	-	-
0225-1	sub	mx	-	-	ph	minor	-	-	Basalt	-	-
0226-1	sub	mx	-	-	mx	major	-	√	Basalt	-	-
0228-2	sub/eu	mx	-	-	mx	-	-	-	Basalt	Bas	-
0301-1	sub	mx	-	-	mx	minor	-	-	Basalt	Bas	-
0301-2	sub/eu	-	-	-	mx	major	-	-	Basalt	-	-
0301-3	sub	mx	-	-	mx	minor	-	-	Basalt	-	-
0301-6	eu	mx	-	-	mx	minor	-	-	Basalt	-	-
0301-10	an	mx	-	-	ph	major	-	√	Basalt	-	-
0302-2	sub	mx	-	-	mx	major	-	-	Basalt	-	-
0302-4	sub	mx	-	-	mx	minor	-	-	Basalt	-	-
0302-5	sub/eu	mx	-	-	mx	major	-	-	Basalt	-	-
0621-1	sub	mx	-	-	mx	minor	-	-	Basalt	-	-
0622-2	sub/eu	mx	-	-	mx	major	-	-	Basalt	-	-

Appendix A. cont.

0622-3	sub	mx	-	-	mx	minor	-	-	Basalt	-	-
0622-4	sub	mx	-	-	mx	minor	-	-	Basalt	-	-
0622-5	an/sub	ph	-	-	mx	major	-	-	Basalt	-	-
0622-6	sub	ph	-	-	mx	minor	-	-	Basalt	-	-
0625-1	sub	mx	-	-	mx	minor	-	-	Basalt	-	-
0625-2	an/sub	-	-	-	mx	minor	-	-	Basalt	-	-
0625-5	an/sub	mx	-	-	mx	minor	-	-	Basalt	-	-
0626-1	sub/eu	ph	-	-	mx	-	-	-	Basalt	Bas	-
0626-3	an/sub	mx	-	-	mx	minor	-	√	Basalt	-	-
0626-4	sub/eu	mx	-	-	mx	minor	-	-	Basalt	-	-
0626-5	eu	mx	-	-	mx	minor	-	-	Basalt	-	-
0628-1	eu	mx	-	-	mx	minor	-	-	Basalt	-	-
0628-2	sub	mx	-	-	mx	major	-	√	Basalt	-	-
0628-3	sub	mx	-	-	mx	major	-	-	Basalt	-	-
0628-5	sub	mx	-	-	mx	minor	-	-	Basalt	-	-
0629-2	sub/eu	ph	-	-	mx	minor	-	-	Basalt	-	W
0629-3	an/sub	mx	-	-	mx	minor	-	-	Basalt	-	-
0629-4	an/sub	mx	-	-	mx	major	-	-	Basalt	-	-
0630-1	sub	mx	-	-	mx	major	-	-	Basalt	-	-
0701-1	eu	mx	-	-	-	minor	-	-	Basalt	-	-
0701-2	sub	mx	-	-	mx	minor	-	-	Basalt	-	-
0702-1	sub	mx	-	-	mx	minor	-	-	Basalt	-	-
0702-6	sub	mx	-	-	mx	minor	-	-	Basalt	-	-
0704-2	sub	mx	-	-	mx	minor	-	-	Basalt	-	-
0705-1	sub	ph	-	-	mx	minor	-	-	Basalt	-	-
0705-3	sub/eu	mx	-	-	mx	-	-	-	Basalt	Bas	-
0705-4	sub	mx	-	-	mx	minor	-	-	Basalt	-	-
0706-1	sub	mx	-	-	mx	minor	-	-	Basalt	-	-
0706-2	sub	mx	-	-	mx	minor	-	-	Basalt	-	-
0707-4	sub	mx	-	-	mx	minor	-	-	Basalt	-	-

Appendix A. cont.

0707-5	sub	ph	-	-	mx	minor	-	-	Basalt	-	-
0707-6	an/sub	mx	-	-	mx	-	-	-	Basalt	Bas	-
0707-7	an/sub	mx	-	-	mx	major	-	-	Basalt	-	-
0709-1	sub	mx	-	-	mx	minor	-	-	Basalt	-	-
0709-2	an/sub	ph	-	-	mx	minor	-	-	Basalt	-	-
0709-3	sub	ph	-	-	mx	-	-	-	Basalt	AB	-
0709-4	an/sub	ph	-	-	mx	minor	-	-	Basalt	-	-
0709-5	sub	mx	-	-	mx	minor	-	-	Basalt	Bas	-
0710-3	sub	mx	-	-	mx	major	-	-	Basalt	-	-
0710-5	an/sub	mx	-	-	mx	minor	-	-	Basalt	-	-
KV03-02	sub/eu	ph	-	-	mx	minor	√	-	Basalt	Bas	-
KV03-05	an	ph	-	-	mx	minor	-	-	Basalt	Bas	W
KV03-06	sub	ph	-	-	mx	minor	-	-	Basalt	AB	-
KV03-07	an/sub	mx	-	-	mx	minor	√	-	Basalt	Bas	-
KV03-08	sub	mx	-	-	mx	minor	√	-	Basalt	Bas	-
KV03-11	sub	mx	-	-	mx	-	-	-	Basalt	AB	-
KV03-12	sub	ph	-	-	mx	-	-	-	Basalt	Bas	-
KV03-14	an	mx	-	-	mx	major	-	-	Basalt	-	-
KV03-16	sub	ph	-	-	mx	major	-	√	Basalt	-	-
KV03-17	an/sub	mx	-	-	mx	-	-	-	Basalt	Bas	-
KV03-19	sub	ph	-	-	mx	rims	-	-	Basalt	PB	-
KV03-20	sub/eu	ph	-	-	mx	-	-	-	Basalt	AB	-
KV03-21	sub	ph	-	-	mx	minor	-	-	Basalt	Bas	-
KV03-22	sub	ph	-	-	mx	minor	-	-	Basalt	-	-
KV03-23	sub	mx	-	-	mx	minor	-	-	Basalt	-	-
KV03-26	sub	mx	-	-	mx	minor	-	-	Basalt	-	D
KV03-27	sub	mx	-	-	mx	minor	-	-	Basalt	Bas	-
KV04-01	sub	mx	-	-	ph	minor	-	-	Basalt	AB	-
KV04-03	sub	mx	-	-	mx	minor	-	-	Basalt	AB	-
KV04-04	sub/eu	mx	-	-	mx	minor	-	-	Basalt	Bas	-

Appendix A. cont.

KV04-06	sub	mx	-	-	mx	minor	-	-	Basalt	Bas	-
KV04-07	sub	mx	-	-	mx	minor	-	-	Basalt	-	-
KV04-10	sub	ph	-	-	mx	minor	-	-	Basalt	Bas	-
KV04-13	sub/eu	mx	-	-	mx	minor	-	-	Basalt	AB	-
KR-3	an	mph	-	-	-	-	√	-	Basalt	Bas	-
0218-1	sub/eu	mx	mx		-	minor	-	-	Foidite	F	-
0218-4	sub	-	mx	mx	-	major	-	-	Foidite	-	-
0219-2	eu	mx	mx	-	-	minor	-	-	Foidite	-	-
0220-4	sub	mx	mx	-	-	minor	-	-	Foidite	F	-
0220-6	an/sub	mx	-	mph	-	minor	-	-	Foidite	MF	-
0221-4	sub/eu	mx	mx	-	-	minor	-	-	Foidite	F	-
0221-5	sub	mx	mx	-	-	major	-	-	Foidite	-	-
0221-6	sub	mx	mx	-	-	major	√	-	Foidite	-	-
0222-1A	an/sub	ph	mx	-	-	minor	√	√	Foidite	-	-
0222-1B	an/sub	ph	mx	-	-	minor	-	√	Foidite	F	-
0222-2S	sub	mx	mx	mx	-	minor	-	-	Foidite	MF	-
0225-2	sub/eu	mx	mx	-	-	minor	-	√	Foidite	F	-
0301-4	sub/eu	-	mx	-	-	minor	-	-	Foidite	F	-
0301-5	sub	mx	mx	-	-	minor	-	-	Foidite	-	-
0301-8	an/sub	mx	mx	-	-	minor	-	-	Foidite	-	-
0301-9	eu	mx	-	mph	-	minor	-	-	Foidite	MF	-
0302-1	sub	mx	mx	-	-	minor	-	-	Foidite	-	-
0622-1	sub	mx	mx	-	-	minor	-	-	Foidite	-	-
0622-7S1	sub	mx	mx	-	-	minor	-	-	Foidite	-	-
0622-7S2	sub	mx	mx	-	-	minor	-	-	Foidite	-	-
0622-8	sub	mx	mx	-	-	minor	-	-	Foidite	-	-
0623-2	sub/eu	mx	mx	-	-	-	-	-	Foidite	-	-
0623-3	sub	-	mx	-	-	-	-	-	Foidite	F	-
0623-4	an/sub	ph	mx	-	-	minor	√	-	Foidite	F	D
0623-5	an	mx	mx	-	-	minor	-	-	Foidite	-	-

Appendix A. cont.

0623-6	an/eu	mx	mx	-	-	minor	-	√	Foidite	F	-
0623-7S	sub	mx	mx	-	-	-	√	√	Foidite	F	-
0625-3	sub	mph	mx	-	-	minor	-	-	Foidite	-	-
0625-6	sub	mx	mx	-	-	minor	-	-	Foidite	-	-
0625-8	sub	ph	mx	-	-	minor	-	-	Foidite	-	-
0629-1	sub	mx	mx	-	-	minor	-	-	Foidite	-	-
0702-2	sub	mx	mx	-	-	major	-	-	Foidite	-	-
0702-3	an/sub	mx	mx	-	-	minor	-	-	Foidite	-	-
0702-5	sub	mx	mx	-	-	minor	-	-	Foidite	-	-
0702-7	sub	mx	mx	mx	-	minor	-	-	Foidite	-	-
0702-8	sub	mx	mx	-	-	minor	-	-	Foidite	-	L
0702-9	an/sub	mx	mx	mx	-	-	√	-	Foidite	MF	D
0704-1	an/sub	ph	mx	-	-	-	√	-	Foidite	-	-
0705-5	sub/eu	mx	mx	-	-	-	√	-	Foidite	-	-
0708-1	sub	mx	mx	-	-	major	-	-	Foidite	-	-
0708-2	an	mx	mx	-	-	major	-	-	Foidite	-	-
0710-1	an	mx	-	mx	-	-	√	√	Foidite	-	-
0710-2	an	mx	mx	mx	-	-	√	-	Foidite	MF	-
0710-4	an/sub	mx	mx	-	-	minor	-	-	Foidite	-	-
0710-6	an/sub	mx	mx	-	-	minor	-	-	Foidite	-	-
0712-1	an	mx	mx	-	-	minor	-	-	Foidite	-	-
0712-2	sub	ph	mx	mx	-	minor	-	-	Foidite	MF	-
0713-1	an/sub	mx	ph	-	-	minor	-	-	Foidite	-	-
0713-2	an/sub	mx	mx	-	-	minor	-	-	Foidite	-	-
0713-3	an/sub	mx	mx	-	-	major	-	-	Foidite	-	-
0713-4	sub	mx	mx	-	-	minor	-	√	Foidite	F	-
KV03-01	sub	mx	mx	-	-	minor	-	-	Foidite	F	-
KV03-03	an/sub	mx	mx	-	-	minor	√	-	Foidite	-	-
KV03-04	an/sub	mx	mx	-	-	minor	-	-	Foidite	F	-
KV03-10	an	mx	mx	-	-	minor	-	-	Foidite	F	-

Appendix A. cont.

KV03-13	sub	mx	mx	-	-	minor	√	√	Foidite	-	-
KV03-15A	sub/eu	mx	mx	-	-	minor	-	-	Foidite	-	-
KV03-15B	sub	mx	mx	-	-	minor	-	-	Foidite	F	-
KV03-18	sub	mx	-	-	mx	-	-	√	Foidite	F	-
KV04-5	sub	mx	ph	-	-	-	-	√	Foidite	F	-
KV04-8	sub	mx	ph	-	-	-	-	-	Foidite	F	L
KV04-9	sub	mx	mx	-	-	-	-	-	Foidite	F	-
KR-1	an/eu	mx	mph	-	-	-	√	√	Foidite	F	-
KR-2	an/sub	mx	-	-	-	minor	-	-	Foidite	F	-
KR-5	an	mx	mph	mph	-	-	-	-	Foidite	MF	-
0223-3	sub/eu	mx	-	-	-	minor	-	-	Undiff.	U	-
0302-3	sub/eu	mx	-	-	-	major	-	-	Undiff.	U	-
0626-2	sub	ph	-	-	-	minor	√	√	Undiff.	U	D
0628-4	eu	mx	-	-	-	minor	-	-	Undiff.	U	-
0702-4	an/eu	mx	-	-	-	minor	-	-	Undiff.	U	-
KR-6	eu/sub	mph	-	-	-	-	√	-	Undiff.	U	-
KR-7	eu/sub	mx	-	-	-	-	-	-	Undiff.	U	-

Key:
√ **=** presence of secondary mineral (calcite, zeolite, or clay)
olivine crystal shape: eu = euhedral, sub = subhedral, an = anhedral
other mineral size: ph (>0.5 mm) = phenocryst, mph (0.1 - 0.5 mm) = microphenocryst, mx = matrix
Rock Type: PB = picrobasalt, AB **=** alkalic basalt**,** Bas = basanite, F = foidite, MF = melilite foidite,
U = undiffereniated (no plagioclase or nepheline)
(*****) = rock name based on normative analysis (XRF), (rs) = rock samples w/no thin section
Xeno – (Xenolith type)**:** D = dunite, L = lherzolitic, W = wehrlitic
Level of iddingsite alteration from least to greatest: none, minor (0.01 -0.1 mm rims on olivine), major (>0.1 mm rims on olivine)
see text for rock type classification criteria

Appendix B. Summary of well location, thickness of Koloa lavas, contact, and other information subdivided into four districts

Well #	Koloa (m)	Position	√	Notes (contact)
Lihue Basin				
0020-03	≥88 m	22º 00' 19.0" N 159º 20' 58.3" W		
0022-01	≥152 m	22º 00' 13.2" N 159º 22' 40.6" W	√	
0023-01(PKR)	175 m	22º 00' 54.0" N 159º 23' 19.0" W		Reviewed by Reiners et al., 1999
0121-01(SW)	210 m	22º 01' 31.0" N 159º 21' 47.0" W		Reviewed by Reiners et al., 1999
0123-01	229 m	22º 01' 26.0" N 159º 23' 12.0" W		Reviewed by Reiners et al., 1999
0124-01(NEK)	190 m	22º 01' 33.0" N 159º 24' 20.0" W		Reviewed by Reiners et al., 1999
0126-01	135 m	22º 01' 27.6" N 159º 26' 21.1" W		Reviewed by Reiners et al., 1999
0222-01 (AH)	50 m	22º 02' 55.0" N 159º 22' 41.0" W		Ananlyzed by S. Izuka (2005)
0320-02	≥70 m	22º 03' 47.3" N 159º 20' 53.2" W	√	No weathered horizon, although well is close to Koloa/WCB contact, Koloa lavas may be ponded high against cliff of shield lavas.
0327-01	70 m	22º 03' 31.0" N 159º 27' 29.0" W	√	
0419-01	48 - ≥76 m	22º 04' 35.0" N 159º 19' 15.0" W		Loose coral and sand to a depth of 15 m, lower coral horizon at 48 m is thin (1 m) and may be a flucuation of Koloa eruptions.
0419-03	≥55 m	22º 04' 39.0" N 159º 19' 40.0" W		6 m thick red clay horizon at 23 m, may be an erosional horizon within the Koloa lavas.
0518-01	52 - ≥91 m	22º 05' 24.0" N 159º 18' 42.0" W		Alternating rock and clays to 52 m, below clay horizon cinder and rock are mixed to depth of well.
0518-02	≥61 m	22º 05' 24.0" N 159º 18' 42.0" W	√	

Appendix B. cont.

0518-04	28 - ≥81	22º 05' 23.0" N 159º 18' 44.0" W		Underlying the rocks at a depth of 28 m is a 22 m section of soft brown clay, below the clay horizon hard rock continues until the depth of the well (81 m).
0523-02	132 m	22º 05' 20.0" N 159º 23' 21.0" W		Contact between WCB and Koloa lavas represented by a 10 m horizon of soil and clay.
0618-05	≥69 m	22º 06' 15.6" N 159º 18' 36.3" W		0618-01 through 07 are mapped in same location and reveal similar stratigraphy.
0620-01	32 - ≥142 m	22º 06' 04.6" N 159º 20' 13.5" W	√	
5721-01	≥99 m	21º 57' 55.0" N 159º 21' 10.0" W	√	
5821-01	≥134 m	21º 58' 18.1" N 159º 21' 11.1" W	√	
5821-02	≥87 m	21º 58' 21.0" N 159º 21' 50.0" W	√	
5824-01	54 - 235m	21º 58' 25.0" N 159º 24' 08.0" W		25 m clay horizion bounds minimum, consistently hard or medium to 235 m.
5824-03	≥61 m	21º 58' 40.2" N 159º 24' 30.0" W	√	
5824-05	≥105 m	21º 58' 22.0" N 159º 24' 27.0" W	√	
5923-01	219 m	21º 59' 01.0" N 159º 23' 53.0" W		Coral horizon at 219 m, underlain by a 55 m section of mostly clay.
5923-03	≥64 m	21º 59' 12.0" N 159º 23' 44.0" W	√	
5923-05	≥84 m	21º 59' 9.4" N 159º 23' 45.8 W	√	
5923-06	≥73 m	21º 59' 19.7" N 159º 23' 41.6" W	√	
5923-07	≥41 m	21º 59' 01.0" N 159º 23' 52.8" W	√	

Appendix B. cont.

5923-08 (HTZ)	266 m	21º 59' 45.1" N 159º 23' 16.9" W		Reviewed by Reiners et al., 1999
5824-07	≥124 m	21º 58' 38.0" N 159º 24' 48.0" W	√	
5824-06	≥152 m	21º 58' 32.3" N 159º 24' 55.8" W	√	

Koloa

Well #	Koloa Thickness	Position		Notes (contact)
5430-01	≥120 m	21º 54' 57.6" N 159º 30' 27.0" W	√	
5426-01	≥58 m	21º 54' 24.5" N 159º 26' 53.2" W		
5426-02	103 m	21º 54' 26.0" N 159º 26' 51.5" W		Analyzed by J. Mink
5826-01	≥117 m	21º 58' 04.7" N 159 26' 01.7" W	√	
5530-02	≥200 m	21º 55' 59.0" N 159º 30' 47.0" W	√	Macdonald et.al.(1960) has Koloa lavas to depth of well.
5530-04	200 m	21º 55' 41.0" N 159º 30' 24.5" W		Well is plotted in WCB's near dashed contact with Koloa lavas. However, field data (sample 0623-7s) would indicate Koloa lavas in this area. Given the depth of Koloa lavas in 5530-02 only 0.5 km to theSW and the lack of erosional horizons in the well log,Koloa lavas may be as deep as in 5530-02.
5825-01	≥90 m	21º 58' 26.0" N 159º 25' 08.0" W	√	
5825-02	64 - ≥125 m	21º 58' 26.0" N 159º 25' 24.0" W		Minimum is bounded by a 58 m section of "soft material", below 58 m hard/medium rock to extent of well.
5825-03	≥98 m	21º 58' 09.0" N 159º 25' 35.0" W	√	

Appendix B. cont.

5529-01	≥162 m	21º 55' 24.5" N 159º 29' 54.0" W	Logger has Koloa lavas to 34 m, unlikely Koloa lavas are that thin in this location, ~1 km east of 5530-02. Koloa lavas to the depth of the well seems probable and well log 5529-02 supports this notion.
5529-02	≥162 m	21º 55' 06.3" N 159º 29' 54.0" W	Logged as Koloa lavas to 151 m, after a small (5 m) section of Palikea Breccia, Koloa lavas are found to the extent of the well.
5529-03	≥220 m	21º 55' 27.6" N 159º 29' 54.8" W	Drilled directly adjacent to 5529-01. Expect similar stratigraphy.
5531-01	207 - ≥289 m	21º 55' 3.1" N 159º 31' 15.4" W	Stratigraphy alternates between hard and soft layers untill the appearance of clay at 207m, where a 20 m section of clay overlies continued alterations between hard and soft layers to the depth of the well.
5631-01	54 m	21º 56' 29.0" N 159º 31' 41.0" W	Stratigraphy below 54 m lacks erosional horizons. Also, well is in close proximity of dashed contact for shield lavas to the north.
5429-01	≥182 m	21º 54' 48.9" N 159º 29' 57.4" W	Koloa lavas are logged by D.C. Cox to the depth of the well
5428-01	133 - ≥295 m	21º 54' 55.0" N 159º 28' 33.0" W	Analyzed by J. Mink

Hanapepe

Well #	Koloa Thickness	Position		Notes (contact)
5635-01	21 m	21º 56' 34.2" N 159º 35' 53.4"		Near dashed contact for WCB
5537-01	≥45 m	21º 55' 16.6" N 159º 37' 53.4" W	√	
5634-01	132 m	21º 56' 07.0" N 159º 34' 43.0" W		Well is located near dashed Koloa/WCB contact, 21 m package of black sand at 132 m is contact.

Appendix B. cont.

North Coast

Well #	Koloa Thickness	Position		Notes (contact)
0618-01	≥69 m	22º 06' 15.6" N 159º 18' 36.3" W		Alluvium and clay down to 43 m, which correpsonds with 0419-01. Below this horizon to depth of well is "hard lava".
0719-01	≥180 m	22º 07' 34.0" N 159º 20' 06.0" W		Koloa lavas are logged to the depth of the well at 180 m (minus ~16 m of Palikea) by D.C. Cox.
0720-02	26 m	22º 07' 25.2" N 159º 20' 31.7" W		Logged by D.C. Cox
0818-01	≥132 m	22º 08' 24.5" N 159º 18' 54.9" W	√	No large erosional gaps. Koloa rocks were sampled at the banks of Anahola stream which lie 61 m below well on adjacent cliff; well terminates at black sand.
0818-02	135 m	22º 08' 24.0" N 159º 18' 55.0" W		Alternating horizons of weathered and hard/soft rock until 135 m, where there is a ~10 m section of coral. Coral horizon correlates well with the black sand horizon of 0818-01.
0918-01	≥24 m	22º 09' 50.0" N 159º 18' 48.0" W	√	
0919-02	18 - ≥45 m	22º 09' 46.0" N 159º 19' 14.0" W		This well is near contact for WCB.
1019-03	≥20 m	22º 10' 37.0" N 159º 19' 07.0" W	√	
1020-01	140 m	22º 10' 34.7" N 159º 19' 23.0"W		Well logged by D.C. Cox, Koloa lavas are found to wells' extent (189 m), however, a 50 m package of Palikea breccia was subtracted from Koloa thickness yielding a net Koloa thickness of at least 140 m.
1120-03	≥27 m	22º 11' 45.0" N 159º 20' 12.0" W		Clay, sand, and coral (~14 m thick) in stratigraphic sequence; hard lavas below 14 m are Koloa.
1120-05	≥26 m	22º 11' 47.0" N 159º 20' 06" W		Sand, clay, and coral to 12m; lavas below may be Koloa lavas.
1120-09	≥27 m	22º 11' 38.0" N 159º 20' 17.0" W		Sand and clay to 14 m, lavas below 14 m are Koloa lavas.
1120-12	≥26 m	22º 11' 45.0" N 159º 20' 03.0" W		Sand and clay to 18 m, lavas below 18 m are Koloa lavas.

Appendix B. cont.

1120-25	≥27 m	22º 11' 34.0" N 159º 20' 51.0" W	√	
1120-26	86 - ≥140 m	22º 11' 48.1" N 159º 20' 54.0" W		Minimum bounded by 30 m section of clay, mostly coherent units below (according to logger).
1120-27	≥62 m	22º 11' 46.6" N 159º 20' 48.0" W	√	
1120-30	150 - ≥186 m	22º 11' 43.4" N 159º 20' 48.9" W		Only 0.3 km's from previous well, no large clay horizon exist. There is a large (~30m) section of cinder and sand which bounds the minimum and correlates with sand horizon in 1120-26.
1123-01	≥40 m	22º 11' 33.0" N 159º 23' 14.0" W	√	
1126-03	≥296 m	22º 11' 38.6" N 159º 26' 11.4" W	√	
1127-01	176 m	22º 11' 55.0" N 159º 27' 06.0" W		Below 176 m to the depth of the well (228 m) is a package of loose, weathered, clay material.
1127-02	≥120 m	22º 11' 18.0" N 159º 27' 32.0" W	√	
1221-03	≥67 m	22º 12' 17.4" N 159º 21' 39.7" W	√	
1225-02	30 - ≥98 m	22º 12' 47.3" N 159º 25' 28.0" W		Ash and cinder (presumably Koloa) is mixed with rock to a depth of 30 m. Below the 30 m horizon is underlain by a 15 m section of red clay; lavas continue to the depth of the well (98m).
1225-03	30 - ≥50 m	22º 12' 23.4" N 159º 25' 28.7" W		Given the close proximity of this well with 1225-02, is very similar. Both have same ~15 m section of red clay followed by a return to lava flows to the depth of the well.
1325-01	≥68 m	22º 13' 25.7" N 159º 25' 19.4" W		At 13m depth a clay horizon continues down well for another 22m. Contact for Koloa lavas and WCB is below depth of well.
1229-01	≥53 m	22º 12' 55.2" N 159º 29' 41.7" W		Well is close to the coast at the mouth of the Hanalei River, sand and mud horizons dominate well stratigraphy to a depth of 53 m. Koloa rocks may be below sediment package, and must have traversed the ancestral Hanalei River, according to Macdonald et. al., (1960).

Appendix B. cont.

1229-02	≥52 m	22º 12' 39.4" N 159º 29' 41.7" W		Same as above.
1327-01	≥70 m	22º 13' 35.0" N 159º 27' 47.3" W	√	
1327-02	65 - ≥183 m	22º 13' 18.7" N 159º 27' 18.6" W		At 65 m "hard" lavas yield to brown clay for another 9-10 m down well. After this small clay horizon, lavas continue uninterupted to the depth of the well (183 m).

Key
≥ = Koloa rocks go to at least the depth of the well
√ = No large erosional gaps (as defined by methods section), thus, Koloa lavas are to the depth of the well
Old Hawaiian datum is used for all lat and long which are in degrees, minutes, and seconds

Assumptions
1. There are commonly ≥30 m sedimentary intervals between Koloa lavs and WCB.

2. Sand layers indicate a paleo shoreline or estuary, and possibly a wave cut bench. Sandy layers may indicate paleo shorelines, hence the contact between Koloa lavas and WCB's.

3. Alternation of hard and soft rock layers, in addition to thin (≤1 m), alternating clay layers are common in the Koloa Volcanics (S. Izuka, 2004, pers. comm.; Macdonald et al., 1960)

4. Shield lavas of the Waimea Canyon Basalts are massive and reveal fewer erosional unconformities than are found in the Koloa lavas.

Appendix C. Normative analysis of 60 Koloa lavas.

Sample	**0218-1**	**0219-2**	**0219-3.b**	**0220-3**	**0220-4**	**0220-6**	**0221-4**	**0222-1.b**	**0222-2S**	**0225-2**
Normative Minerals										
Plagioclase	12.9	14.9	27.2	14.9	6.2	2.6	18.4	10.5	9.9	14.2
Orthoclase	-	-	5.44	-	-	-	-	-	-	-
Nepheline	14.7	11.9	9.7	11.9	18.0	19.0	8.7	17.2	15.6	11.6
Leucite	4.0	5.6	-	5.6	7.6	7.7	3.4	2.9	4.9	4.2
Diopside	36.5	34.7	27.5	34.7	19.0	19.5	30.2	22.6	17.6	27.9
Olivine	21.4	21.7	20.9	21.7	27.5	30.0	26.2	26.8	30.7	27.7
Larnite	0.2	0.4	-	0.4	8.6	10.3	2.0	8.0	10.3	3.5
Ilmenite	5.7	6.4	5.1	6.4	7.4	5.6	6.2	6.5	5.3	6.0
Magnetite	3.1	3.2	3.0	3.2	3.4	3.3	3.4	3.3	3.3	3.3
Apatite	1.5	1.3	1.1	1.3	2.2	2.0	1.5	2.3	2.4	1.7
Total	**100.0**	**100.0**	**100.0**	**100.0**	**100.0**	**100.0**	**100.0**	**100.0**	**100.0**	**100.0**

Sample	**0228-2**	**0301-1**	**0301-4**	**0301-9**	**O622-6**	**0623-3**	**0623-4**	**0623-6**	**0623-7s**	**0626-1**
Normative Minerals										
Plagioclase	24.2	19.4	7.5	10.9	34.1	12.5	9.2	5.1	11.1	15.1
Orthoclase	4.9	6.7	-	-	4.5	-	-	-	-	6.0
Nepheline	8.3	11.5	17.6	15.5	4.7	11.4	12.9	16.3	13.3	12.7
Leucite	-	-	7.8	6.2	-	3.2	5.2	7.1	5.4	-
Diopside	30.7	32.1	21.7	34.9	28.6	25.8	25.1	27.3	25.2	33.2
Olivine	23.8	21.4	26.5	22.0	21.0	30.7	34.2	26.4	27.5	24.2
Larnite	-	-	7.9	0.8	-	5.7	3.5	5.7	5.1	-
Ilmenite	4.3	4.9	6.3	5.5	3.7	5.4	4.9	6.8	7.2	4.5
Magnetite	3.0	3.0	3.2	3.1	2.8	3.4	3.2	3.3	3.3	3.1
Apatite	0.9	1.0	1.7	1.1	0.7	2.0	1.7	2.1	2.0	1.2
Total	**100.0**	**100.0**	**100.0**	**100.0**	**100.0**	**100.0**	**100.0**	**100.0**	**100.0**	**100.0**

Appendix C. cont.

Sample	**0702-9**	**0705-3**	**0705-5**	**0707-6**	**0709-3**	**0709-5**	**0710-2**	**0712-2**	**0713-4**	**KV03-1**
Normative Minerals										
Plagioclase	8.8	23.2	16.1	20.4	31.7	11.0	6.6	10.8	11.0	6.3
Orthoclase	-	6.56	-	5.6	5.6	7.9	-	-	-	-
Nepheline	13.6	9.0	11.2	10.2	7.4	16.2	16.5	11.3	12.8	15.6
Leucite	5.0	-	3.85	-	-	0.2	6.0	4.4	6.2	7.9
Diopside	22.6	31.3	33.8	32.8	27.7	37.4	20.6	18.3	21.3	29.1
Olivine	31.6	21.5	23.7	22.9	19.7	18.0	29.5	31.4	31.5	24.8
Larnite	7.8	-	0.4	-	-	-	9.8	10.3	6.1	4.3
Ilmenite	5.3	4.7	6.3	4.3	4.1	5.1	5.6	7.4	6.2	6.9
Magnetite	3.3	3.0	3.2	2.9	2.9	2.9	3.4	3.5	3.2	3.4
Apatite	2.1	0.9	1.5	1.0	1.0	1.4	2.0	2.6	1.7	1.7
Total	**100.0**	**100.0**	**100.0**	**100.0**	**100.0**	**100.0**	**100.0**	**100.0**	**100.0**	**100.0**

Sample	**KV03-2**	**KV03-4**	**KV03-5**	**KV03-6**	**KV03-7**	**KV03-8**	**KV03-10**	**KV03-11**	**KV03-12**	**KV03-15B**
Normative Minerals										
Plagioclase	28.8	6.8	30.3	30.3	26.3	18.4	11.2	27.3	22.6	9.1
Orthoclase	6.9	-	5.3	6.8	5.0	5.8	-	6.1	6.6	-
Nepheline	8.6	16.0	5.9	8.0	8.4	11.2	16.1	10.0	12.8	14.8
Leucite	-	7.8	-	-	-	-	5.0	-	-	5.3
Diopside	34.1	30.2	25.5	34.8	32.0	33.9	34.4	34.2	38.4	28.2
Olivine	12.4	22.8	23.7	11.7	20.4	22.4	21.2	13.6	11.4	27.9
Larnite	-	4.2	-	-	-	-	1.8	-	-	4.4
Ilmenite	5.3	7.0	5.1	4.5	4.2	4.3	5.6	4.8	4.4	5.6
Magnetite	2.9	3.4	3.1	2.8	2.9	3.0	3.2	2.9	2.7	3.1
Apatite	1.1	1.8	1.1	1.2	0.9	1.0	1.6	1.0	1.2	1.5
Total	**100.0**	**100.0**	**100.0**	**100.0**	**100.0**	**100.0**	**100.0**	**100.0**	**100.0**	**100.0**

Appendix C. cont.

Sample	KV03-17	KV03-18	KV03-19	KV03-20	KV03-21	KV03-27	KV04-1	KV04-3	KV04-4	KV04-5
Normative Minerals										
Plagioclase	11.0	13.1	22.4	33.8	26.9	12.3	36.9	29.6	25.3	13.5
Orthoclase	2.6	2.5	3.6	4.7	7.2	4.1	3.5	5.2	5.3	-
Nepheline	16.1	12.3	7.3	2.8	6.8	18.2	1.8	5.8	8.1	10.6
Leucite	3.3	2.8	-	-	0.0	-	-	-	-	5.3
Diopside	35.1	35.0	30.8	26.9	30.4	37.0	25.1	29.3	29.4	22.5
Olivine	23.0	25.6	27.0	24.4	19.3	18.5	26.3	22.3	23.9	31.2
Larnite	-	-	-	-	-		-	-	-	5.9
Ilmenite	4.5	4.5	4.5	3.8	5.2	5.3	3.1	4.1	4.1	6.2
Magnetite	3.1	3.2	3.2	2.8	3.0	3.2	2.8	3.0	3.0	3.2
Apatite	1.3	1.1	1.3	0.8	1.3	1.3	0.6	0.9	0.9	1.7
Total	**100.0**	**100.0**	**100.0**	**100.0**	**100.0**	**100.0**	**100.0**	**100.0**	**100.0**	**100.0**

Sample	KV04-6	KV04-8	KV04-9	KV04-10	KV04-13	KR-5	KR-3	KR-2	KR-1	Makaleha
Normative Minerals										
Plagioclase	24.0	13.7	14.1	28.1	41.2	7.6	23.7	10.3	15.3	9.2
Orthoclase	5.0	11.0	-	5.3	5.2	-	7.8	-	-	-
Nepheline	7.7	4.7	10.4	6.8	0.3	15.6	11.3	16.9	8.8	14.6
Leucite	-	-	5.1	-	-	4.6	-	2.3	3.3	5.5
Diopside	27.5	26.0	27.2	28.6	24.4	22.5	39.3	33.6	26.6	24.2
Olivine	27.4	28.8	28.4	22.9	20.9	29.4	8.3	23.3	28.8	27.7
Larnite	-	4.3	3.4	-	-	7.9	-	2.5	-	7.7
Ilmenite	4.4	6.4	6.4	4.5	4.2	6.7	5.5	6.4	6.5	5.7
Magnetite	3.2	3.4	3.5	3.0	2.9	3.4	3.0	3.2	3.3	3.4
Apatite	0.9	1.7	1.7	0.9	0.9	2.2	1.1	1.7	1.6	2.1
Total	**100.0**	**100.0**	**100.0**	**100.0**	**100.0**	**100.0**	**100.0**	**100.0**	**100.0**	**100.0**

References

Bianco, T.A., Ito, G., Becker, J.M., and Garcia, M.O., 2005, Secondary Hawaiian volcanism formed by flexural arch decompression: Geochem. Geophys. Geosyst., 6, Q08009, doi:10.1029/2005GC000945

Bizimis M., Sen G., Salters V. J. M., and Keshav S., 2005, Hf-Nd-Sr isotope systematics of garnet pyroxenites from Salt Lake Crater, Oahu, Hawaii: Evidence for a depleted component in Hawaiian volcanism: Geochem. Cosmochem. Acta, v. 69, p. 2629-2646.

Chen, C.-Y., Frey, F. and Garcia, M.O., Evolution of alkalic lavas at Haleakala Volcano, East Maui, Hawaii: Major, trace element and isotopic constraints: Contrib. Mineral. Petrol., v. 105, p. 197-218.

Clague, D.A. and Frey, F.A., 1982, Petrology and trace-element geochemistry of the Honolulu Volcanics, Oahu: Implications of the oceanic mantle beneath Hawaii: J. Petrol., v. 23, p. 447-504.

Clague, D.A., Dao-Gong, C., Murnane, R., Beeson, M.H., Lanphere, M.A., Dalrymple, B., Friesen, W., and Holcomb, R.T., 1983, Age and petrology of Kalaupapa basalt, Molokai, Hawaii: Pacific Sci., v. 36, no. 4, p. 411-420.

Clague, D.A., and Dalrymple, G.B., 1987, The Hawaiian-Emperor volcanic chain Part 1, Geologic evolution: USGS Prof. Paper, 1350, p. 5-54.

Clague, D.A., and Dalrymple, G.B., 1988, Age and petrology of alkalic postshield and rejuvenated-stage lavas from Kauai, Hawaii: Contrib. Mineral. Petrol., v. 99, p. 202-218.

Clague, D. A., R. T. Holcomb, J. M. Sinton, R. S. Detrick, and M. E. Torresan (1990), Pliocene and Pleistocene alkalic flood basalts on the seafloor north of the Hawaiian Islands, Earth Planet. Sci. Lett., v. 98, p. 175–191.

Clague, D.A., Paduan, J.B., McIntosh, W.C., Cousens, B.L., Davis, A.S., and Reynolds, J.R., 2005, A submarine perspective of the Honolulu Volcanics, Oahu: J. Volcanol. Geotherm. Res., v. 151, p. 279-307.

Cross, W., 1915, Lavas of Hawaii and their relations: USGS Prof. Paper 88, pp. 97.

Dana, J.D., 1849, Geology: U.S. Exploring Exped. Rep., vol. 10, pp. 756, (esp. p. 262-279).

Dana, J.D., 1890, Characteristics of Volcanoes, New York, pp. 399.

Enviromental Systems Research Institute, 2004, ArcGIS 9: Using ArcMap: ESRI, New York, pp. 585.

Everden, J.F., Savage, D.E., Curtis, G.H., and James, G.T., 1964, Potassium-argon dates and the Cenozoic mammalian chronology of North America: Am. J. Sci., v. 262, p. 145-198.

Faure, G., 1986, Principles of Isotope Geology: John Wiley & Sons Inc., 2nd Ed., pp. 589.

Feigenson, M.D., 1984, Geochemistry of Kauai volcanics and a mixing model for the origin of Hawaiian alkali basalts: Contrib. Mineral. Petrol., v. 87, p. 109-119.

Francis, P., Oppenheimer, C., Stevenson, D., 1993, Endogenous growth of persistently active volcanoes: Nature, v. 366, p. 354-357.

Frey, F.A., Blichert-Toft, J.,Regelous, M., Boyet, M. 2005, Origin of depleted components in basalt related to the Hawaiian hot spot: Evidence from isotopic and incompatible element ratios: Geochem. Geophys. Geosyst., 6, Q02L07, doi:10.1029/2004GC000757

Folk, R.L., 1974, Petrology of Sedimentary Rocks: Hemphill Publishing Co., Austin, TX, pp. 182.

Garcia, M., Foss, D., West, H. and Mahoney J., 1995, Geochemical and isotopic evolution of Loihi Volcano, Hawaii: J. Petrol., v. 36, p. 1647-1674

Gramlich, J.W., Lewis, V.A., and Naughton, J.J., 1971, Potassium-argon dating of Holocene basalts of the Honolulu Volcanic series: Geol. Soc. Am. Bull., v. 82, p. 1399-1404.

Gurriet, P., 1987, A thermal model for the origin of post-erosional alkalic lava, Hawaii: Earth Planet. Sci. Lett., v. 82, p. 153-158.

Hearty, P.J., Karner, D.B., Renne, P.R., Olson, S.L., and Fletcher, S., 2005, $^{40}Ar/^{39}Ar$ age of a young rejuvenation basalt flow: implications for the duration of volcanism and the timing of carbonate platform development during the Quaternary on Kaua`i, Hawaiian Islands: New Zeal. J. Geol. Geophys., v. 48, p. 199-211.

Hinds, N.E.A., 1930, The geology of Kauai and Niihau: Bull. B.P., Bishop Mus, v. 71, pp. 103.

Hitchcock, C.H., 1909, Hawaii and its Volcanoes, Honolulu, pp. 314.

Holcomb, R.T., Reiners, P.W., Nelson, B.K., and Sawyer, N.E., 1997, Evidence for two shield volcanoes exposed on the island of Kauai, Hawaii: Geology, v. 25, no. 9, p. 811-814.

Jackson, E.D., and Wright, T.L., 1970, Xenoliths in the Honolulu Volcanic Series, Hawaii: J. Petrol., v. 11, p. 405-430.

Kay, R.W., and Gast, P.W., 1973, The rare-earth content and origin of alkali-rich basalts: J. Geol., v. 81, p. 653-682.

Kind, R., Li, X., Yuan, X., Woelbern, I., and Kumar, P., 2005, Rejuvenation of the Pacific lithosphere by the Hawaiian plume: EOS Trans. AGU 86(52) Fall Meet. Suppl., V54A-05.

Lamphere, M.A., and Dalrymple, G.B., 1980, Age and strontium isotopic composition of the Honolulu Volcanic Series, Oahu, Hawaii: Am. J. Sci., v. 280-A, p. 736-751.

Lassiter, J.C., Hauri, E.H., Reiners, P.W., and Garcia, M.O., 2000, Generation of Hawaiian post-erosional lavas by melting of a mixed lherzolite/pyroxenite source: Earth Planet. Sci. Lett. v. 178, p. 269-284.

Le Bas, M.J., Le Maitre, R. W., Streckeisen, A., and Zanettin, B., 1986, A chemical classification of volcanic rocks based on the total alkali silica diagram: J. Petrol., v. 27, p. 745-750.

Le Bas, M.J., 1989, Nephelinitic and basanitic rocks: J. Petrol., v. 30, p. 1299-1312.

Le Maitre, R.W., Streckeisen, A., Zanettin, B., Le Bas, M.J., Bonin, B., Bateman, P., Bellieni, G., Dudek, A., Efremova, S., Keller, J., Lameyre, J., Sabine, P.A., Schmid, R., Sorensen, H., and Woolley, A.R., 2002, Igneous rocks: a classification and glossary of terms: Cambridge Univ. Press, 2nd Ed., pp. 236.

Li, X., Kind, R., Yuan, X. Wolbern, I., and Hanka, W., 2004, Rejuvenation of the lithosphere by the Hawaiian plume: Nature, v. 427, p. 827-829.

Lipman, P., D. A. Clague, J. G. Moore, and R. T. Holcomb, 1989, South Arch Volcanic Field—Newly identified young lava flows on the sea floor south of the Hawaiian Ridge: Geology, v. 17, 611–614.

Maaloe, S., James, D., Smedley, P., Petersen, S., and Garmann, L.B., 1992, The Koloa Volcanic suite of Kauai, Hawaii: J. Petrol., v. 33, p. 1-24.

Macdonald, G. A., 1968, Composition and origin of Hawaiian lavas: Geol. Soc. Am. Mem., v. 116, p. 477-522.

Macdonald, G.A., Abbot, A.T., and Peterson, F.L., 1983, Volcanoes in the Sea: The Geology of Hawaii: Univ. Haw. Press, 2nd Ed., pp. 517.

Macdonald, G.A., Davis, D.A., and Cox, D.C., 1960, Geology and groundwater resources of the island of Kauai, Hawaii: Haw. Div. Hydrog. Bull. 13, pp. 212.

Macdonald, G.A., and Katsura, T., 1964, Chemical composition of Hawaiian lavas: J. Petrol., v. 5, p. 82-133.

McDougall, I., 1964, Potassium-argon ages from lavas of the Hawaiian Islands: Geol. Soc. Am. Bull., v. 75, p. 107-128.

McDougall, I., 1979, Age of shiedl-building volcanism of Kauai and linear migration of volcanism in the Hawaiian Island chain: Earth Planet. Sci. Lett., v. 46, p. 31-42.

Natland, J., 1980, The progression of volcanism in the Samoa linear volcanic chain: Am. J. Sci., v. 280-A, p. 709-735.

Naughton, J.J., Macdonald, G.A., Greenberg, V.A., 1980, Some additional potassium-argon ages of Hawaiian rocks: the Maui volcanic complex of Molokai, Maui, Lanai, and Kahoolawe: J. Vocanol, Geotherm. Res., v. 7, p. 339-355.

Nesse, W.D., 1991, Introduction to Optical Mineralogy: Oxford Univ. Press, 2nd Ed., p. 335.

Ozawa, A., Tagami, T., Garcia, M.O., 2005, Unspiked K-Ar ages of Honolulu rejuvenated and Koolau shield volcanism on Oahu, Hawaii: Earth Planet. Sci. Lett., v. 232, p. 1-11.

Palmiter, D., 1975, Geology of the Koloa Volcanic Series of the south coast of Kauai, Hawaii: M.S. Thesis, Univ. Hawaii, pp. 87.

Powers, S., 1920, Notes on Hawaiian petrology: Am. J. Sci., 4th ser., v. 50, p. 256-280.

Reiners, P.W., and Nelson, B.K., 1998, Temporal-compositional-isotopic trends in rejuvenated-stage magmas of Kauai, Hawaii, and implications for mantle melting processes: Geochem. Cosmochem. Acta, v. 62, p. 2347-2368.

Reiners, P.W., Nelson, B.K., and Izuka, S.K., 1999, Structural and petrologic evolution of the Lihue basin and eastern Kauai, Hawaii: Geol. Soc. Am. Bull., v. 111, p. 674-685.

Rhodes, J.M., 1996, Geochemical stratigraphy of lava flows sampled by the Hawaii Scientific Drilling Project: J. Geophys. Res., v. 101, p. 11,729-11,746.

Rhodes, J.M., and Vollinger, M.J., 2004, Composition of basaltic lavas sampled by phase-2 of the Hawaii Scientific Drilling Project: Geochemical stratigraphy and magma types: Geochem. Geophys. Geosyst., 5, p. 1-38.

Ribe, N.M., 2004, Through thick and thin: Nature, v. 427, p. 793-795.

Ribe, N.M., and Christensen, U.R., 1999, The dynamical origin of Hawaiian volcanism: Earth Planet. Sci. Lett., v. 62, p. 517-531.

Robinson, J.E., and Eakins, 2006, Calculated volumes of individual shield volcanoes at the young end of the Hawaiian ridge: J. Volcanol. Geotherm. Res., v. 151, p. 309-317.

Sano, H., 2006, Unspiked K-Ar dating of the rejuvenated and shield-building volcanism on Kaua'i, Hawai'i: M.S. Thesis, Kyoto University.

Schmincke H. U., 1973, Magmatic evolution and tectonic regime in the Canary, Madeira and Azores island groups: Geol. Soc. Am. Bull., v. 84, p. 633-648.

Sherrod, D. R., Nishimitsu, Y., Takahiro, T., 2003, New K-Ar ages and the geologic evidence against rejuvenated-stage volcanism at Haleakala, East Maui, a postshield-stage volcano of the Hawaiian island chain: Geol. Soc. Am. Bull., v. 115, p. 683-694.

Sherrod, D.R., Sinton, J.M., Watkins, S.E., and Brunt, K.M., 2005, Digital geologic map of the State of Hawaii: USGS map series, in review.

Sinton, J.M., 2005, Geologic Mapping, Volcanic Stages and Magmatic Processes in Hawaiian Volcanoes: EOS Trans. AGU 86(52) Fall Meet. Suppl., V51A-1471.

Spengler, S. and Garcia, M.O., 1988, Geochemical evolution of Hawi Formation lavas, Kohala Volcano, Hawaii: The hawaiite to trachyte transition: Contrib. Mineral. Petrol., v. 99, p. 90-104.

Stearns, H.T., 1946, Geology of the state of Hawaii: Haw. Div. Hydrog. Bull., 8, pp. 106.

Tagami, T., Nishimitsu, Y., and Sherrod, D., 2003, Rejuvenated-stage volcanism after 0.6 m.y. quiescence at West Maui volcano, Hawaii: New evidence from K-Ar ages and chemistry of Lahaina Volcanics: J. Volcanol. Geotherm. Res., v. 120, p. 207-214.

Walker, G.P.L., 1990, Geology and volcanology of the Hawaiian Islands: Pacific Sci., v. 44, p. 315-347.

White, R.W., 1966, Ultramafic inclusions in basaltic rocks from Hawaii: Contr. Mineral. Petrol., v. 12, p. 245-314.

Winchell, H., 1947, Honolulu Series, Oahu, Hawaii: Geol. Soc. Am. Bull,, v. 58, p. 49-78.

Woodhead, J.D., 1992, Temporal geochemical evolution in oceanic intra-plate volcanics: a case study from the Marquesas (French Polynesia) and comparison with other hotspots: Contrib. Mineral. Petrol., v. 111, 458-467

Yang, H.J., Frey, F.A., Clague, D.A., 2003, Constraints on the source components of lavas forming the Hawaiian North Arch and Honolulu Volcanics: J. Petrol., v. 44, p. 603-627.

Xu, G., Frey, F.A., Clague, D.A., Weis, D., Beeson, M.H., 2005, East Molokai and other Kea-trend volcanoes: Magmatic processes and sources as they migrate away from the Hawaiian hot spot: Geochem. Geophys. Geosyst., 6, Q05008, doi:10.1029/2004GC000830